INTERACTION OF ENVIRONMENTAL CALCIUM/PHOSPHATE AND pH WITH GLASS IONOMER RESTORATIVES

WANG XIAOYAN

(BDS) Beijing Medical University,
(MD) Peking University

A THESIS SUBMITTED

FOR THE DEGREE OF DOCTOR OF PHILOSOPHY

DEPARTMENT OF RESTORATIVE DENTISTRY

NATIONAL UNIVERSITY OF SINGAPORE

2006

Acknowledgements

I would like to thank Faculty of Dentistry, National University of Singapore and School and Hospital of Stomatology, Peking University for giving me the opportunity to undertake this research.

I would like to thank and express my sincere gratitude to my supervisor Dr. Adrian Yap U Jin. I am strongly motivated by his passion and knowledge in research work. His invaluable advice, encouragement, patience and care guided me through my research journey in Singapore.

I am also grateful to my co-supervisors Dr. Hien Ngo from Colgate Australian Clinical Dental Research Center, Adelaide University, Australia, Dr. Zeng Kaiyang from Department of Mechanical Engineering, National University of Singapore, and my thesis committee member Dr. Anil Kishen from Department of Restorative Dentistry, National University of Singapore, for their advice, guidance and help in this research project.

I would also like to thank Assistant Professor Chen Jiaping from Department of Chemical & Biomolecular Engineering, Associate Professor Hsu Chin-ying, Stephen, Senior Laboratory Officer Mr Chan Swee Heng from Faculty of Dentistry, National

University of Singapore, and Senior Laboratory Officer Ms Shen Lu from Institute of Material Research and Engineering, for their assistance in conducting the research.

Special thanks are due to colleagues of our team, Chung Sew Meng, Soh Mui Siang and Wu Xiaowa, for their generous help and assistance.

Heartfelt thanks also go to all my friends in Singapore and China, especially my fellow colleagues in Dentistry Research Laboratory, for their help.

I would also like to express my appreciation to Professor Gao Xuejun, current Head of Department of Cariology, Endodontology and Operative Dentistry, School and Hospital of Stomatology, Peking University, Professor Wang Jiade, former Head of Department of Cariology, Endodontology and Operative Dentistry, School and Hospital of Stomatology, Peking University, and Professor Yu Guangyan, Dean of School and Hospital of Stomatology, Peking University, for their support and concern.

Finally, but most of all, I am deeply grateful to my family, especially my husband Peng Xin, for their endless love, patience and understanding.

Table of Contents

List of Tables and Figures

Tables

Figures

Summary

Glass-ionomer cements (GICs) are biocompatible, anticariogenic and can chemically adhere to tooth structure. These positive characteristics account for their popularity in dentistry. The clinical performance of GIC restoratives, however, varies in different patients. Intra-oral environment of patients is complex and consists of mechanical, biological, thermal and chemical factors. GICs, being hydrophilic and salt-based, are susceptible to degradation by the intra-oral chemical environment. While GICs are vulnerable to acids, some components e.g. calcium and phosphate in the oral environment may have positive effects on GICs. Little information is currently available on the co-effects of pH and inorganic constitutes of saliva on GICs. This new knowledge will lead to better understanding of the clinical performance of GICs, provide guidance to their clinical use and facilitate development of new materials.

The effects of environmental calcium/phosphate and pH on two highly viscous GIC (HVGIC) restoratives were investigated in this study. Results suggest that the effects of environmental calcium and phosphate on both calcium and strontium based HVGICs are pH dependent. When pH was at 7 and 5, variations in environmental calcium and phosphate levels did not significantly affect the hardness, elastic modulus and surface structure. However, at pH 3, hardness and elastic modulus of these GICs were increased by the addition of environmental phosphate. The improved properties

were strongly correlated to a modified surface reaction layer arising from the interaction between environmental phosphate and GICs when exposed to acids (pH 3).

The structure, compositions and physico-mechanical properties of the surface reaction layer were characterized using a series of surface analytic techniques. When subjected to higher levels of environmental phosphate, the surface reaction layer was thinner and mechanical properties of the surface reaction layer were higher. This layer consisted of two distinct zones, an inner degradation zone and an outer phosphate complexation zone. The outer zone was closely related to the presence of environmental phosphate and may be responsible for the reduction of the inner degradation zone. Results of ion release from GICs suggest that the phosphate uptake in the outer zone may be the result of ligand exchange between environmental phosphate anions and intrinsic carboxyl groups. The results of ion release also confirmed the inhibition effect of environmental phosphate on acid degradation of GICs.

Moreover, the clinically related properties of wear resistance and shear strength of GICs in acidic conditions were also improved when phosphate was present. Although fluoride released by GICs in acidic conditions was slightly decreased by environmental phosphate, the fluoride release was kept at a substantial level. The findings of the current study suggest that the introduction of local phosphate to GICs may result in better clinical performance of glass-ionomer restoratives *in vivo*.

Notice

Sections of the results and related research in this thesis have been presented, published, accepted for publication or are submitted.

International Journal Papers

1. Yap AUJ, Wang XY, Wu XW, Chung SM. Comparative hardness and modulus of tooth-colored restoratives: A depth-sensing microindentation study. Biomaterials 2004;25:2179-2185.

2. Wang XY, Yap AUJ, Ngo HC. Effect of early water exposure on strength of glass ionomer restoratives. Operative Dentistry 2006;31:584-589.

3. Wang XY, Yap AUJ, Ngo HC, Chung SM. Environmental degradation of glass-ionomer cements: A depth-sensing microindentation study. Journal of Biomedical Materials Research, Part B: Applied Biomaterials (Accepted for publication).

Conference Papers

1. Xiaoyan WANG, Adrian YAP, Vicky WU, Sew Meng CHUNG. Comparative hardness and modulus of direct tooth-colored restorative materials. NHG Annual Scientific Congress, Oct 2003, Singapore.

2. Adrian YAP, Vicky Xiaowa WU, Xiaoyan WANG, Sew Meng CHUNG. Effects of thermal fatigue on the mechanical properties of tooth-coloured restorative materials. NHG Annual Scientific Congress, Oct 2003, Singapore.

3. X.Y. Wang, A.U.J. Yap, K.Y. Zeng. Effect of environmental calcium/phosphate on acid resistance of glass ionomers. 19th IADR/SEA, Sept 2004, Thailand.

4. Xiaoyan WANG, Adrian YAP, Qihui Sam, Sihan Lee. Effect of early water contact on shear punch strength of highly viscous glass-ionomers. 8th NUS-NHG Scientific Congress, Oct 2004, Singapore.

5. Xiaoyan WANG, Adrian YAP. Effect of environmental pH on surface hardness and indentation modulus of glass ionomers. NHG Annual Scientific Congress, Oct 2004, Singapore.

6. Xiaoyan WANG, Adrian YAP. Effect of aqueous environment on surface properties of highly viscous glass-ionomers. NHG Annual Scientific Congress, Oct 2004, Singapore.

7. X.Y. Wang, A.U.J. Yap, H.C. Ngo, K.Y. Zeng. Interaction of environmental calcium/phosphate with glass ionomers. IADR 83rd general session, Mar 2005, USA.

8. X.Y. Wang, A.U.J. Yap, H. Ngo, K.Y. Zeng, L. Yang, J.P. Chen. Surface characterizations of glass-ionomers in acidic environments with calcium/phosphate supplement. 20th IADR/SEA, Sept 2005, Malaysia.

9. Xiaoyan WANG, AUJ YAP. Effect of environmental calcium/phosphate and pH on fluoride release from glass-ionomers. Combined Scientific Meeting, Nov 2005, Singapore.

10. Xiaoyan WANG, AUJ YAP. Influence of calcium/phosphate supplements to acidic conditions on clinically related properties of glass-ionomers. Combined Scientific Meeting, Nov 2005, Singapore.

Awards

X.Y. Wang, A.U.J. Yap, K.Y. Zeng. Effect of Environmental Calcium/Phosphate on Acid Resistance of Glass Ionomers.

Awarded Best Paper in Dental Materials --- Laboratory Research at 19th Annual Scientific Meeting, International Association for Dental Research --- Southeast Asian Division, 2004, Thailand.

Chapter 1

Introduction

The use of tooth-colored restorative materials has increased significantly due to rising aesthetic demands by patients. Contemporary direct tooth-colored restorative materials include glass-ionomer cements (GICs), resin-modified glass-ionomer cements (RMGICs), polyacid-modified resin composite (compomer), giomers and composite resins. GICs and composite resins possessing distinctive characteristics are on the two extreme ends of the continuum of direct tooth-colored restorative materials (Figure1-1).

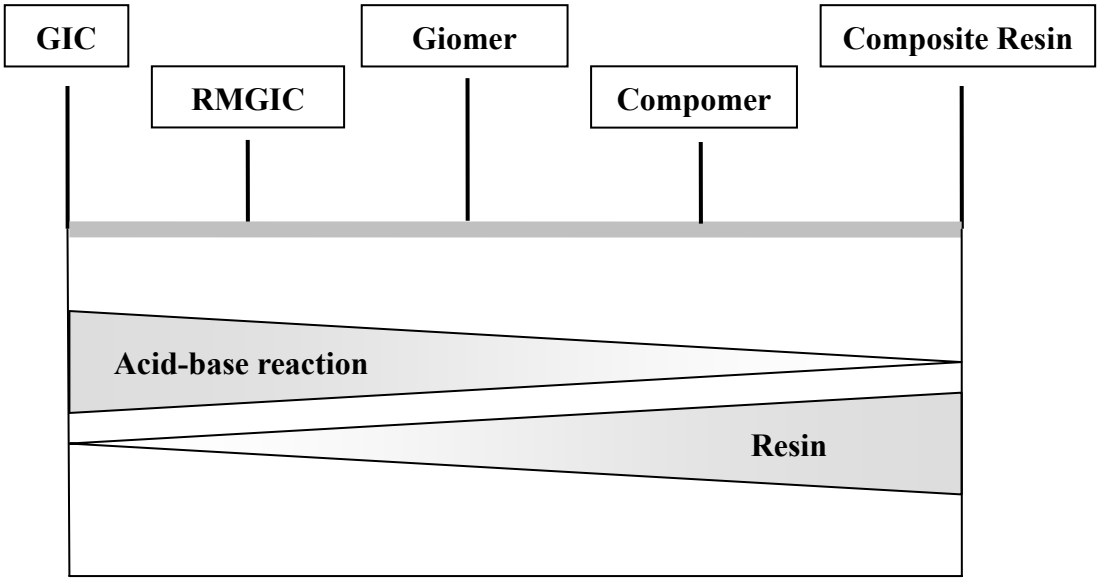

Figure 1-1 Continuum of direct tooth-colored restorative materials

An ideal restorative material should have comparable properties to tooth tissue. No existing materials, however, completely fulfill this criterion. GIC sets by an acid-base reaction and has the advantages of fluoride release, chemical adhesion with tooth structure and excellent biocompatibility. Composite resin, on the other hand, is cured by free radical addition polymerization and has the merits of excellent aesthetics and good handling property. Modern hybrid direct tooth-colored restorative materials have been developed based on GIC and/or composite technique to incorporate the advantages of both materials.

Since GICs were first reported by Wilson and Kent (1972), both polyacid liquid and basic glass powder have been continuously modified to achieve optimum mechanical, aesthetic and handling properties. Alterations in powder and liquid formulation or powder to liquid ratio result in GICs with a variety of physico-mechanical properties and clinical applications.

Based on their clinical applications, GICs can be categorized using the following classifications (Wilson and Mclean, 1988a):

Type I	Luting and bonding cement
Type II	Restorative cement
	(a) aesthetic
	(b) reinforced
Type III	Lining or base cements

Luting and bonding GICs are composed of finer powder particles at a low powder:liquid ratio to achieve an optimum film thickness. Lining GIC has similar powder to liquid ratio as luting GIC, while base GIC consists of higher percentage of glass powder for base purpose. Restorative GIC has the highest content of glass particles compared to other types of GICs. Amongest GIC restoratives, metal-reinforced GIC (MRGIC) has been developed by adding metals or sintering silver with glass particles. With increased physical properties, MRGIC is, however, lack of aesthetic properties and wear resistance. In addition, highly viscous GIC (HVGIC) with rapid set and great physical properties has been subjected to occlusal defects. Regarding HVGICs, excess calcium ions are removed from the surface of glass particles and higher powder to liquid ratio is adopted (Mount, 2002). With improved physical and handling properties, HVGICs are also named “packable” GIC.

According to their setting reactions, GICs can also be classified as conventional GICs and resin-modified GICs (RMGICs). Conventional GIC consists of polycarboxylic acids and basic fluoroaluminosilicate glass particles. It sets by an acid-base reaction between the polyacids and glass particles, which is capable of fully curing in the dark. RMGIC is composed of water-soluble resin monomers in addition to conventional polycarboxylic acids and glass particles. This type of GIC is hardened not only by acid-base reaction but also by free radical addition polymerization of resin monomers. Both conventional and resin-modified GICs can be used as luting, bonding, lining, base and restorative materials.

1.1 Clinical performance of glass-ionomer restoratives

GICs are commonly used in deciduous teeth as alternatives to dental amalgam. In permanent teeth, they are mainly employed in cervical lesions, atraumatic restorative technique (ART), tunnel and sandwich techniques due to their excellent bonding and moderate mechanical properties. In addition, GICs are also indicated in patients with high caries risk, such as patients with xerostomia, taking advantage of the cariostatic potential of fluoride release from glass-ionomer materials.

1.1.1 Longevity of glass-ionomer restoratives *in vivo*

Several clinical trials have been conducted on the longevity of GICs over the last decade or so. Some clinical trials published in full text since 1991 are summarized in Table 1-1. These studies longitudinally observed restorative GICs for at least 2 years. Those studies involving non-restorative GICs or specifically recruiting subjects with high risk of caries were excluded. It can be seen that longevity of glass-ionomer restoratives varied widely between different clinical surveys. Like other dental restoratives, the longevity of glass-ionomer restoratives is influenced by operator, material and patient factors (Manhart *et al*., 2004).

a. Operator effect

GICs are prepared immediately before insertion in cavities and are fragile for some time after hardening. Taifour *et al.* (2002) examined glass-ionomer restoratives

Table 1-1 Longevity of glass-ionomer restoratives

Authors	Observation Period (years)	Black Class	Restorative Materials	Sample Size	Survival Rate	Survival criteria
Yu *et al.* (2004)	2	I[#] II[#] I[#] II[#]	Fuji IX GP (HVGIC, GC, Japan) Fuji IX GP (HVGIC, GC, Japan) KetacMolar (HVGIC, ESPE, Germany) KetacMolar (HVGIC, ESPE, Germany)	20[a] 15[a] 17[a] 20[a]	89.2% 49.1% 93.8% 55.0%	Present, good or marginal defect less than 0.5mm
Mandari *et al.* (2003,2001)	6 2	I[#]	Fuji II (GIC, GC, Japan)	177[b] 212[b]	72% 96%	Perfect or satisfied marginal adaption and anatomic form without secdonary caries[+]
Gao *et al.* (2003)	2.5	I[#]	Fuji IX GP (HVGIC, GC, Japan) KetacMolar (HVGIC, ESPE, Germany)	12[b] 17[b]	92% 88%	Retention
Mallow *et al.* (1998)	3	I[#]	Fuji II (GIC, GC, Japan)	39[b]	59%	Present, good or marginal defect less than 0.5mm
Hubel and Mejare (2003)	3	II*	Fuji II (GIC, GC, Japan) Vitremer (RMGIC, 3M, USA)	62[a] 53[a]	81% 94%	Perfect or satisfied marginal adaption and anatomic form without secdonary caries[+]
Espelid *et al.* (1999)	3	II*	Vitremer (RMGIC, 3M, USA) KetacSilver (MRGIC, ESPE, Germany)	49[a] 49[a]	98% 73%	Perfect or satisfied marginal adaption and anatomic form without secdonary caries[+]
Qvist *et al.* (1997)	3 8	I/II*	KetacFil (GIC, ESPE, Germany)	515[a]	63% 58%	Retention (including censored restorations)
Kilpatrick *et al.* (1995)	2.5	II*	KetacFil (GIC, ESPE, Germany) KetacSilver (MRGIC, ESPE, Germany)	46[a] 46[a]	77% 59%	Perfect or satisfied marginal adaption and anatomic form without secdonary caries[+]
Ostlund *et al.* (1992)	3	II*	ChemFil (GIC, Dentsply, USA)	25[a]	40%	Perfect or satisfied marginal adaption and anatomic form without secdonary caries[+]

Table 1-1 (Continued)

Authors	Observation Period (years)	Black Class	Restorative Materials	Sample Size	Survival Rate	Survival criteria
Welbury *et al.* (1991)	5	II*	KetacFil (GIC, ESPE, Germany)	119[a]	67%	Perfect or satisfied marginal adaption and anatomic form without secdonary caries[+]
Franco *et al.* (2006)	5	V	Vitremer (RMGIC, 3M, USA)	28[b]	96.4%	Retention
Onal and Pamir (2005)	2	V	Vitremer (RMGIC, 3M, USA)	24[a]	100%	Retention
Brackett *et al.* (2003, 1999)	2	V	Fuji II LC (RMGIC, GC, Japan) KetacFil (GIC, ESPE, Germany) PhotacFil (RMGIC, ESPE, Germany)	37[a] 34[a] 34[a]	96% 93% 93%	Retention
Loguercio *et al.* (2003)	5	V	Vitremer (RMGIC, 3M, USA)	16[a]	93%	Retention
Ermis (2002)	2	V	Vitremer (RMGIC, 3M, USA)	20[a]	95%	Retention
Folwaczny *et al.* (2001)	3	V	Fuji II LC (RMGIC, GC, Japan) PhotacFil (RMGIC, ESPE, Germany)	51[a] 31[a]	96% 90%	Retention
Neo and Chew (1996)	3	V	KetacFil (GIC, ESPE, Germany)	50[a]	96%	Retention
Powell *et al.* (1995)	3	V	KetacFil (GIC, ESPE, Germany)	37[b]	97.3%	Retention

[#]ART restoration; *Restorations in primary teeth; [a]Number at start; [b]Number at final recall; [+]Modified USPHS Ryge criteria

GIC: Conventional GIC; RMGIC: Resin-modified GIC; HVGIC: Highly viscous conventional GIC; MRGIC: Metal-reinforced GIC

manipulated and placed by 8 operators and found a significant difference in survival rate of GIC restorations between different operators after 3 years. In another study on GICs handled by general practitioners, although proper powder to liquid ratio for preparation was indicated by manufacturers, GICs were quite often mixed in a much lower powder to liquid ratio and may have less-than optimum physical properties (Billington *et al.*, 1990).

To minimize the operator effect, manufacturers introduced GIC in capsulated form. The capsulated materials are standardized with fixed powder to liquid ratio and mixed by shaking or rotating machines ensuring optimum properties (Nomoto *et al.*, 2004). Meantime, light-cured and fast-set GICs of quick initial set were also developed. This leads to less sensitivity to early moisture contamination and therefore optimum properties of GICs. In addition, well-informed instructions for material usage reduce technique difference between experienced practitioners and inexperienced ones. Application of surface coating on GICs is generally employed to overcome early moisture sensitivity and dehydration of glass-ionomer restoratives (Mount, 1999).

b. Material type

Physico-mechanical properties of GICs vary enormously among different types of GICs and commercial products. This also accounts for the varied clinical performance of glass-ionomer restoratives. Conventional GICs are auto-cured within several minutes, while RMGICs are light-initiated and polymerized instantaneously by

incorporation of photoinitiator. The additional water-soluble resin monomers bestow RMGICs more aesthetic property than conventional ones (Yap *et al.*, 1999). Auto-cured HVGICs were developed by stripping excess calcium ions from the surface of glass particles. HVGICs have improved mechanical properties *via* modifications of glass particle size, size distribution and glass surface reactivity (Young *et al.*, 2004).

HVGICs were originally developed for atraumatic restorative technique (ART). This technique is noted by removal of tooth decay with hand instruments and filling cavity with GICs (Frencken *et al.*, 1996). The survival rate of ART restoratives using contemporary HVGICs is higher than early conventional GICs as shown in Table 1-1. However, Yu *et al.* (2004) reported that ART using HVGICs was only suitable for Class I lesion but not for Class II cavity.

GICs are generally not considered as routine restoratives in stress-bearing posterior teeth due to their inadequate strength. In early clinical trials, conventional GICs (40%) in Class II cavities of primary teeth had lower success rate compared to amalgam (92%) (Ostlund *et al.*, 1992). With improvement of glass-ionomer materials, the longevity of conventional GICs in later studies was higher than before. Additionally, RMGICs performed better than early conventional GICs in Class II restorations and were comparable to amalgam in deciduous teeth (Table 1-1).

In case of Class V restorations, although the longevity was slightly different between various commercial products (Brackett *et al.*, 2003, 1999; Ermis, 2002),

GICs generally had satisfactory performance in restoring cervical defects as shown in Table 1-1.

c. Patient effect

Besides the operator and material factors, patient factor has a significant influence on glass-ionomer restoratives. In a clinical survey for causes of restoration failure, the ranking of failure factors was in decreasing order of patient, operator and material factors (45%, 35% and 20%, respectively) (Maryniuk and Kaplan, 1986). It is well-known that the oral environment is complex and varies among individuals. The intra-oral mechanical, biological, thermal and chemical environments may independently or conjunctly influence the longevity of dental restorations *in vivo*.

Pyk and Mejare (1999) evaluated 242 tunnel restorations of reinforced GICs for 3.5 years and found failure of restorations in molar was four times higher than premolar. Mjör and Jokstad (1993) observed that glass-ionomer restoratives in upper molar suffered more bulk fracture. In another study of tunnel restorations, patients with high caries activity experienced significantly more failure of restorations (Strand *et al.*, 1996). When GICs were applied in xerostomic patients, all restorations presented shorter survival time (Wood *et al.*, 1993). Moreover, some studies reported deterioration of cervical GIC restoratives and dissolution of GIC open-sandwich restorations (Abadalla *et al.*, 1997; Van Dijken, 1994; Van Dijken *et al.*, 1999). Pluim and Arends (1986) evaluated solubility of GICs *in vivo* and found some patients had a larger material loss than others. In another study, a patient with diabetes taking

sugarless diet had minimal degradation of GICs *in vivo* and very little *S. mutans* counts (Mesu and Reedijk, 1983). The aforementioned studies suggest the oral environment may play an important role in the performance of glass-ionomer restorative *in vivo*.

1.1.2 Failure of glass-ionomer restoratives *in vivo*

In terms of *in vivo* evaluation of dental restoratives, the most commonly used criterion is the United States Public Health Service (USPHS) system, also named Ryge criteria. In most clinical trials, the restoratives are qualitatively judged by anatomy form, marginal adaptation, color match, marginal discoloration, surface roughness, as well as secondary caries following Ryge criteria (Ryge *et al.*, 1981).

Clinical studies have shown that bulk fracture and loss of anatomy form are the main reasons for the failure of GIC restoratives in general practice (Mjör, 1997; Mandari *et al.*, 2001, Burke *et al.*, 2001). For xerostomic patients, the most frequently observed failure for glass-ionomers were loss of anatomy, marginal deterioration and erosion of material (McComb *et al.*, 2002; Hu *et al.*, 2002).

Glass-ionomers suffered more bulk fracture when inserted in a large Class I cavity. Bulk fracture of Class II restoratives was mostly located at the isthmus (Smales *et al.*, 1990; Qvist *et al.*, 1997). These results may be ascribed to the low capacity of GICs to undergo strain without fracture. It also indicates that GIC is not suitable for stress-bearing sites.

Loss of anatomy is indicative of material deterioration. The intrinsic structure and properties of materials, as well as chemical erosion, may be simultaneously responsible for wear of glass-ionomer restoratives (Mair *et al.*, 1996; Maeda *et al.*, 1999). According to McKinney *et al.* (1987), the wear patterns of GIC restoratives in occlusal contact area (OCA) and contact free area (CFA) were the same. He highlighted the importance of the chemical environment in the degradation process of glass-ionomer restoratives. In most cases, the functional glass-ionomer restoratives were maintained *in situ* while dissolution was observed which may lead to a shorter duration of restorations (Van Dijken, 1994; Van Dijken *et al.*, 1999; Abadalla *et al.*, 1997; Gao *et al.*, 2003). The early GICs had poor resistance to chemical degradation. This property was improved in newer glass-ionomer materials developed later.

For glass-ionomer restoratives, color changes and discoloration are minor problem and the development of secondary caries is negligible. Hu *et al.* (2002) observed patients after radiation therapy for two years and found no secondary caries around GICs restoratives, even when glass-ionomer restoratives were lost. Compared with composite resins and amalgam, GICs significantly reduced recurrent caries in xerostomic patients without taking topical fluoride supplementation (McComb *et al.*, 2002; Haveman *et al.*, 2003; Wood *et al.*, 1993). Although Mjör (1996) reported recurrent caries as the main cause for replacement of glass-ionomer restoratives, a possible reason is that GICs are usually placed in high caries risk patients in which other dental materials may have worse performance. Burke *et al.* (2001) analyzed

patient factor related to failure of restorations. He highlighted that GIC had the least secondary caries among different dental materials and more patients provided with glass-ionomers had poor oral hygiene and higher caries susceptibility. In a systematic review paper, Randall and Wilson (1999) concluded that although GICs had positive effects against secondary caries for some patients, the evidence that GIC was associated with prevention of secondary caries was not strong. More well designed and controlled clinical trials are warranted.

1.2 Recent studies on chemical environment and GICs *in vitro*

Thus far, specific patient factors influencing the *in vivo* performance of GICs among individual patients are still not clear. As the chemical environment is an important one, *in vitro* studies have been carried out to evaluate chemical degradation of glass-ionomers.

The intra-oral chemical environment is very complex. Inorganic and organic substances in the chemical environment come from saliva, plaque, gingival fluids, preventive agents, foods and beverages, *etc*. The quality and quantity of environmental chemicals *in vivo* vary from time to time and among individuals (Edgar, 1992). This topic will be reviewed in greater detail in chapter 2.2.

Being a salt-based material with abundant inorganic ions, GICs are hydrophilic and more sensitive to an acidic and ionic chemical environment. Many *in vitro* studies had demonstrated the evidence of acid dissolution of GICs (Fukazawa *et al*., 1990;

Nomoto and McCabe, 2001). In a recent study, it was found that storage in saliva significantly improved surface hardness of GICs, which might be related to calcium and phosphate present in saliva (Okada *et al.*, 2001). This indicates that some "positive" factors in the intra-oral chemical environment may improve mechanical properties of GICs, and thus may extend longevity of glass-ionomers restoratives *in vivo*. A review of the interaction between chemical environment and GICs is included in chapter 2.3.

By now, few studies have systematically investigated the factors with the most potential "positive" effects, calcium and phosphate (the abundant inorganic ions *in vivo*), on glass-ionomer restoratives. Knowledge of how we can improve the clinical performance of glass-ionomer restoratives will give a new insight and provide additional guidance to their clinical use as well as facilitate the development of new materials.

Chapter 2

Literature Review

The two fundamental components of GICs are aluminosilicate glass and polyelectrolytes. GICs set *via* an acid-base interaction between polycarboxylic acids and basic silicate glass particles. Although this reaction may last over a period of weeks or even months, GICs gain most properties during the first 24 hours after initial hardening. After mixing polycarboxlic acids with basic glass powder, acidic protons of polyacids attack glass particles, metal cations are then released and attached to polycarboxylic anions forming salt bridge, which leads to cross-linking of polymer chains. With increasing inter- and intra-molecular bridging points, the matrix moves from a gel structure to a solid one (Maeda *et al.*, 1999). Aluminum polyacrylates, which are stiffer and more insoluble than calcium polyacrylates, can slowly displace calcium polysalts in matrices (Wasson and Nicholson, 1993), then continue the development of physical properties of GICs after initial setting (Pearson and Atkinson, 1991; Mitra and Kedrowski, 1994). An inorganic network of pure silicate or mixed silicate/phosphate also forms with time and corresponds to the post-hardening process (Wasson and Nicholson, 1991; Wilson, 1996).

Set GIC can be regarded as a composite of polysalt matrices penetrated by silicate/phosphate inorganic network and unreacted glass particles sheathed by siliceous gel (Figure 2-1).

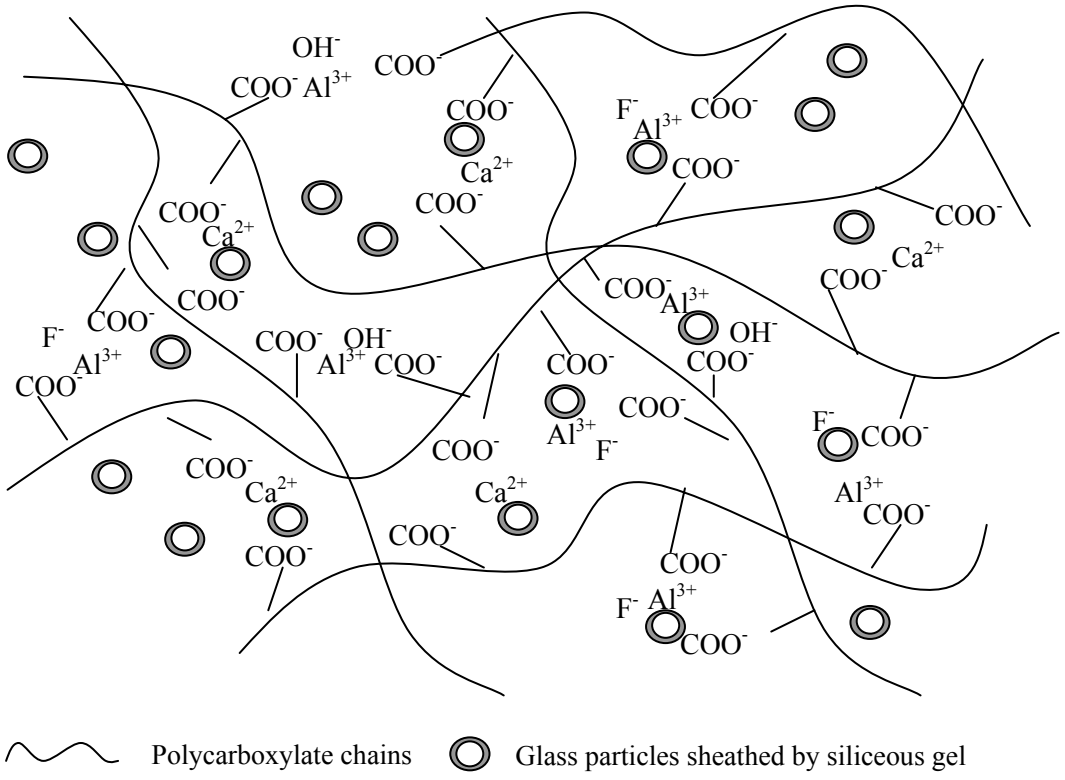

Figure 2-1 Diagram of set GIC structure

Being a water-based material, the components of GIC may react with the intra-oral aqueous environment. In the hydrogel matrices cross-linked by ionic bridges, cement-forming and non-cement-forming ions, such as aluminum, strontium/calcium, silicon, phosphorus, fluorine and sodium, together with aqueous hydrogen and hydroxide ions, can be mobile (Okada *et al.*, 2001). The potential ion-exchange ability enables GICs bio-interaction with oral environment and tooth (Yoshida *et al.*, 2000), as well as prevention of caries of adjacent tooth (Forsten, 1991).

2.1 Development of GICs

One of the main limitations of GICs is the lack of physico-mechanical properties. This limits the use of GICs to deciduous teeth and non-stress bearing areas of permanent teeth. Several approaches have been employed to improve the physico-mechanical properties of GICs. They include modification of the glass and polyelectrolyte components, and inclusion of resins.

2.1.1 Modification of the glass

a. Composition

The original glass employed was calcium fluoroaluminosilicate glass with the formula SiO_2-Al_2O_3-CaF_2-$AlPO_4$-Na_3AlF_6. Silica and alumina form the skeletal structure of glass (Figure 2-2).

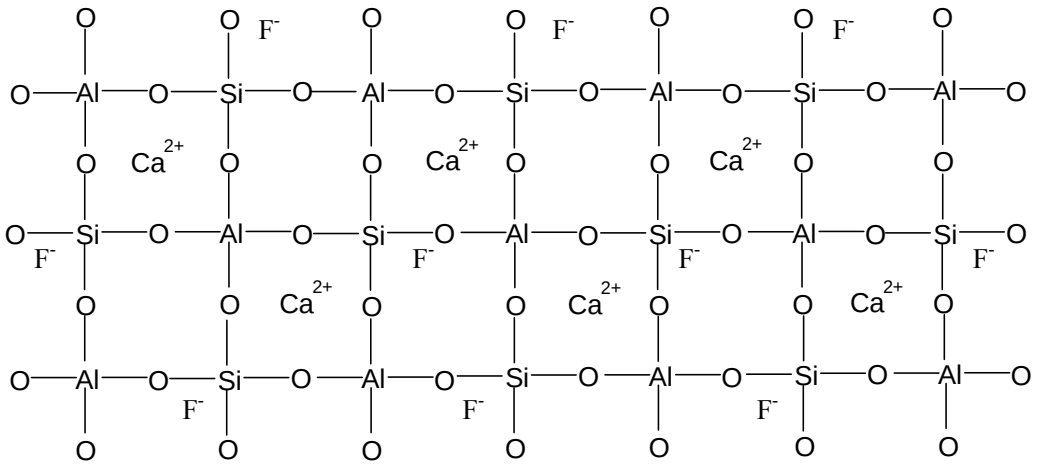

Figure 2-2 Skeletal structure of calcium fluoroaluminosilicate glass

(Modified according to Saito *et al.*, 1999)

Replacement of silica with alumina makes the glass network ionic and vulnerable to reaction with acids. CaF_2 or Na_3AlF_6 is used as flux in manufacturing process to decrease melting temperature. Higher concentration of silica relates the glass to transparency while alumina and calcium fluoride are responsible for the opacity of the glass. For optimum setting time, opacity and compressive strength, a ratio for SiO_2:Al_2O_3 of about 2:1 is recommended (Wilson and McLean, 1988a). The variation of metal oxide ratio in calcium fluoroaluminosilicate glass is important for improving handling properties and decreasing early water sensitivity of set GICs (Wilson and McLean, 1988a). In commercial products, the composition ratio of silica, alumina, fluorine and calcium varies according to manufacturers.

During the glass manufacturing process, phase separation causes formation of droplets with calcium-rich surface. Calcium is thus preferentially leached out and activates the setting process by forming calcium polycarboxylates. Minimization of the calcium-rich surface of the glass increases working time and decreases water sensitivity (Schmitt *et al.*, 1983). Strontium, barium or lanthanum has been used to replace calcium in the glass to improve radio-opacity (Smith, 1998). Due to the similarity between calcium and strontium, calcium can be substituted by strontium totally or partially without disrupting the glass structure. Darling and Hill (1994) reported a hydrolytically stable zinc silicate glass of short setting time and high compressive strength. In this glass system, the setting reaction was influenced by network connectivity of the glass and not by aluminum to silicon ratio.

Bioactive glass (SiO_2-Na_2O-CaO-P_2O_5) has been attempted to be blended with traditional glass particles to improve mineralization ability. The mixed glass, however, compromised mechanical properties (Yli-Urpo *et al.*, 2005a, b). To increase strength, glass fibers or amalgam alloy powder have also been added and silver was sintered to glass particles. These reinforced materials exhibited increased flexural strength, but wear resistance and fracture toughness were poor (Wilson and McLean, 1988a). Gu *et al.* (2005) investigated incorporation of hydroxyapatite/zirconia particles of nano-size into glass powder and reported superior mechanical properties of the modified GIC.

b. Particle size

The particle size and size distribution of the glass powder are also important for setting, handling and mechanical properties of GICs.

Originally, glass particles with a maximum size of 50 μm were adopted for restorative glass-ionomers. Following modifications to decreased acid reactivity of the glass, particle size of the glass was also decreased. Fast-set and condensable GICs contain glass particles in μm or nm scale. Examples include KetacMolar Quick and Fuji IX Fast (Guggenberger *et al.*, 1998; Yap *et al.*, 2003a). Theoretically, finer glass particles have greater surface and faster setting reaction. They may, however, lead to lower bulk density and powder to liquid ratio, and result in decreased strength (Gu *et al.*, 2004).

In terms of particle size distribution of the glass powder, Prentice *et al.* (2005) found that increasing the proportion of smaller particles (3.34 μm) resulted in higher

strengths, while increasing the proportion of larger particles (9.60 μm) led to decreased viscosity of the unset cement. Gu *et al.* (2004) also reported GICs had lower strength when fine glass particles (< 5 μm) were absent. Mitsuhashi *et al.* (2003) found that the incorporation of more fine glass particles decreased fracture toughness of GICs. He recommended particle size of up to 10 μm for glass powder to maintain smooth surfaces and high fracture toughness.

More investigations on optimisation of glass composition, particle size and size distribution are warranted to achieve operator-friendly handling characteristics and greater strength of GICs.

2.1.2 Modification of the polyelectrolyte

When polyacrylic acid is used solely in glass-ionomers, the cement takes a long time to set and the liquid gels in a short time. To overcome gelation of the low molecular weight polyacrylic acid, copolymers of acrylic acid and di- or tri-carboxylic acids were introduced. The most frequently used polyacids are derived from polyacrylic acids or copolymers of acrylic-itaconic acids [poly(AA-*co*-IA)], acrylic-maleic acids [poly(AA-*co*-MA)], and acrylic-methacrylic acids (Figure 2-3) (Culbertson, 2001).

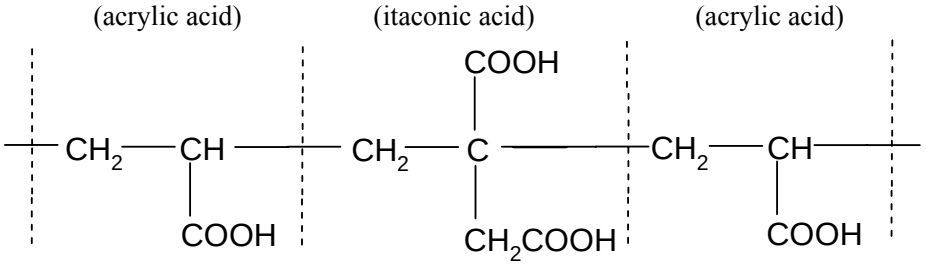

Copolymer of acrylic and itaconic acids

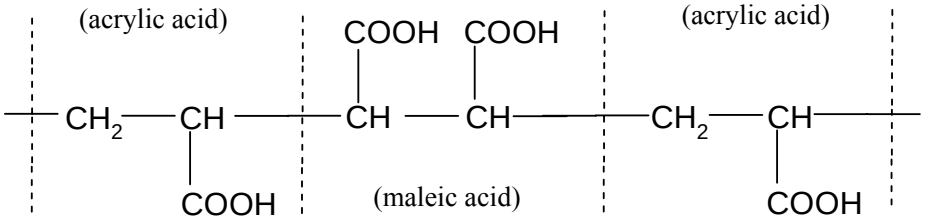

Copolymer of acrylic and maleic acids

Figure 2-3 Major acids used in GICs (From Hosoda, 1993)

These copolymers have more reactivity due to increased carboxyl groups per unit. In addition, incorporation of tartaric acid in polyacid system significantly improves the handling property and increases setting reaction rate (Culbertson, 2001).

Increasing concentration and/or molecular weight of polymeric acids improve physical properties of GICs. Handling properties are, however, compromised (Wilson *et al.*, 1989). Optimizing the molecular weight and concentration ratio of polyacids can minimize viscosity of polyacids but only to a certain extent. There are two optimal ways to increase mechanical properties of GICs without sacrificing handling characteristics. One is adopting a higher powder to liquid ratio; another is adding the polyacids in dried form to glass powder yielding a water-hardening cement (McLean *et al.*, 1984).

Changing the type of polyelectolyte has also been accepted. Poly(vinylphosphonic acid) (PVA) was used in experimental GIC. However, the PVA and its copolymers reacted too actively with glass particles and were not feasible (Braybook and Nicholson, 1993). To improve the rigid matrix of polyacrylic acid and copolymers, new monomers have been used to modify or copolymerize with acrylic acid functioning as a spacer. In these modified polyelectolytes, carboxylic acid group is attached to the backbone *via* a long flexible chain and is more free and less sterically hindered. The most widely investigated are amino acid containing monomer (Culbertson *et al.*, 1999) and *N*-vinylpyrrolidone (NVP) (Xie *et al.*, 1998a, b, c). Polyelectrolytes based on these modifications gain some mechanical properties and may improve performance of GICs.

2.1.3 Inclusion of resins

New generation hybrid glass-ionomers has been designed to achieve improved handling and esthetic characteristics. This type of material, known as resin modified GICs (RMGICs), has two mechanisms of curing. They include an acid-base reaction and an activated free-radical polymerization forming a matrix network of polycarboxylates and polymers (McCabe, 1998). Commonly, the light-initiated cure of this material is accomplished by copolymerization of methacrylate group. The unsaturated methacrylate group can be incorporated by tether to polyacids *via* monomers, such as 2-hydroxyethyl methacrylate (HEMA), glycidyl methacrylate, and

2-isocyanatoethyl methacrylate (IEM) (Figure 2-4). The polymerizable monomer HEMA is hydrophilic and is linked to polyacids by hydrogen bonding. Glycidyl methacrylate and IEM are grafted to the polyacids *via* reaction with the pendent carboxylic acid of the backbone (Culbertson *et al.*, 2001).

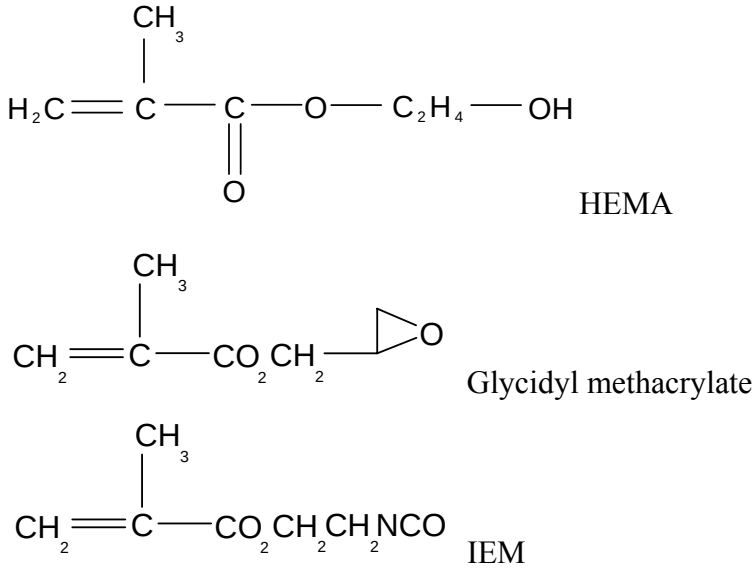

Figure 2-4 Structure of monomers tethered to polyacids

Other approaches to the hybrid cements are the development of polymerizable polyalkenoic acid functionalized monomer, which achieves polyacid structure in situ and is ready to react with basic glass. The structure of some commercial monomers is listed in Figure 2-5. However, these modified polyacids are usually hydrophobic and combined with monomers in commercial products. The hybrid material, namely compomer, is hardened *via* free-radical polymerization. The acid-base reaction occurs only after material hardening and absorption of water. These materials do not cure in the dark and are not true GICs.

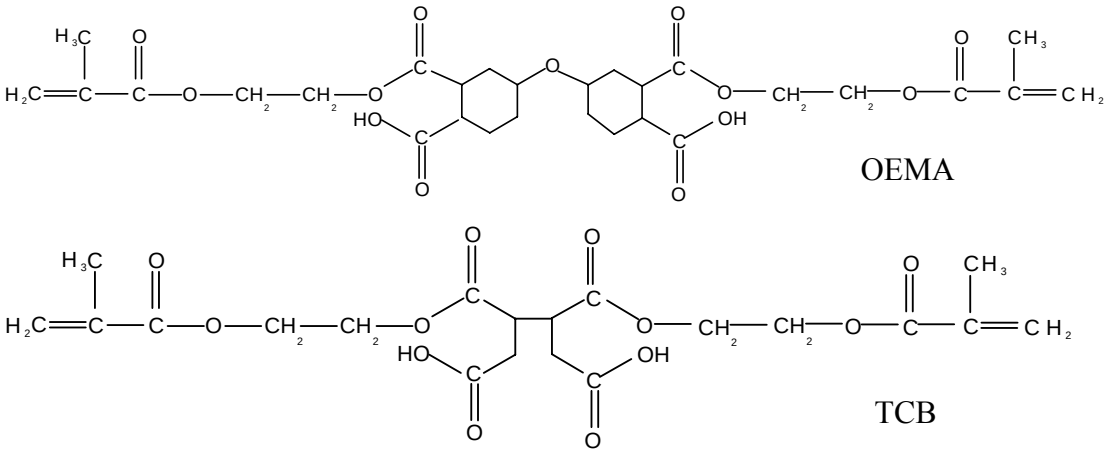

Figure 2-5 Structure of monomers present in hybrid cement system

(From Hammersfahr, 1994)

RMGICs have less moisture sensitivity than conventional GICs. The command light-cured mode of RMGICs also meets the requirements of clinician satisfyingly. Advantages of fluoride release and chemical bond to teeth are preserved for RMGICs (Forsten, 1994; McLean, 1996). However, the intrinsically hydrophilic characteristic causes RMGICs to have lower mechanical strength than composite resins and even some chemical-cured GICs.

Progressing from the original glass-ionomers, modern chemical and light-cured GICs have achieved improved physical/mechanical properties and handling characteristic, as well as aesthetic appearance (Guggenberger *et al.*, 1998; McCabe, 1998). Modern GICs have made important and significant impact on restorative and preventive dentistry and have been accepted widely in the dental community.

2.2 Complex chemical environment *in vivo*

The intra-oral chemical environment is very complex. The main constituents are saliva and metabolite of plaque. Together with preventive agents, foods and beverages dosed at intervals also contribute to the chemical environment. The ionic components in plaque are close to those in saliva with the exception of pH, which is near neutral in saliva. Most soft drinks with carbohydrates are of low pH values of 2.48 ~ 3.20 (Larsen and Nyvad, 1999) and the carbohydrates intake may quickly decrease plaque pH to about 4.0 (Muhlemann *et al.*, 1977). Depending on the intended use, preventive agents will contain different chemical substances. In view of the aforementioned, it is not surprising that the intra-oral chemical environment is varied among individuals and also inconsistent within the same individual over time.

Water is the predominant component of saliva and plaque fluid, as well as the chemical environment. Solutes in the chemical environment can be simply classified into inorganic and organic components. The organic component involves numerous proteins and the inorganic component mainly consists of sodium, potassium, calcium, phosphate, chloride and carbonate, in addition to other trace ions. These components maintain physiological functions of oral cavity, for instance, facilitating digestion of starch, lubrication of oral surfaces, dilution of substance introduced to the mouth and neutralization/buffering of acids (Edgar, 1992). With regards to caries prevention, calcium and phosphate in saliva are critical for remineralization of decayed tooth structure. The inorganic constituents of saliva and plaque fluid are briefly summarized

in Table 2-1. The wide variation of the inorganic component concentration indicates large variations between individuals and even within an individual at various time. The organic components will not be reviewed at length, since they are beyond the scope of current research.

Table 2-1 Concentration of selected inorganic constituents of whole saliva and plaque fluid

	Whole saliva*	**Rested and starved plaque fluid***
pH	5.0 ~ 8.0	5.69 ~ 7.08
Bicarbonate	0 ~ 40 mg/100ml	------
Sodium	0 ~ 80 mg/100ml	8.9 ~ 38.9 mM
Potassium	60 ~ 100 mg/100ml	41.0 ~ 85.1 mM
Calcium	2 ~ 11 mg/100ml	1.2 ~ 12.0 mM
Phosphorus (inorganic)	6 ~ 71 mg/100ml	10.1 ~ 54.5 mM
Chloride	50 ~ 100 mg/100ml	22.2 ~ 42.8 mM
Fluoride	0.01 ~ 0.04 ppm	0.002 ~ 0.029 mM

*The saliva data are from Edgar (1992) and plaque fluid data are from Margolis and Moreno (1994).

The following factors should be considered with regards to the variation of the intra-oral environment.

2.2.1 Biological variation

The compositions of unstimulated and stimulated saliva as well as saliva from various glands are different. It has been demonstrated that calcium concentration is higher in submandibular saliva and phosphorus is higher in unstimulated saliva (Suddick *et al.*, 1980).

In addition, the circadian rhythm of an individual influences both flow rate and composition of saliva (Humphrey and Williamson, 2001). Circadian low flow normally takes place during sleep while peak flow happens during simulation period, e.g. chewing or acidic taste stimuli. Salivary electrolytes and proteins also vary according to the rhythm, e.g. low levels of calcium and phosphate in the early morning (Edgar, 1992). When saliva flow increases to peak value, salivary pH accordingly increases and cation level remains constant. For anions, carbonate and chloride increase with the peaked saliva flow, while phosphorus decreases (Ferguson and Botchway, 1980).

With regards to gender and age, Dodds *et al.* (2005) reported that salivary secretion declined with increasing age and females had lower flow rate than males.

2.2.2 Diet

Both diet component and diet behavior have significant effects on the chemical environment. During and after food consumption, intra-oral pH value may be lowered. The duration of pH drop depends on consumption frequency, salivary buffering,

clearance and flow rate (Bibby *et al.*, 1986).

The frequent consumption of acidic foods and drinks has been shown to soften dental hard tissues and contribute to erosion and abrasion of teeth (Lussi *et al.*, 1995, 1997). The pH, phosphate, calcium and fluoride content of some beverage and foods are shown in Table 2-2.

Table 2-2 The pH and selected inorganic content in different beverage and foodstuffs*

	pH	Phosphate (mM)	Calcium (mM)	Fluoride (ppm)
Coca Cola	2.6	5.43	0.84	0.13
Fanta orange	2.9	0.12	0.75	0.05
Sprite light	2.9	0.00	0.26	0.06
Ice tea	3.0	0.08	0.56	0.83
Pepsi light	3.1	3.94	0.90	0.04
Grapefruit juice fresh squeezed	3.1	0.23	3.50	0.08
Grapefruit juice	3.2	2.58	3.14	0.16
Vinegar	3.2	2.18	3.40	1.20
Apple juice	3.4	1.74	4.03	0.11
Red wine	3.4	3.25	1.90	0.16
Red Bull	3.4	<0.01	1.70	0.36
Kiwi juice fresh squeezed	3.6	5.30	4.15	0.06
Salad dressing	3.6	1.64	0.28	0.14
White wine	3.7	3.16	0.91	0.35
Orange juice	3.7	5.54	2.20	0.03
Yoghurt kiwi	4.1	34.0	42.5	0.06
Yoghurt orange	4.2	43.0	31.6	0.05
Carrot juice	4.2	8.35	5.00	0.09
Carlsberg beer	4.4	7.33	2.23	0.28
Milk	6.7	18.9	29.5	0.01

*Data from Lussi *et al.* (2004)

2.2.3 Other Factors

Certain medications, Sjögren's syndrome and radiation therapy may result in salivary hypofunction. Saliva flow is dramatically decreased and the oral chemical environment is significantly changed, thus increasing the caries risk of patients (Lacatusu *et al.*, 1996). Some patients may recover and have normal saliva secretion while in others the condition is irreversible due to permanent damage of salivary glands.

In these cases, the saliva is more viscous with decreased buffering capacity. Some studies reported increased salivary concentrations of protein and inorganic ions, such as sodium, calcium, magnesium and chloride, due to lower flow rate and condensed saliva (Schwarz *et al.*, 1999). On the contrary, reduced protein secretion rate was shown in some patients (Pedersen *et al.*, 2005). For these patients, saliva pH is low and *Streptococcus mutans* and *Lactobacillus* species carriage are high (Schwarz *et al.*, 1999).

As can be seen, the intra-oral chemical environment is very varied. This may account for the different performance of glass-ionomer restoratives in clinical studies. These variations should be considered for proper evaluation of glass-ionomer restoratives *in vivo*.

2.3 Interaction between chemical environment and GICs

Understanding the interaction between dental materials and their intra-oral environment will provide useful knowledge for the enhancement of materials and clinical processes. As *in vivo* trial is usually long-term and costly, numerous *in vitro* studies have been carried out to evaluate and compare dental materials. Commonly, one or more parameters of the oral environment are mimicked in *in vitro* studies. Results from *in vitro* studies must, however, be properly interpreted and conclusions should be cautiously drawn when translating to clinical applications.

2.3.1 Saliva

Saliva is the primary constituente of intra-oral chemical environment. As natural saliva is varied/unstable and more than 90% of saliva is water, most *in vitro* studies use water as the storage medium for evaluating dental materials. In International Organization for Standardization (ISO) standards for GICs, distilled water is recommended (ISO 9917, 1991). Nicholson *et al.* (2001) reported that GICs behaved differently in ionic and acidic solutions compared to water. Many recipes for artificial saliva have been developed to try making *in vitro* study closer to real intra-oral conditions (Leung and Darvell, 1997). The ideal artificial saliva should be the exact replication of natural saliva, however, this is impossible due to the inconsistency of natural saliva.

Table 2-3 *In vitro* studies on artificial saliva and GICs

Authors	Artificial saliva composition	Results
Hayacibara *et al.* (2004)	Ca 1.5mM, PO_4 0.9mM, KCl 150mM, Tris buffer 20mM, NaN_3 0.02%, pH 7.0	KetacFil, Vitremer and Fuji Ortho LC had less F^- release in artificial saliva compared with those in distilled water. The concentration of Al^{3+} was below the limitation of analysis method.
Williams *et al.* (1997)	NaCl 0.4g/l, KCl 0.4g/l, $CaCl_2$ 0.6g/l, Na_2HPO_4 0.6g/l, $CO(NH_2)_2$ 1.0g/l, Mucin 4.0g/l, $Mg_2P_2O_7$ 0.0016g/l, Na_2S 0.0016g/l	Compared with deionized water, artificial saliva reduced ion release (F^-) from MiracleMix, ChelonSilver, KetacSilver, OpusSilver and OpusFil.
Karantakis *et al.* (2000)	$CaCl_2$ 1mM, NaH_2PO_4•$2H_2O$ 1mM, NaCl 35mM, CH_3COONa•$3H_2O$ 15mM, pH 7	There was no significant difference in the amounts of fluoride release from Argion, Fuji II LC and Vitremer in water vs. artificial saliva.
Levallois *et al.* (1998)	NaCl 125.64mg/l, KCl 963.90 mg/l, KSCN 189.20mg/l, KH_2PO_4 654.50mg/l, $CO(NH_2)_2$ 200.00mg/l, $CaCl_2$•$2H_2O$ 227,80mg/l, Na_2SO_4•$10H_2O$ 763.20mg/l, NH_4Cl 178.00mg/l, $NaHCO_3$ 630.80mg/l, pH 5.1	Fuji II LC and Vitremer released significantly more fluoride in water than in artificial saliva.
Hattab and Amin (2001)	NaCl 0.400g/l, KCl 0.004g/l, $CaCl_2$•$2H_2O$ 0.445g/l, NaH_2PO_4•$2H_2O$ 0.78g/l, Na_2S•xH_2O (x=7-9) 0.005g/l, urea 1.0g/l, pH 5.5	For KetacFil, Fuji II and KetacSilver, the release of F^- in artificial saliva was significantly less than in deionized water.
el Mallakh and Sarkar (1990)	NaCl 0.4g/l, KCl 0.4g/l, $CaCl_2$•H_2O 0.795g/l, Na_2HPO_4•H_2O 0.69g/l, Na_2S•$9H_2O$ 0.005g/l, pH 5.525	Ketac-Fil, Ketac-Silver, Fuji-II and Miracle Mix released more fluoride in de-ionized water than in artificial saliva.
Turssi *et al.* (2002,2003)	Ca 1.5mM, PO_4 0.9mM, KCl 150mM, Tris buffer 0.1mM, pH 7.0	Fuji II LC and Fuji II Improved showed similar surface roughness and morphology in artificial saliva as those in distilled water.
Yip *et al.* (2004)	Acetate buffer 0.05M, $CaHPO_4$ 2.2mM, pH 5.0	Fuji IX Fast and KetacMolar showed an increase in surface roughness after stored in artificial saliva (3weeks).
Mckenzie *et al.* (2003b)	NaCl 0.50g/l, $NaCO_3$ 4.20g/l, $NaNO_2$ 0.03g/l, KCl 0.20g/l	Storage in artificial saliva gave ChemiFil Superior, ChemFlex, Fuji II LC and Vitremer of lower surface hardness than in natural saliva and water.
Mojon *et al.* (1996)	Mucin 40g/l, NaCl 0.85g/l, KCl 1.2g/l, $MgCl_2$•$6H_2O$ 0.05g/l, $CaCl_2$•$6H_2O$ 0.15g/l, K_2HPO_4 0.35g/l, NaF 0.0042g/l, Sorbitol 30g/l, CKNS 0.1g/l, pH 6.7	Water had a greater softening effect than artificial or natural saliva on Fuji I, while the difference between water and natural saliva was not significant.
Kanchanavasita *et al.* (1998a,b)	K_2HPO_4 0.200g/l, $Ca_3(PO_4)_2$ 0.300g/l, KSCN 0.330g/l, $NaHCO_3$ 1.500g/l, NaCl 0.700g/l, KCl 1.200g/l, $(NH_2)_2CO$ 0.130g/l, pH 6.7	Vitremer, Fuji II LC, Vitrebond and Fuji Lining LC stored in artificial saliva were relatively softer than those in water and showed a decrease in surface hardness with time. But similar flexural values were presented for these GICs in water and artificial saliva.
Musanje *et al.* (2001)	Na 28.16mM, K 25.74mM, NH_4 4.10mM, Cl 29.84mM, PO_4 4.67mM, SCN 2.24mM, Lac 0.78mM, Cit 0.95mM, Urate 0.11mM, Urea 3.30mM, CO_2 0.04g, pH 6	ChemFil showed a marked decrease in flexural strength and elastic modulus in artificial saliva compared with those in water vapor.

Most studies on GICs and artificial saliva have focused on fluoride release (Table 2-3). Previous studies have shown that GICs released less fluoride in artificial saliva than in water, regardless of glass-ionomer type and artificial saliva component (Hayacibara *et al.*, 2004; Hattab and Amin, 2001; Williams *et al.*, 1997; Levallois *et al.*, 1998; el Mallakh and Sarkar, 1990). These results suggest that GICs interact with components in saliva, of which calcium is the most probable. A CaF_2 layer may form on the surface of GICs (Levallois *et al.*, 1998).

A few studies have concentrated on effects of artificial saliva on physico-mechanical properties of glass-ionomers, which are equivocal (Table 2-3). Glass-ionomers presented rougher or unchanged surface morphology in artificial saliva (Turssi *et al.*, 2002, 2003; Yip *et al.*, 2004). Some researchers reported decreased surface hardness and flexural strength of GICs in artificial saliva compared to water (Kanchanavasita *et al.*, 1998a; Musanje *et al.*, 2001), while others demonstrated comparable strength of GICs in artificial saliva and in water (Kanchanavasita *et al.*, 1998b; Mojon, 1996). The different GICs and artificial saliva used may account for these varied results. However, studies on whether and how the special components in artificial saliva interact with GICs have not been addressed.

The studies investigating effects of natural saliva on GICs are very limited. In a recent study, Okada *et al.* (2001) reported that a glass-ionomer (Fuji IX) in natural saliva showed higher surface hardness than in water. He postulated that salivary calcium and phosphate might diffuse into GICs forming a thin layer of calcium

phosphate, aluminum phosphate and polyacrylate salts. However, in a previous study, the surface hardness of a luting GIC was found to be similar whether in natural saliva or in water (Mojon *et al.*, 1996). McKenzie *et al.* (2003a) also commented that natural saliva had no more effect than water on surface hardness of both conventional and resin-modified GICs. In a further study, he reported that compressive and biaxial strength of GICs were also not affected by natural saliva (McKenzie *et al.* 2003b). It should be noted that the natural saliva and its pH were not characterized and different glass-ionomer products were evaluated in these studies.

In summary, it can be concluded that GICs may interact with saliva depending on material type. However, the interactive factors in intra-oral environment, whether positive or negative, are not specified and require investigations.

2.3.2 Intra-oral pH

Although GIC is more stable than other dental cements, this salt-based material is still vulnerable to acid attack due to its composition. Clinical trials have shown dissolution of both conventional and resin-modified GICs (Van Dijken, 1994; Van Dijken *et al.*, 1999; Abadalla *et al.*, 1997; Gao *et al.*, 2003). *In vivo* studies have reported that the dissolution of GIC is not related to salivary buffing capacity or saliva pH. Pluim and Arends (1987) postulated that the dissolution of GIC *in vivo* may be caused by acids from dental plaque and/or food and beverage. In an *in vitro* study, Mesu and Reedijk (1983) have found that *in vitro* acid erosion testing closely predicts

the clinical durability of GICs. A standard acid erosion test is recommended by ISO (ISO 9917, 2003).

Many *in vitro* studies have investigated effects of environmental pH on GICs. Walls *et al.* (1988) exposed GICs to pH 4 ~ pH 10 conditions and found that they had good resistance to erosion at pH 6 and higher, but were prone to erosion at pH 4. The greater erosion of GICs in lower pH solutions was confirmed by Fukazawa *et al.* (1987) and Eisenburger *et al.* (2003). They put forward that dissolution of GICs was mainly influenced by the concentration of H^+ ion at the cement surface. Nomoto and McCabe (2001) found that GIC specimens exposed to acidic buffered solutions had higher erosion depth than in pure acids of the same pH. This phenomenon may be explained by the fact that the pH remained stable in buffered solutions.

Fukazawa *et al.* (1990) reported that erosion of GICs was also acid anion dependent. GICs immersed in citric acid degraded faster and more severely than those in lactic and acetic acids due to different chelating ability of acid anions. In a recent study, McKenzie *et al.* (2003a) reported that GIC performed better in Coca-Cola than in orange and apple juice. In the latter media, GIC specimens were dissolved after 6 months. He pointed out that Cola contains phosphoric while the fruit juices contain some carboxylic acids.

Dissolution of GIC is also material dependent. Fukazawa *et al.* (1987) reported that the matrix structure of GIC influenced the diffusion process of acid. GICs based on maleic acid copolymers are less resistant to acid attack than those based on acrylic

acid copolymers (Setchell *et al.*, 1985; Wilson *et al.*, 1986).

The exact mechanism of acid erosion of GIC is still not very clear. Acids can disrupt ionic bonds which are abundant in GIC matrix. When the number of broken salt bridge reaches a threshold level, the matrix may be decomposed. Using Scanning Electron Microscopy (SEM), Roulet and Walti (1984) observed the dissolution of polyacrylate matrices with extruding filler particles left. Fano's study with confocal laser microscopy showed that acid erosion (pH 3.5) affected not only the matrix but also the gel layer circling glass particles (Fano *et al.*, 2001).

On the other hand, Nicholson *et al.* (1999) assumed that both conventional GICs and RMGICs showed the ability to neutralize surrounding acidic solutions. The surface area of set GIC is critical to adjustment of surrounding pH (Patel *et al.*, 2000). This fact may be linked to calcium polyacrylate and unreacted polyacids in set GIC, which may act as chemical buffer and alter environmental pH.

Although both environmental pH and salivary inorganic ions play important roles in the clinical performance of GICs *in vivo*, there are few studies investigating the concurrent effects of environmental pH and salivary inorganic ions in this process.

2.3.3 Other factors

a. Professional topical fluoride agents

Caries prevalence in many countries has declined remarkably due to the cariostatic effect of fluoride (Brunelle and Carlos, 1990; Karlsbeek and Verrips, 1990).

Fluoride agents are usually used in preventive programs for high caries risk patients. These fluoride agents are commonly manufactured in gel, solution or varnish forms. Fluoride is incorporated as acidulated phosphate fluoride (APF), stannous fluoride and sodium fluoride of different concentration (Stephen, 1994).

el-Badrawy *et al.* (1993) compared effects of different fluoride gels on conventional GICs and found APF (pH 5) and sodium fluoride containing citric acid (pH 5.8) significantly affected both matrices and particles of GIC, while neutral sodium fluoride had no such effect. He highlighted that both the pH and the acid used in fluoride agents contributed to this degradation of GICs. RMGICs also exhibited the same trends when exposed to APF. The degradation was, however, lesser in extent (Triana *et al.*, 1994; el-Badrawy and McComb, 1998).

Billington *et al.* (1987) found that exposure to 2% neutral NaF solution reduced hardness of GICs. This phenomenon was explored further by Hadley *et al.* (2000). They discovered that GICs containing fluoride, whether intrinsic or admixed, showed more surface disintegration in NaF solution than those without fluoride. It was hypothesized that NaF breaks Al-based salt bridge by F^- reaction with AlF^{2+} crosslinks in Al-polycarboxylate matrix.

b. Bleaching agents

Bleaching for now is very popular in the practice of esthetic dentistry. Due to their ability at oxidization, hydrogen peroxide and peroxide releasing agents (carbamide peroxide and sodium perborate) are generally the main components of

bleaching agents. The concentration of oxidizing agents is lower in home-used products (10~16% carbamide peroxide) than in in-office items (30~35% hydrogen or carbamide peroxide) (Attin *et al.*, 2004).

There are limited studies investigating the effect of bleaching agents on GICs. Yap and Wattanapayungkul (2002) demonstrated that application of 35% carbamide peroxide and hydrogen peroxide did not affect surface hardness of GICs. Mair and Joiner (2004) added 6% hydrogen peroxide to a phosphate buffer of pH 5.5 and found this bleaching gel had no effects on GICs compared with those in water and phosphate buffer. However, Jefferson *et al.* (1992) reported that 10% carbamide peroxide at pH 4.5 decreased surface content of aluminum and may cause matrix decomposition in GICs. It seems that the pH of bleaching agents is more critical than the oxidizer in the interaction between bleaching agents and glass-ionomers.

As fore mentioned, GICs being hydrophilic and salt-based, are susceptible to degradation by the intra-oral chemical environment. Although GICs are vulnerable to acids, some components e.g. calcium and phosphate in the oral environment may have positive effects on GICs. Little information is currently available on the co-effects of environmental pH and inorganic constituents of saliva on GICs. This new knowledge will lead to better understanding of the clinical performance of glass-ionomer restoratives, provide guidance to their clinical use and facilitate development of new materials.

2.4 Strategies and methods for characterizing GICs

A wide range of surface analytical techniques have been used to characterize glass-ionomers and their interactions with the chemical environment. These include scanning electron microscopy (SEM), laser scanning confocal microscopy (LSCM), atomic force microscopy (AFM), surface profiler, nano-indentation testing, acoustic microscopy, solid state nuclear magnetic resonance spectroscopy (NMR), Raman spectroscopy (RM), Fourier transform infrared spectroscopy (FTIR), secondary ion mass spectrometry (SIMS), X-ray photoelectron spectroscopy (XPS), electron probe microanalysis (EPMA) and energy dispersive X-ray analysis (EDS) amongst others (el-Badrawy *et al*., 1993; Fano *et al*., 2001; Denisova *et al*., 2004; Wilder *et al*., 2000; Mohamed-Tahir and Yap, 2004; Towler *et al*., 2001; Lloyd *et al*., 1999; Young *et al*., 2000, 2004; Jones *et al*., 2003; Okada *et al*., 2001; Yli-Urpo *et al*., 2005b). These methods provide valuable information on the structural, chemical and physico-mechanical characteristics of GICs. Each technique, however, has its advantages and limitations. To truly understand a material and its interaction with the environment, the use of more than one method is required. The techniques commonly used for surface characterization of GICs are summarized in Table 2-4.

Despite their valuable functions, for some techniques, an ultra high vacuum environment and special sample preparation are required. Water-containing materials such as GICs may be damaged due to dehydration and cracking caused by the vacuum and sample preparation. The most surface analysis equipments are also very expensive, not readily available and require special training to operate.

Table 2-4 General information of the surface analytical techniques used for GICs

Technique	Application	Principle	Depth Resolution	Special Requirement
SEM/EDS	Topographical imaging and elemental microanalysis (not for light element)	An electron beam bombards the sample and creates various signals such as secondary and backscattered electrons. These signals are collected and displayed on the cathode ray tube thus forming an image. The energy and intensity distribution of X-ray signals are measured by energy dispersive spectroscopy for determination of elemental composition.	sub μm	Vacuum and conductive sample
FTIR-ATR	Qualitative and quantitative analysis of chemical bond information	The infrared spectrum is obtained by a measurement of the intensity of a beam of infrared radiation before and after interaction with the sample.	2-3 μm	---
SIMS	Topographical mapping; Qualitative and quantitative analysis of element and chemical bond information; Depth profiling	When an energetic beam of ions or neutrals bombards the sample, secondary electrons are ejected and detected by a mass spectrometer.	outer 1-2 monolayer	Vacuum
XPS	Qualitative and quantitative analysis of element and chemical bond information (not for trace element)	An monochromatic low-energy X-ray beam bombards the sample and causes emission of photoelectrons, which is used to identify the element.	3nm	Vacuum
EPMA	Qualitative and quantitative analysis of element information at ppm level	An electron beam bombards the sample and emits X-ray photons, which is recorded as WDS spectra and used to identify the element composition.	1μm	Vacuum

Table 2-4 (Continued)

Technique	Application	Principle	Depth resolution	Special Requirement
NMR	Qualitative and quantitative analysis of chemical bond information	In an external magnetic field, an energy transfer of a nucleus takes place at a wavelength that corresponds to radio frequencies. This transfer is measured and processed to yield an NMR spectrum for the nucleus concerned.	---	---
AFM	Topographical imaging at atomic resolution	An extreme sharp probe integrated on a tiny cantilever scans over a sample surface at a distance over which atomic forces act. The cantilever deflection caused by the forces is measured by a photo detector mapping the topography of the sample.	10nm	---
LSCM	Topographical imaging; Series optical imaging	A laser beam is focused in a fluorescent sample. The emitted fluorescent light is recollected by the objective lens and the reflected into a photo detection device forming an image.	0.5μm	Sample treated with fluorescent dyes
Micro-/Nano-indentation	To characterize hardness, elastic modulus and fracture toughness	An indenter tip with a known geometry is penetrated into the sample by applying a load. Through analysis the area of the indentation or the applied load and the corresponding penetration depth, hardness and/or elastic modulus is calculated. Fracture toughness is determined by directly measuring radial cracks as a function of indentation load.	---	---
Mechanical profiler	Surface roughness	A sharp stylus is drawn across the sample surface. The surface roughness is obtained by amplification and analysis of the deflection of the stylus.	0.5nm	---

(From Brundle *et al*., 1992; Watson, 1991; Chung *et al*., 2005; Li and Bhushan, 2002)

In this study, micro- and nano-indentation testing, SEM, EDS, FTIR-ATR, and surface profilometry were used to characterize GICs. These techniques are summarized in the following sections.

2.4.1 Indentation testing

Indentation testing is the most commonly used technique to determine mechanical properties of dental materials, since it is semi-destructive allowing repeatable measurements of the same specimen and easy to operate. According to the indentation load, macro-, micro- and nano-indentation testing are catalogued.

2.4.1.1 Micro-indentation testing

Micro-indentation testing has been widely used for mechanical characterization of dental materials. Generally, a load at micro level has been applied providing a sufficient penetration depth to determine the bulk mechanical properties of these materials (Okada *et al.*, 2001; Chung *et al.*, 2005).

In this study, a depth-sensing micro-indentation testing was used to examine mechanical properties (plasticity and elasticity) of GICs. This novel method has advantages of deriving hardness and elastic modulus values in a single test using small size specimens (Yap *et al.*, 2004). The detail of this method will be covered in Chapter 4.

2.4.1.2 Nano-indentation testing

Nano-indentation testing is able to determine hardness and elastic modulus precisely at nanometer penetration depth, thus, it is commonly used for mechanical characterization of microstructure. When equipped with a continuous stiffness measurement (CSM) technique, nano-indentation testing provides depth-profile of mechanical properties. In the CSM technique, in addition to the normal load on specimens, an oscillating force is simultaneously superimposed on the indenter causing in-phase and out-of-phase components of the displacement response. Thereby, an accurate determination of continuous contact stiffness along the loading curve is reached. With the continuous record of contact stiffness/load/displacement, hardness and elastic modulus of specimens are derived as a function of indenter penetration depth using the following equations (Li and Bhushan, 2002; Shen *et al.*, 2003).

$$H = \frac{P_{\max}}{A_{\max}} \tag{2-1}$$

$$E = \frac{\sqrt{\pi}}{2}\frac{1}{\sqrt{A_{\max}}}S\left(1-\nu^2\right) \tag{2-2}$$

where P_{max} is the maximum indentation load, A_{max} is the maximum projected contact area, S is contact stiffness and ν is Possion's ratio.

In addition, the relation between contact stiffness and indenter penetration depth can be used to study the uniformity of materials. It can be theoretically derived as follows:

From Eq. (2-2), one obtains

$$S = \frac{E}{1-\nu^2}\frac{2}{\sqrt{\pi}}\sqrt{A_{\max}} \quad (2\text{-}3)$$

The contact area for a perfect Berkovich indenter is given by

$$A_{\max} = 24.56h_p^2 \quad (2\text{-}4)$$

where, h_p is the true contact depth during indentation.

Substituting Eq. (2-4) to Eq. (2-3), stiffness can be derived as

$$S = \frac{E}{1-\nu^2}\frac{2}{\sqrt{\pi}}\sqrt{24.56}h_p \quad (2\text{-}5)$$

According to Eq. (2-5), for a uniform material with a constant elastic modulus (E), S is linearly proportional to h_p. While for a non-uniform material, E is not constant and changes with h_p, so the linear relationship between S and h_p does not exist.

By now, few studies have used nano-indentation testing for characterizing mechanical properties of GICs (Towler *et al*., 2001; Xu, 2003). The CSM technique has not been used to study changes in mechanical properties of GICs after exposure to various chemical environments. In this study, a nano-indentation testing equipped with CSM technique was used to mechanically characterize the surface of GICs after interaction with environmental calcium/phosphate and pH.

2.4.2 SEM/EDS

SEM is the main surface analytical method for studying the microstructure of GICs. Assisted by EDS x-ray microanalysis, SEM has been used to demonstrate the morphologic characteristics and compositions of conventional and modified GICs,

such as highly viscous GIC (HVGIC), fast set HVGIC, metal-reinforced GIC and bioglass/hydroxyapatite added GIC (Xie *et al*., 2000; Yap *et al*., 2003a; Sarkar, 1999; Yli-Urpo *et al*., 2005b; Arita *et al*., 2003). It has been used to determine the mechanism of OCA or CFA wear (Yap *et al*., 2001b; van Duinen *et al*., 2005; Momoi *et al*., 1997). Moreover, the effects of environment (water, acid and saliva, *etc*.), clinical treatment (finishing, surface coating, acid etching and periodontal scaling, *etc*.) and prophylaxis agents (fluoride agents and bleaching agents) on GICs have also been evaluated using SEM/EDS (Fukazawa *et al*., 1990; Smith, 1988; Barkmeier *et al*., 1992; el-Badrawy *et al*., 1993; Turker and Biskin, 2003).

Since GIC is water-based material, cracks have been observed on the surface of specimens with SEM due to the high vacuum and sample preparation requirement (Swift and Dogan, 1990; Yip *et al*., 2004). Modified SEM techniques, such as field emission SEM, environmental SEM and cyto-SEM were developed to overcome the problems of water-containing specimens (Tanumiharja *et al*., 2001; Turssi *et al*., 2002; Nomoto *et al*., 2003). However, the high costs of these instrumentations limit their availability.

2.4.3 FTIR-ATR

FTIR technique provides chemical bond information through analysis of an infrared radiation beam. Attenuated total reflectance (ATR) technique allows for sampling solid specimens. In ATR technique, an IR beam is directed into a crystal

with a high refractive index and creates an evanescent wave. The IR beam is changed after weak interaction with the sample and is detected by a spectrometer. The evanescent wave penetrates only a few micrometers into the sample, thus, the surface of solid samples can be analyzed by FTIR with ATR technique (Brundle *et al*., 1992). FTIR-ATR has been used to study the chemical composition and setting reaction of GICs (Young, *et al*., 2004; De Maeyer *et al*., 2002). The effect of artificial saliva on compositions of GICs was also interpreted using FTIR spectra (Yip and To, 2005).

In the FTIR spectra interpretation, the peak assignment to components in GICs is slightly different due to the varied compositions of GIC products and resonance effect. The peak assignment for GICs in different studies is summarized and listed in the following table (Table 2-5).

Table 2-5 FTIR peak assignment for GICs

Studies	Compound	Wavenumber (cm^{-1})	Assignment
Young (2002)	Mono- or divalent-PAA	1540	COO- (asym)
		1420	COO- (sym)
	Al-PAA	1600	COO- (asym)
		1460	COO- (sym)
	glass	940	Si-O stretch
Young *et al*. (2000)	Ca-PAA	1580	COO- (asym)
	Al-PAA	1620	COO- (asym)
De Maeyer *et al*. (2002)	glass	1000 ~ 1200	Si-O (asym)
Deb and Nicholson (1999)	Sr-PAA	1550	COO- (asym)
	Ca-PAA	1551	COO- (asym)
	Al-PAA	1614	COO- (asym)
Matsuya *et al*. (1996)	Hydrated silica gel	1050	Si-O-Si stretch
		950	Si-OH

*asym: asymmetric; sym: symmetric

2.4.4 Mechanical profiler

Profilometry is the most popular method used to measure surface topography of GICs. Among the stylus instruments used for measurement of surface roughness, mechanical profiler has advantages of better lateral resolution and a larger height measurement range (up to several micrometers) (Sherrington and Smith, 1988). Using a stylus based profilometer, many studies have examined the changes in surface roughness of GICs after different treatments, such as finishing/polishing, thermo-cycling, acid erosion, bleaching agents, *etc*. (Yap *et al*., 2002; Muraguchi *et al*., 2004; Mohamed-Tahir and Yap, 2004; Wattanapayungkul *et al*., 2004).

Thus, with the wide selection of techniques used for characterization of GICs, only the aforementioned techniques will be used for the surface characterization of GICs after interaction with environmental calcium/phosphate and pH in this study. Combining the structural information, elemental constitutes, chemical bond, mechanical properties and surface texture of the surface, the interaction occurring between GICs and environmental calcium/phosphate and pH will be explored.

Chapter 3

Research Objectives and Research Program

3.1 Aims

The overall aims of this research are:

1. To study the effects of environmental calcium/phosphate and pH on GICs in terms of
   (a) surface hardness and elastic modulus;
   (b) clinically related properties: strength, wear resistance and fluoride release.
2. To investigate surface physico-mechanical, chemical and microstructural characteristics of GICs.
3. To analyze ion release from GICs.
4. To propose a mechanism of interaction of GICs with environmental calcium/phosphate and pH.

3.2 Research program

To achieve these aims, the study was divided into the following phases:

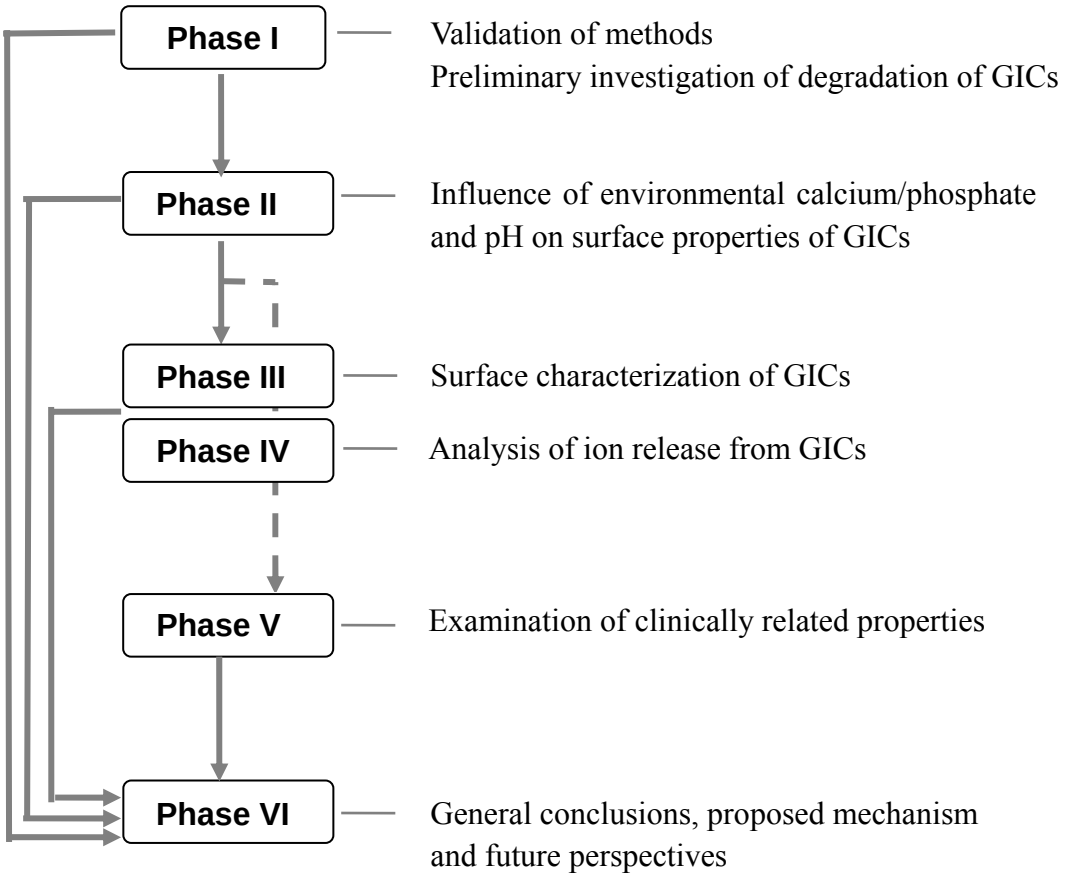

Phase I

Environmental Degradation of GICs: A Preliminary Study

The aims of this phase (Chapter 4) were to (1) examine the suitability of the depth-sensing micro-indentation testing for GICs, and (2) preliminarily investigate the effects of environmental conditions, such as water, 100% humidity and ionic media of varying pH, on hardness and elastic modulus of GICs using the micro-indentation method.

In this phase, two RMGICs and three HVGICs conditioned in water and 100% humidity were used to evaluate the suitability of the depth-sensing micro-indentation technique. To investigate the effect of environmental pH on GICs, ionic media with constant calcium/phosphate level and varying pH of 7, 5 and 3 were employed. They represent the pH of saliva, critical pH for demineralization of hydroxyapatite and acidic beverage respectively.

Phase II

Influence of Environmental Calcium/Phosphate and pH on GICs

The aim of this phase (Chapter 5) was to investigate the effects of environmental calcium/phosphate and pH on surface properties of GICs.

In this phase, a series of ionic media with varying calcium/phosphate levels and pH were employed. The surface mechanical properties (hardness and elastic modulus) and surface micro-structural feature of two HVGICs (calcium and strontium based)

were examined using the depth-sensing micro-indentation testing and SEM. The changes in surface mechanical properties and surface micro-structural feature were evaluated and correlated with environmental calcium/phosphate and pH of storage media.

Phase III

Surface Characterization of GICs Exposed to Acidic Conditions: Effects of Environmental Calcium/Phosphate

The aim of this phase (Chapter 6) was to explore the mechanism of interaction of GICs with environmental calcium/phosphate and pH *via* characterization of the surface of GICs after interaction with environmental calcium/phosphate at pH 3.

The surface of GICs was characterized using (1) Nano-indentation testing for surface mechanical properties, (2) Attenuated Total Reflectance Fourier Transform Infrared Spectrometers (FTIR-ATR) and Energy Dispersive X-ray analysis (EDS) for chemical compositions, and (3) Scanning Electron Microscopy (SEM) and profilometer for surface morphology feature.

Phase IV

Ion Release by GICs Exposed to Acidic Conditions: Effects of Environmental Calcium/Phosphate

The aim of this phase (Chapter 7) was to further explore the mechanism of interaction of GICs with environmental calcium/phosphate and pH *via* analysis of

ion/ligand release from GICs in pH 3 ionic media with varying levels of environmental calcium/phosphate.

In this phase, the ions/ligands were determined using Inductively Coupled Plasma Optical Emission Spectrometry (ICP-OES), Ion Selective Electrode (ISE) and Ultraviolet-Visible (UV-Vis) spectroscopy.

Phase V

Effects of Environmental Calcium/Phosphate on OCA Wear and Shear Strength of GICs subject to Acidic Conditions

The aim of this phase (Chapter 8) was to investigate the effects of environmental calcium/phosphate and pH on clinically related properties of GICs under acidic conditions.

Shear strength and wear resistance of GICs were measured using customized shear-punch and OCA wear testing.

Phase VI

General Conclusion, Proposed Mechanism and Future Perspectives

The last phase summed up all the research findings (Chapter 9). The mechanism of interaction of GICs with environmental calcium/phosphate and pH was interpreted based on a postulated model. Limitations of this study and recommendations for future work were also addressed.

Chapter 4

Environmental Degradation of GICs: A Preliminary Study

4.1 Introduction

All modern day tooth-colored restoratives are based on glass-ionomer and/or composite resin technology. GICs are water-based materials, in which water is bound to coordination sites of polycarboxylate matrices and siliceous hydrogel surrounding glass particles (Ngo, 2002). Despite this, water contamination and dehydration during initial setting reaction can result in dissolution or cracking of materials leading to decreased physical properties (Wilson and McLean, 1998b). In addition, GICs being salt-based cements are vulnerable to acids and ionic solutions (Eisenburger *et al.*, 2003; McKenzie *et al.*, 2003a).

To improve the physical and handling properties of traditional GICs, RMGICs were developed by incorporating water-soluble resin monomers, while HVGICs were modified by removing excess calcium ions from glass particles, decreasing particle size and increasing powder to liquid ratio (Guggenberger *et al.*, 1998). Contrary to common knowledge, a commercial HVGIC showed higher strength with early water exposure (Leirskar *et al.*, 2003). Increase in hardness was also observed when a HVGIC was conditioned in natural saliva. This may be due to the material's interaction with calcium and phosphate present in saliva (Okada *et al.*, 2001). The results suggest that these modified GICs may behave differently from traditional GICs in various oral conditions.

Hardness and elastic modulus are basic mechanical properties of restorative materials, which measure the resistance to load penetration and elasticity respectively. Hardness relates to the plastic deformation of restoratives under occlusal stress, while elastic modulus is responsible for the integrity of interface between restoratives and tooth structure (Sabbagh *et al.*, 2002). Hardness is usually measured using indentation testing in which a sharp diamond indenter is pressed into the material. The hardness number is then calculated by dividing the peak load over the projected contact area of the indent impression (Chandler, 1999). Elastic modulus of dental materials is commonly measured with a three-point bending method, which requires large beam specimen (2 mm × 2 mm × 25 mm) and high surface quality (ISO 4049:2000).

Recently, a depth-sensing micro-indentation technique was successfully used by Yap *et al.* (2004) to derive hardness and elastic modulus of dental materials in a single test. In the depth-sensing micro-indentation testing, indentation load (P) and corresponding indenter penetration depth (h) were measured continuously. Hardness and elastic modulus were then calculated from the loading and unloading portion of the P-h curve, respectively. Some of the advantages associated with the micro-indentation testing include ease of specimen preparation and small specimen size. The depth-sensing micro-indentation test, like other types of indentation tests, will leave an indent on testing surface and is not a truly non-invasive method. Due to the indent size of microscale, repeatable tests can, however, be performed on different sites of the same sample. In a separate study, Chung *et al.* (2005) found a significantly strong and positive

correlation between this method and ISO 4049 flexural test results.

This study evaluated the suitability of the depth-sensing micro-indentation testing for GICs. This study also preliminarily investigated the influence of various environmental conditions, such as water, 100% humidity and ionic media of varying pH, on hardness and elastic modulus of modified restorative GICs using the depth-sensing micro-indentation approach.

4.2 Materials and methods

The restorative GICs studied included two RMGICs (Fuji II LC [FL]; Photac-Fil Quick [PQ]) and three HVGICs (Fuji IX Fast [FN]; KetacMolar [KM]; KetacMolar Quick [KQ]). The material profiles are listed in Table 4-1.

Table 4-1 Technical profiles of the materials evaluated in present study

Material	Classification	Manufacturer	Batch Number	Shade	Curing time
Fuji II LC Capsule (FL)	RMGIC	GC Corp., Tokyo, Japan	0107105	A2	Light-cured 20s
Photac-Fil Quick Aplicap (PQ)	RMGIC	3M-ESPE, Seefeld, Germany	123075	A2	Light-cured 20s
Fuji IX Fast Capsule (FN)	HVGIC	GC Corp., Tokyo, Japan	0109083	A2	Auto-cured 3min
Ketac-Molar Quick Aplicap (KQ)	HVGIC	3M-ESPE, Seefeld, Germany	132967	A2	Auto-cured 3min 30s
Ketac-Molar Aplicap (KM)	HVGIC	3M-ESPE, Seefeld, Germany	114129	A1	Auto-cured 4min 30s

All materials were in capsule form and manipulated according to manufacturers' instructions. The mixed materials were injected into the square recesses (3 mm long, 3 mm wide and 2 mm deep) of customized acrylic molds and covered with acetate strips (Hawe-Neos Dental, Bioggio, Switerzland). A glass slide was placed over the acetate strip and pressure was applied to extrude excess material. The light-cured materials were polymerized using the Spectrum light unit (Dentsply/Caulk, Delaware, US) with mean intensity greater than 400 mW/cm^2. All specimens were allowed to set at 37 ºC and 100% humidity for 1 hour before being subjected to different storage conditions.

For evaluation of suitability of the depth-sensing micro-indentation testing, 14 specimens for each material were randomly divided into two groups (n=7) and conditioned in 100% humidity (H) and distilled water (W) at 37 ºC for 4 weeks without being disturbed (Yap *et al.*, 2001a). After determination of hardness and elastic modulus, the indent impressions were captured and compared with a custom-designed digital imaging system (Chung *et al.*, 2005).

For observation of effects of environmental pH, a RMGIC (FL) and a HVGIC (FN) produced by the same manufacturer were used. Twenty-one specimens for FL and FN respectively were randomly distributed into three groups (n=7) and separately treated in ionic media of pH 7 (IM7), pH 5 (IM5) and pH 3 (IM3). These ionic media consisted of common components of 1.5 mM $CaCl_2$, 0.9 mM KH_2PO_4 and 150 mM KCl. In addition, 20 mM HEPES for IM7 and 50 mM acetic acid for IM5 and IM3 were added, coupled

with 1 M KOH for adjusting pH to desired value (Appendix A). Hardness and elastic modulus were measured at weekly interval for four weeks.

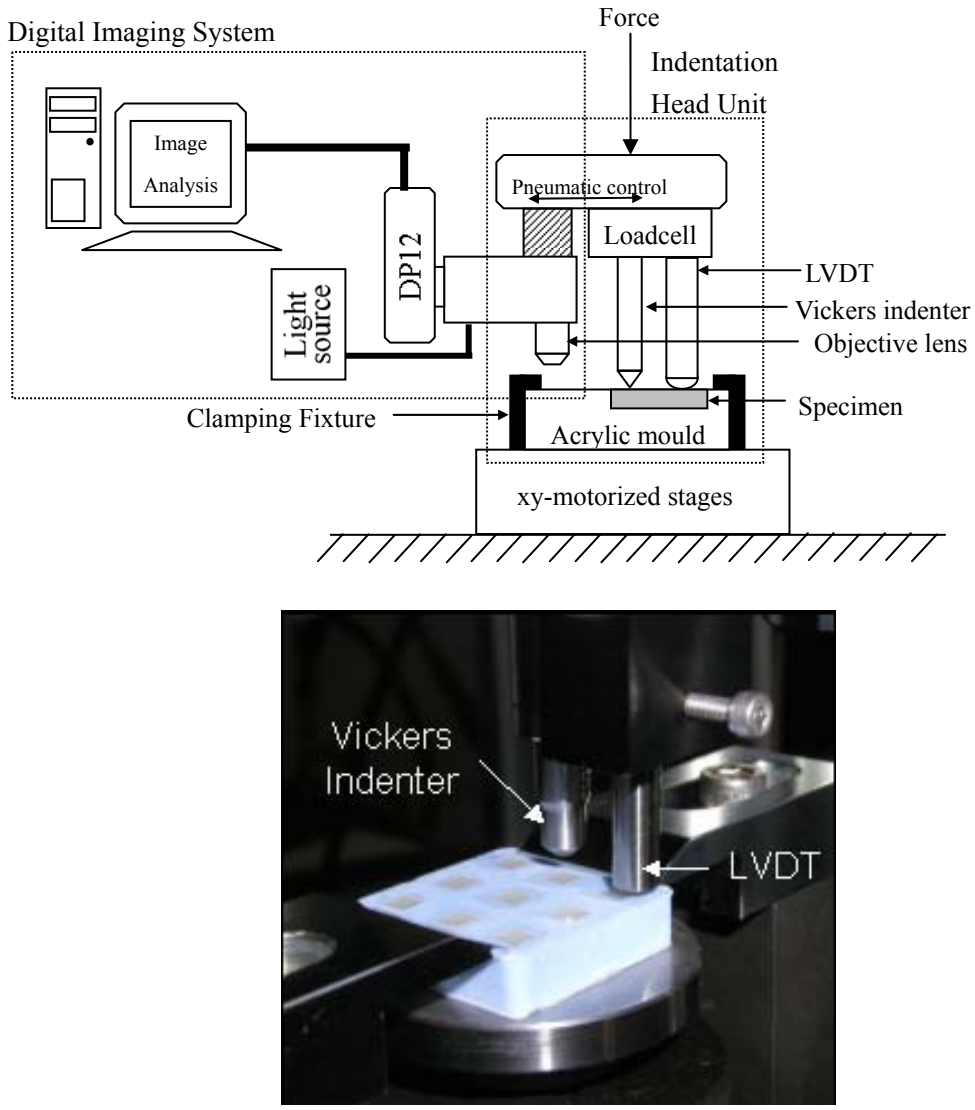

Figure 4-1 Depth-sensing micro-indentation testing set-up

In this study, specimens were kept in moisture by blotting out excessive water gently and fixed tightly on the x-y motorized stage centrally beneath the customized indentation head unit (Figure 4-1). A four-sided diamond Vickers indenter was used and

specimens were indented at a rate of 0.0005 mm/s until a maximum load of 10 N was attained. The peak load was held for 10 seconds and unloaded fully at a rate of 0.0002 mm/s. The indenter penetration depth (h_{max}) were in ranges of 24 ~ 29 μm and 30 ~ 35 μm for HVGICs and RMGICs respectively. Hardness and elastic modulus were derived using in-house developed software (PhCalculator Version 1.1).

Hardness (H) was determined by dividing the peak load over the maximum contact area, while elastic modulus (E_{in}) was calculated using an unloading contact stiffness analysis according to Oliver & Pharr method (Figure 4-2) (Oliver and Pharr, 1992). The equations used were as follows:

$$H = \frac{P_{\max}}{A_{\max}} \tag{4-1}$$

$$E_{in} = \frac{1-\nu_{in}^{\ 2}}{\left(1.142\frac{\sqrt{A_{\max}}}{S} - \frac{(1-\nu_o^2)}{E_o}\right)} \tag{4-2}$$

$$A_{\max} = 24.56\left(h_{\max} - \frac{3P_{\max}}{4S}\right)^2 \tag{4-3}$$

where P_{max} = maximum indentation load,

A_{max} = maximum projected contact area,

h_{max} = indentation depth at maximum load,

E_o = elastic modulus of the indenter,

ν_o = Poisson ratio of the indenter,

ν_{in} = Poisson ratio of the indented material of interests, and

S = unloading contact stiffness.

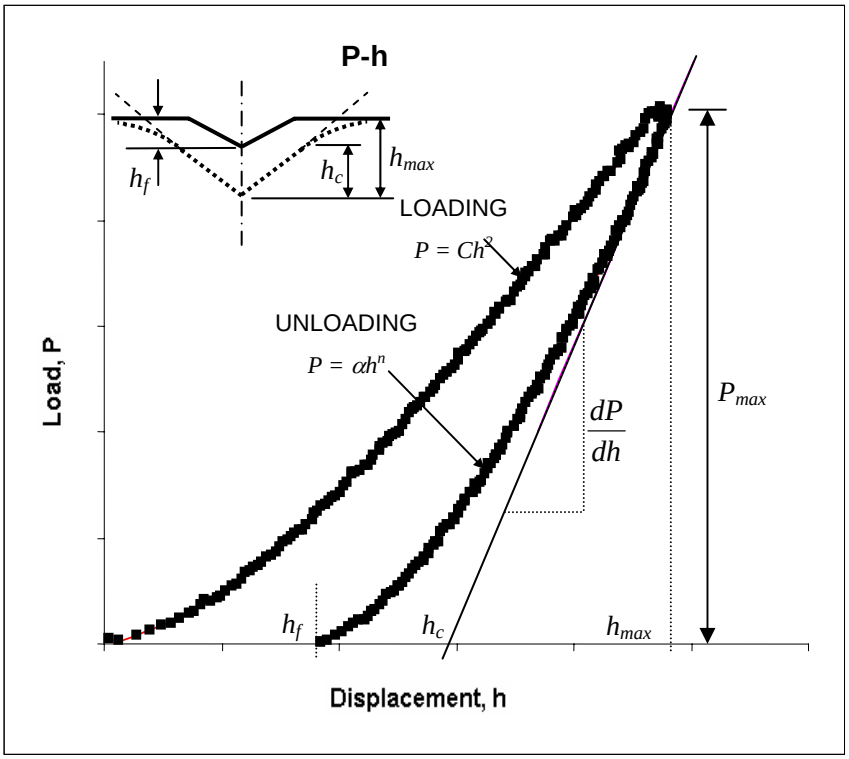

Figure 4-2 A typical *P-h* curve during a loading-unloading cycle

where h_{max} is the maximum indenter displacement at peak indentation load (P_{max}),

$\frac{dP}{dh}$ is the slope of the *P-h* curve during the initial unloading stage,

h_f and h_c are the final (residual) and contact depth of the indent impression respectively.

Results were analyzed using independent-sample T-test and one-way ANOVA/Scheff's post-hoc test at significance level of 0.05.

4.3 Results

Mean value of hardness and elastic modulus of modified GICs in 100% humidity and water are presented in Figure 4-3 and Table 4-2.

(a)

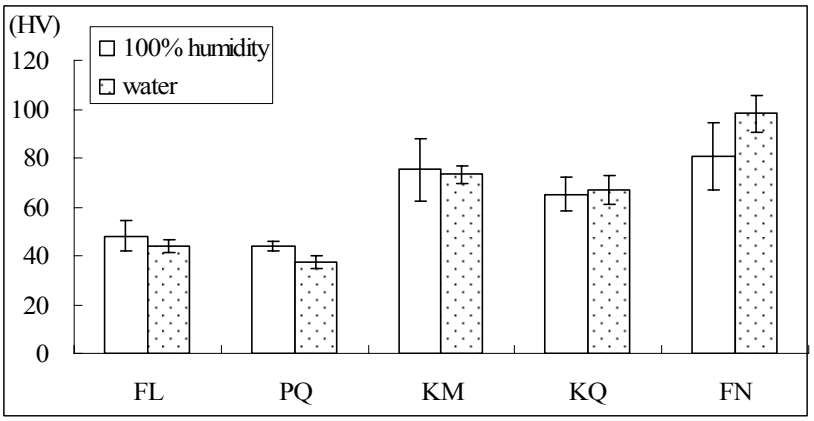

(b)

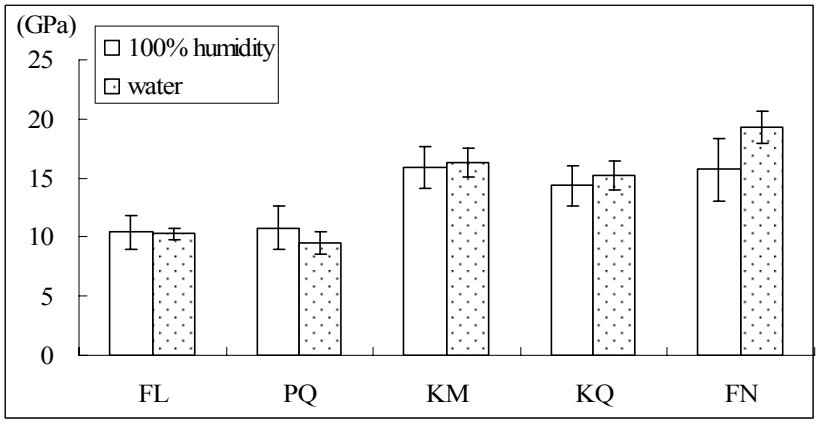

Figure 4-3 Hardness (a) and elastic modulus (b) of GICs in 100% humidity and water

*Vertical lines represent standard deviations

The mean hardness ranged from 65.24 to 98.24 HV and 37.14 to 47.99 HV, while mean elastic modulus ranged from 14.43 to 19.32 GPa and 9.51 to 10.77 GPa for HVGICs and RMGICs respectively. HVGICs (KM, KQ and FN) showed significantly higher hardness and modulus than RMGICs (FL and PQ) in all storage conditions (p<0.05). Storage in water significantly decreased hardness and elastic modulus of PQ (p<0.05), but significantly increased hardness and elastic modulus of FN (p<0.05) (Table 4-3).

Table 4-2 Hardness and elastic modulus of GICs in 100% humidity and water

	Hardness (HV)		Elastic modulus (GPa)	
	100% humidity	Water	100% humidity	Water
FL	47.99 (6.30)	44.03 (2.84)	10.40 (1.36)	10.29 (0.45)
PQ	43.93 (2.12)	37.14 (2.55)	10.77 (0.80)	9.51 (0.85)
KM	75.15 (12.64)	73.21 (3.62)	15.87 (1.76)	16.37 (1.19)
KQ	65.24 (6.72)	66.89 (3.33)	14.43 (1.66)	15.23 (1.20)
FN	80.51 (13.86)	98.24 (7.54)	15.66 (2.68)	19.32 (1.33)

Standard deviation in parentheses (n=7)

Table 4-3 Statistical comparison of hardness and elastic modulus between 100% humidity and water

Variables	Materials		Difference
Hardness (HV)	RMGIC	FL	No significant difference
		PQ	H > W
	HVGIC	KM	No significant difference
		KQ	No significant difference
		FN	W > H
Elastic Modulus (GPa)	RMGIC	FL	No significant difference
		PQ	H > W
	HVGIC	KM	No significant difference
		KQ	No significant difference
		FN	W > H

Results of independent-samples T-test ($p < 0.05$)
> indicates statistically significant difference in hardness/elastic modulus

Effects of pH of ionic media on FL and FN are shown in Figure 4-4, Figure 4-5, and Table 4-4 respectively. Both FL and FN stored in IM7 and IM5 showed relatively consistent hardness and elastic modulus in the 4-week observation period. In IM3 condition, FL showed constant and comparable hardness and elastic modulus with those stored in IM7 and IM5. On the contrary, FN presented decreased hardness in IM3, which was significantly lower than those in IM7 and IM5 at 4 weeks time (Table 4-5).

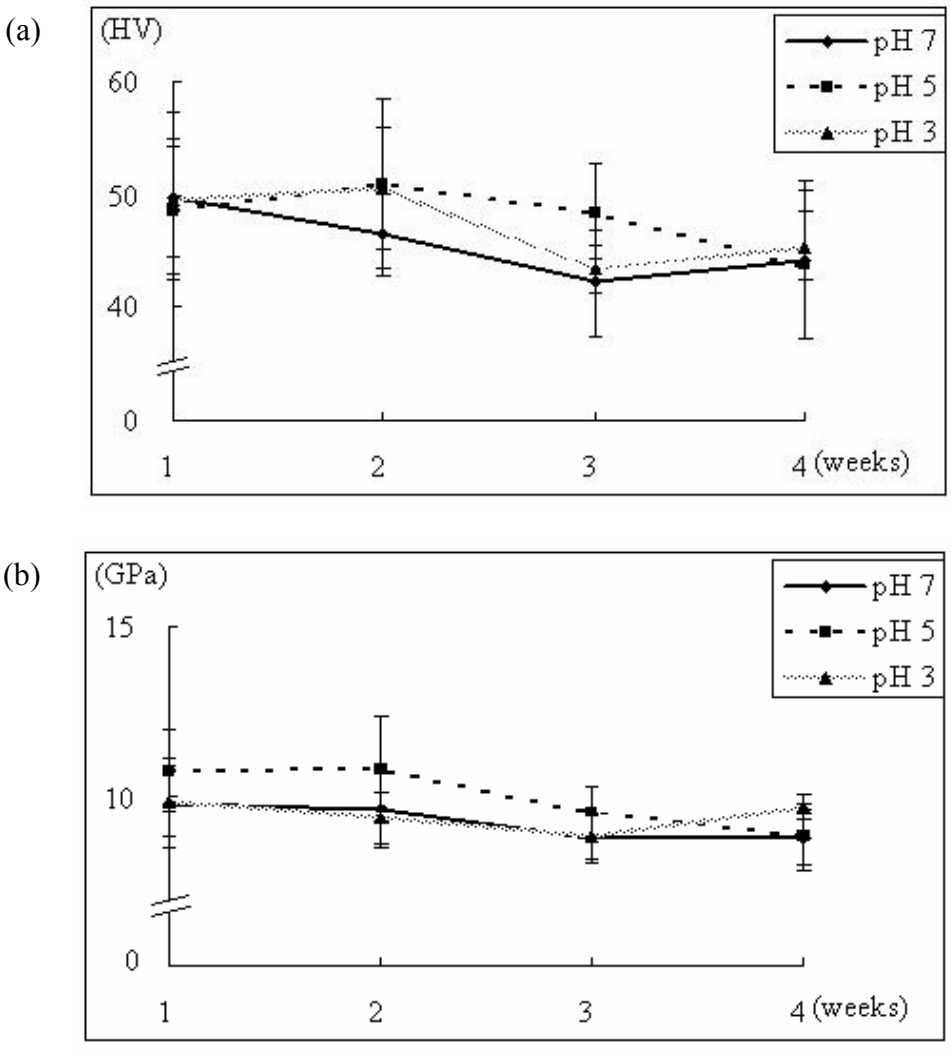

Figure 4-4 Hardness (a) and elastic modulus (b) of FL in ionic media of varying pH

*Vertical lines represent standard deviations

(a)

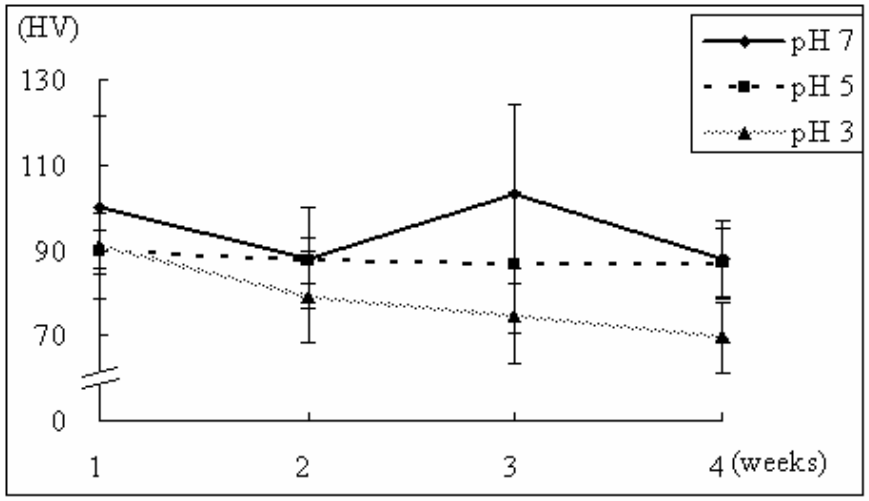

(b)

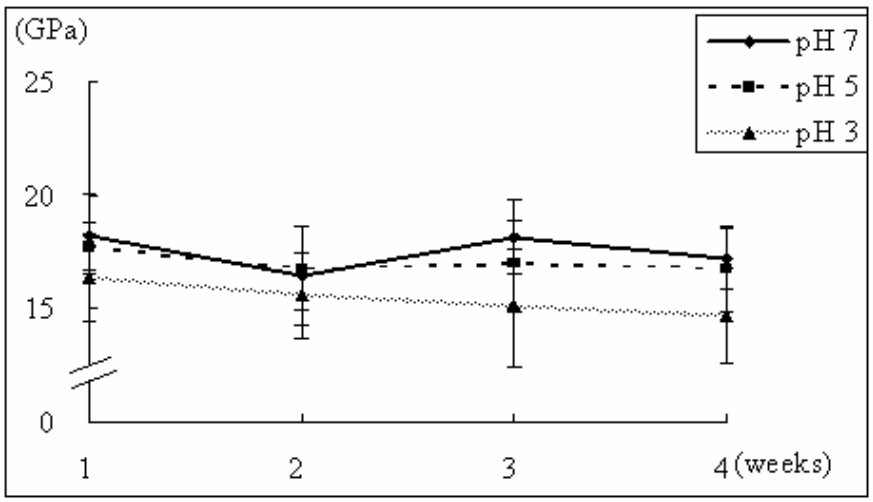

Figure 4-5 Hardness (a) and elastic modulus (b) of FN in ionic media of varying pH

*Vertical lines represent standard deviations

Table 4-4 Hardness and elastic modulus of FL and FN in ionic media of varying pH

		FL		FN	
		Hardness (HV)	Elastic modulus (GPa)	Hardness (HV)	Elastic modulus (GPa)
1 week	**pH 7**	49.86 (7.54)	9.80 (1.36)	100.08 (21.56)	18.27 (1.79)
	pH 5	48.59 (5.76)	10.74 (1.24)	90.17 (4.79)	17.76 (1.10)
	pH 3	49.64 (5.26)	9.87 (1.07)	91.52 (7.37)	16.36 (1.98)
2 week	**pH 7**	46.60 (3.89)	9.62 (1.16)	88.27 (11.88)	16.45 (2.20)
	pH 5	50.99 (7.57)	10.82 (1.56)	87.64 (5.53)	16.78 (1.85)
	pH 3	50.66 (5.36)	9.36 (0.80)	78.76 (10.65)	15.59 (1.91)
3 week	**pH 7**	42.21 (4.78)	8.73 (0.74)	103.21 (21.18)	18.17 (1.67)
	pH 5	48.45 (4.26)	9.53 (0.77)	86.94 (16.67)	16.97 (1.93)
	pH 3	43.38 (2.16)	8.78 (0.65)	74.57 (11.10)	15.05 (2.60)
4 week	**pH 7**	44.26 (7.03)	8.77 (0.81)	88.06 (9.09)	17.21 (1.35)
	pH 5	43.80 (6.64)	9.78 (0.96)	86.92 (8.26)	16.74 (1.92)
	pH 3	45.48 (3.06)	9.70 (0.38)	69.38 (8.11)	14.67 (2.11)

Standard deviation in parentheses (n=7)

Table 4-5 Statistical comparison of hardness and elastic modulus between ionic media of varying pH (after 4 weeks)

Materials	**Variables**	**Difference**
FL	Hardness (HV)	No significant difference
	Elastic modulus (GPa)	No significant difference
FN	Hardness (HV)	IM7, IM5 > IM3
	Elastic modulus (GPa)	No significant difference

Results of one-way ANOVA/Scheff's post-hoc test ($p < 0.05$)
> indicates statistically significant difference in hardness/elastic modulus

The typical indent impressions of GICs are presented in Figure 4-6, whereas the phenomenon of "sink in" (materials around contact area deform downwards with respect to the original surface plane.) and indistinct indentation contour of some GICs are clearly shown. This indicates that it is difficult to optically measure the diagonal length of indentation impressions for glass-ionomer specimens.

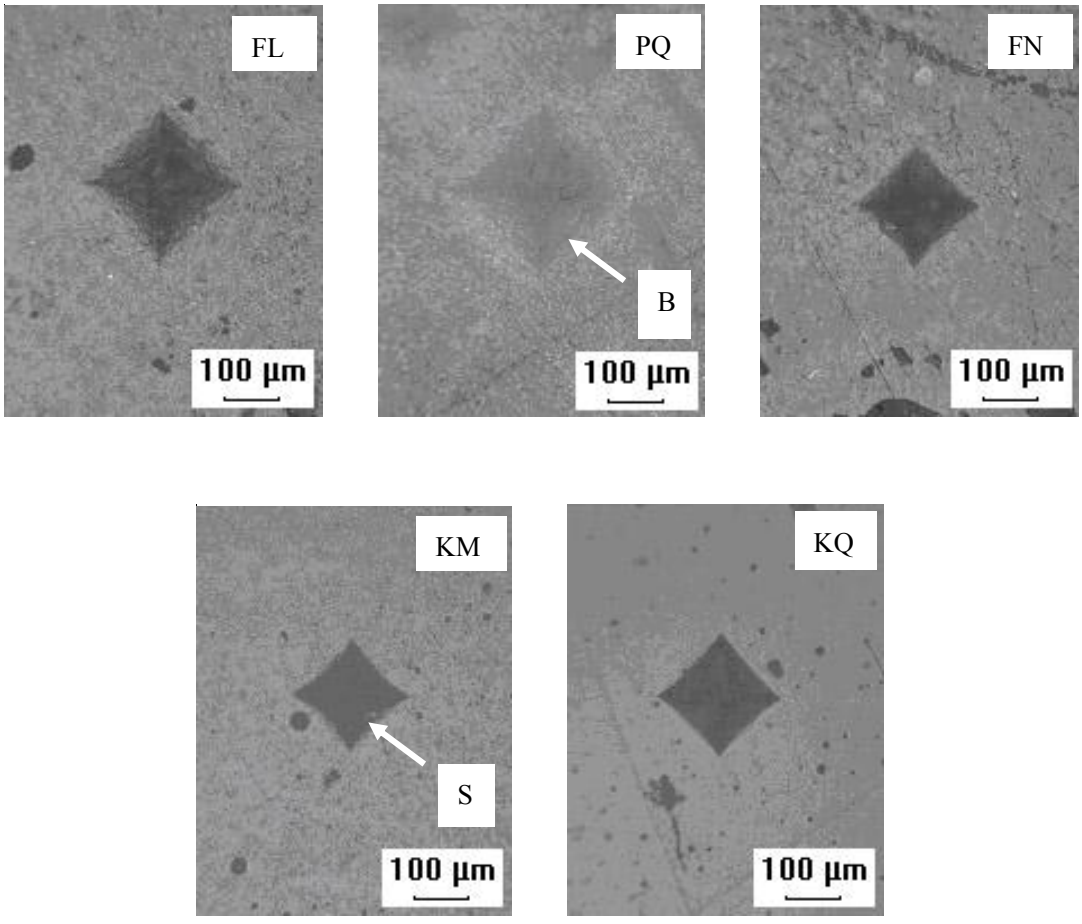

Figure 4-6 Indent impressions of various GICs in water

B, undistinguished boundary; S, "sink-in" indentation shape

4.4 Discussion

Hardness is a parameter describing the resistance of material to permanent deformation and is related to several properties including resistance to plastic deformation, friction and abrasion (Chandler, 1999). Micro-indentation testing is commonly used to evaluate setting reaction and influencing factors of dental materials (Kanchanavasita *et al.*, 1998; Musanje *et al.*, 2001). From a method point of view, the determination of contact area at the maximum load is critical for micro-indentation test. For conventional micro-indentation testing with Vickers indenter tip, hardness is derived from measurement of the diagonal length of the indentation impression. In this study, the indent images of some GICs conditioned in water were blurred and showed indistinguishable boundary (Figure 4-6), which made it difficult to measure the diagonal length and hence the precise calculation of the hardness. In the depth-sensing micro-indentation testing, we used Oliver & Pharr method (1992) for calculating the indenter contact area, which avoided measurement error caused by uncertainty of the diagonal length measurement and "pile-up" or "sink-in" effect (Yap *et al.*, 2004). During indentation test, materials around contact area may deform upwards (pile-up) or downwards (sink-in) with respect to the original surface plane. Sink-in decreases and pile-up increases the contact area, thus, true contact area may be over- or under-estimated. Oliver & Pharr method (1992) works for hard materials which predominantly show "sink-in", but fails with materials which display extensive "pile-up". In this study, "sink in" of the materials around the indent impression was clearly visible in some indentation images (Figure 4-6). With the present setting,

hardness values of HVGICs and RMGICs obtained by the depth-sensing micro-indentation testing were in the same order as those reported in previous studies (Yap *et al.*, 2003a; Ellakuria *et al.*, 2003). In this study, the indentation depth derived from the micro-indentation testing was 24 ~ 35 μm, which covered the size of most glass particles. The test thus reflects the bulk property of GICs (Yap *et al.*, 2003a; Guggenberger *et al.*, 1998). The major advantage of this novel test is that considerable experiment time and materials were saved as hardness and elastic modulus were derived in a single test.

GICs being water-based cements are susceptible to aqueous conditions. Although water is essential for acid-base setting reaction in GICs, water contamination during early setting hydrolytically degrades calcium polycarboxylate matrix and reduces mechanical properties of GICs (Wasson and Nicholson, 1993; Mojon *et al.*, 1996). Thus, all specimens in the present study were kept in 100% humidity for 1 hour immediately after initial setting. This protocol is commonly used in *in vitro* study on GICs and has been reported to give the samples optimum properties (Causton, 1981). On the other hand, set GICs require aqueous environment for maintaining hydro-gel structure and physico-mechanical properties (Wilson *et al.*, 1979). To avoid dehydration of glass-ionomer specimens during indentation testing, in this study, the specimen surface was kept in moisture by blotting out excessive water just before the indentation testing (Yap *et al.*, 2004).

To mimic *in vivo* conditions, the ionic media used in this pilot study consisted of

150 mM KCl providing a constant ionic strength similar to saliva (ten Cate and Duijsters, 1982). Levels of calcium (1.5 mM) and phosphate (0.9 mM) in the ionic media were also comparable to saliva, which was recommended by ten Cate and Duijsters (1982) for demineralization and remineralization of tooth *in vitro*. pH of the ionic media was varied as pH 7, pH 5 and pH 3 representing pH of saliva, critical pH for demineralization of hydroxyapatite and acidic beverage pH respectively (Edgar, 1992; Larsen and Nyvad, 1999).

Regardless of storage conditions, HVGICs showed greater hardness and elastic modulus than RMGICs after conditioning. This is in agreement with the one-year results by Ellakuria *et al.* (2003) using the conventional hardness testing. The improved hardness and elastic modulus of HVGICs may be accounted for as follows. Firstly, removal of excess calcium ions from the surface of glass particles in HVGICs allows formation of insoluble aluminum polycarboxylate at early setting time (Young *et al.*, 2004, Yap *et al.*, 2003a). The insoluble aluminum salts are more resistant to aqueous conditions and improve the mechanical properties (De Maeyer *et al.*, 1998). By contrast, RMGICs consist of polymer and polycarboxylate matrix network. HEMA polymer matrix in RMGICs may retard H^+ mobility, inhibit further acid-base reaction and therefore prevent complete formation of polycarboxylate matrix (Bourke, 1992). Secondly, a dense surface texture with tightly packed glass particles may result in higher surface hardness of GICs (Xie *et al.*, 2000). Thus, larger glass particle size and higher powder to liquid ratio may contribute to the superior mechanical properties of HVGICs

(Yap *et al.*, 2003a; Guggemberger *et al.*, 1998). Thirdly, in RMGICs, HEMA polymer entangled with polycarboxylate matrix may lead to an inferior interface between glass particles and matrices (de Gee, 1999). Possible phase separation due to the inferior interface may result in degradation of the composite structure and lead to lower mechanical properties.

In this study, HVGICs behaved differently from RMGICs when exposed to water after initial setting. Compared to those in 100% humidity, HVGICs presented higher or comparable hardness and elastic modulus while RMGICs showed comparable or decreased mechanical properties in water. The improved hardness and elastic modulus for HVGICs exposed to water further indicate that aqueous environment is critical for set GICs of polycarboxylates structure (Mount, 2002). On the other hand, the reduction in hardness and elastic modulus of RMGICs may be attributed to plasticization arising from water absorption by hydrophilic HEMA in matrices (Kanchanavasita *et al.*, 1998a,b; Yap, 1997). These results suggest that set HVGICs should be prevented from dehydration while RMGIC restoratives should be sealed with a resin after placement.

With regard to environmental pH effects, FN showed decreased hardness in the pH 3 ionic media, while the hardness of FL was unchanged and independent of the ionic medium pH. Generally, GICs perform well in pH 6 to pH 10 conditions and are prone to degradation in pH 4 (Walls *et al.*, 1988). In acidic conditions, the solubility of GICs increases with a decrease in environmental pH (Eisenburger *et al.*, 2003). It is postulated that acids extract metal cations from matrices and glass particles, thus leading to the

degradation of materials (Fukazawa *et al.*, 1990). The unaffected properties of RMGICs exposed to low environmental pH should be attributed to the incorporation of HEMA resin. This entangled polymer-polycarboxylate structure may improve the resistance to acid erosion *via* obstructing movement of H^+ (Bourke *et al.*, 1992). Results from this study suggest that HVGICs are stable in pH 5 surroundings but are vulnerable in pH 3 conditions. Further investigations on the interaction of GICs with environmental calcium/phosphate and pH are warranted.

4.5 Conclusions

The suitability of the depth-sensing micro-indentation testing and the effects of storage conditions on hardness and elastic modulus of modified restorative GICs were investigated in this study. For glass-ionomer materials, the depth-sensing micro-indentation testing was found to be both efficient and effective. In this study, HVGICs were significantly harder and stiffer than RMGICs. When exposed to water, hardness and elastic modulus of HVGICs increased or remained the same. In contrast, RMGICs showed comparable or decreased hardness and elastic modulus in water. Ionic media of varying pH did not affect surface mechanical properties of FL. pH 3 ionic medium, however, had a significant effect on FN. These results suggest that the performance of GICs is material-type and storage condition dependent. Preventing HVGIC restoratives from dehydration and protecting RMGIC restoratives with waterproof coatings after initial setting are recommended.

Chapter 5

Influences of Environmental Calcium/Phosphate and pH on GICs

5.1 Introduction

Set GIC can be regarded as a composite of polycarboxylate matrices and unreacted glass particles sheathed by siliceous gel. The polycarboxylate matrices are cross-linked by calcium/strontium or aluminum polycarboxylate salt bridges (Maeda *et al.*, 1999). Divalent calcium/strontium ions may bridge two polycarboxylate chains with the remaining coordination positions occupied by water molecule. In steric consideration, trivalent aluminum ions may only bridge two polycarboxylate chains and the third valency may be with fluoride or hydroxyl ions (Wilson and McLean, 1988a). The ionic and hydrophilic structure imparts ion-exchange ability in GICs. Hence, GIC is capable of interaction with the oral environment/tooth (Yoshida *et al.*, 2000) and release/uptake of fluoride (Forsten, 1991).

The ionic and hydrophilic structure also render GICs vulnerable to acids and ions present in the intra-oral environment (Eisenburger *et al.*, 2003; Nicholson *et al.*, 2001). With regard to environmental ions, the common monovalent ions, such as Na^+, K^+ and Cl^-, have no significant effect on GICs (McKenzie *et al.*, 2003a). In addition, Billington *et al.* (1987) reported that neutral NaF solution reduced the hardness of GICs. He postulated that F^- may react with ionic salt bridges and break the

cross-linking of matrix (Billington *et al.*, 2000). In another study, Okada *et al.* (2001) reported that a HVGIC in natural saliva had improved surface hardness compared to those in distilled water. This may be related to a possible surface reaction involving salivary calcium and phosphate.

It is known that acids have negative effects on GICs. The acid degradation of GICs depends on environmental pH, acid anion and glass-ionomer type. GICs suffer greater degradation in lower pH solution (Fukazawa *et al.*, 1990; Eisenburger *et al.*, 2003). Citric acid degrades GICs faster and more severely than lactic and acetic acids (Fukazawa *et al.*, 1990). In addition, GICs with maleic acid copolymers were less resistant to acid attack than those with acrylic acid copolymers (Setchell *et al.*, 1985; Wilson *et al.*, 1986). Under acid challenge, matrix salt bridges are hydrolyzed and $Ca^{2+}/Sr^{2+}/Al^{3+}$ cations are released, thus, matrix-glass particle structure is decomposed resulting in degradation of GICs (Fukazawa *et al.*, 1990).

The acids *in vivo* come either by degradation of carbohydrates in stagnant areas of the mouth, consumption of acidic beverage/foodstuffs, or regurgitation of stomach acids. The consumption of soft drinks and juices has been steadily increasing resulting in the high prevalence of dental erosion in children and adolescents (Lussi and Schaffner, 2000; Ganss *et al.*, 2001; Johansson *et al.*, 1996). Most carbonated beverages and juices are of pH 3 and can damage glass-ionomer restoratives (Lussi *et al.*, 2004). Recently, McKenzie *et al.* (2003a, 2004) observed that GICs in CocaCola (~ pH 3.0) showed comparable properties to those in neutral media and much better

than those in other acidic beverages. They postulated that phosphoric acid in CocaCola may form insoluble complexes with calcium and be responsible for maintaining the strength of GICs. This indicates that intra-oral calcium and phosphate may have positive effects on GICs. Few studies have, however, systemically focused on this issue and the effects of environmental phosphate/calcium on GICs at different pH conditions are not known.

In our preliminary study, the HVGIC (FN) showed sensitivity to the pH of ionic storage media with fixed calcium/phosphate level. In this study, the concentrations of calcium/phosphate in ionic storage media were varied between the range found in saliva and beverages. The aim of this study was to investigate the effects of environmental calcium and phosphate on HVGICs at different pH.

5.2 Materials and methods

Two HVGICs Fuji IX Fast ([FN], GC, Japan) and KetacMolar ([KM], 3M ESPE, Germany) were used in this study. FN is strontium based and KM is calcium based. Both of them set by traditional acid-base reaction. These materials were in encapsulated form and activated/mixed according to manufacturers' instructions. Specimen preparation procedures were the same as those in chapter 4. One hundred and five specimens for each material were randomly divided into 15 groups (n=7) and stored in different ionic media for 4 weeks. The compositions of ionic media with varying calcium/phosphate and pH are listed in Table 5-1. Preparation of the ionic

media is shown in Appendix A.

Table 5-1 Compositions of storage media

		$CaCl_2 \cdot 2H_2O$ (mM)	KH_2PO_4 (mM)	KCl (mM)	HEPES (mM)	Acetic Acid (mM)	pH*
Group pH7	pH7-Control	0	0	150	20	---	7
	pH7-A	2.4	0	150	20	---	7
	pH7-B	1.5	0.9	150	20	---	7
	pH7-C	1.2	1.2	150	20	---	7
	pH7-D	0	2.4	150	20	---	7
Group pH5	pH5-Control	0	0	150	---	50	5
	pH5-A	2.4	0	150	---	50	5
	pH5-B	1.5	0.9	150	---	50	5
	pH5-C	1.2	1.2	150	---	50	5
	pH5-D	0	2.4	150	---	50	5
Group pH3	pH3-Control	0	0	150	---	50	3
	pH3-A	2.4	0	150	---	50	3
	pH3-B	1.5	0.9	150	---	50	3
	pH3-C	1.2	1.2	150	---	50	3
	pH3-D	0	2.4	150	---	50	3

*pH was adjusted with 1 M KOH;

HEPES: N-2-hydroxyethylpiperazine-N′-2′-ethanesulfonic acid

The calcium/phosphate levels were varied based on remineralization/ demineralization solutions from ten Cate and Duijsters' study (1982) and were within the range of saliva and beverages (Edgar, 1992; Larsen and Nyvad, 1999). For each pH group, one subgroup (pH-Control) contained neither calcium nor phosphate, two subgroups (pH-A and pH-D) contained either calcium or phosphate, and other two subgroups (pH-B and pH-C) contained both calcium and phosphate of different ratio. pH 7, pH 5 and pH 3 were representative of pH in saliva, critical pH for demineralization of hydroxyapatite and acidic beverage pH respectively. For the purpose of simulating *in vivo* condition and keeping approximately equal ionic

strength of various solutions, KCl was added at a concentration of 150 mM, which was much higher than the concentration of calcium/phosphate. It was assumed that KCl would contribute most to the ionic strength of solution. Given the approximately equal ionic strength of solutions and controlled experimental temperature (37℃), the comparison of effects of calcium/phosphate by concentration was deemed reasonable.

As mentioned in chapter 2.2, calcium, phosphate and pH of the intra-oral environment vary from time to time. In order to study the maximum effects of environmental calcium/phosphate and pH on GICs, all specimens in this study were conditioned continuously in storage media for 4 weeks. Hardness and elastic modulus of specimens were determined using a depth-sensing micro-indentation testing at weekly intervals. This method was described in detail in Chapter 4. Hardness and elastic modulus of FN and KM after 4 weeks were analyzed using one-way ANOVA/Scheff's post-hoc test or Kruskal-Wallis/Mann-Whitney test at significance level of 0.05.

Three specimens of each group were randomly selected for observation of surface structure. Specimens were rinsed with tap water and sectioned. The sectioned surface was dried, sputter coated with gold and examined using a SEM (JSM-5600, JEOL, Japan). Secondary electron microscopic images for each group were obtained at ×500 magnification using an accelerating voltage of 5 kV and a spot size of 22 nm. For pH 3 group, extra images were collected at higher magnification of ×1000.

5.3 Results

Hardness and elastic modulus for FN and KM are presented in Figure 5-1, Figure 5-2 and Table 5-2 to Table 5-5. Hardness ranged from 36.27 to 114.88 HV and 18.41 to 80.47 HV, while elastic modulus ranged from 9.87 to 20.13 GPa and 5.36 to 16.40 GPa for FN and KM respectively. The effects of calcium/phosphate level in storage media on hardness and elastic modulus of both FN and KM were found to be pH dependent.

At pH 7 and pH 5, the hardness and elastic modulus of both FN and KM remained relatively constant as a function of time and were independent on calcium/phosphate level in storage media. No significant differences in hardness and elastic modulus were present among specimens conditioned in ionic media of varying calcium/phosphate levels after 4 weeks (Table 5-6).

At pH 3, FN and KM showed varied hardness and elastic modulus depending on levels of calcium/phosphate in ionic storage media. When exposed to pH 3 conditions without calcium and phosphate (pH 3-Control group), both FN and KM showed decreased hardness and elastic modulus compared to those under pH 7 and pH 5 conditions. FN and KM in pH 3-A group (with calcium and without phosphate) showed similar hardness and elastic modulus to those in pH 3-Control group, while FN and KM in pH 3-D group (high in phosphate level) exhibited higher hardness and elastic modulus than those in pH 3-Control group. After 4 weeks, FN and KM exposed to pH 3 storage media with higher phosphate level had significantly higher hardness and elastic modulus ($p<0.05$) (Table 5-6).

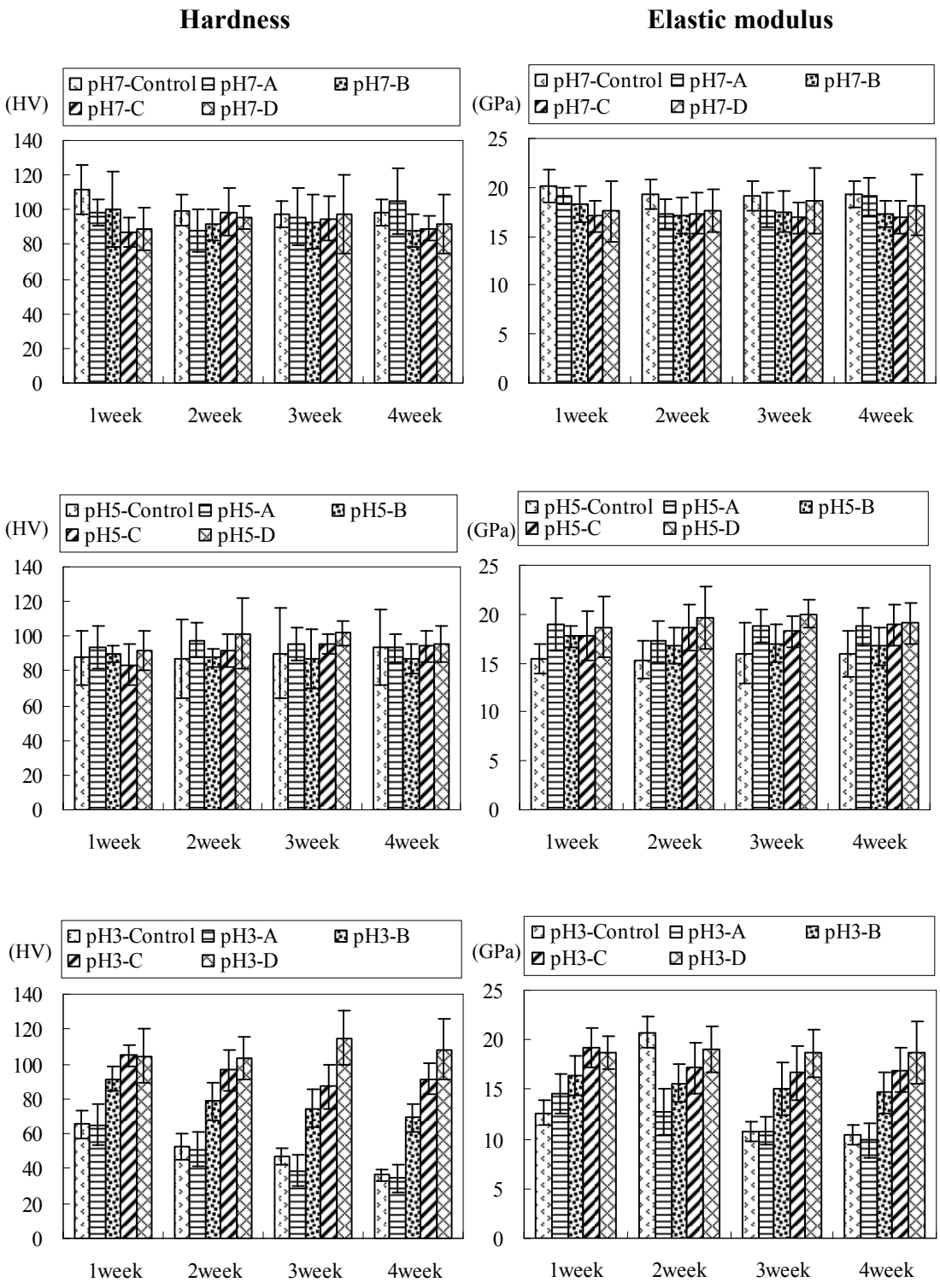

Figure 5-1 Hardness and elastic modulus of FN

*Vertical lines stand for standard deviations.

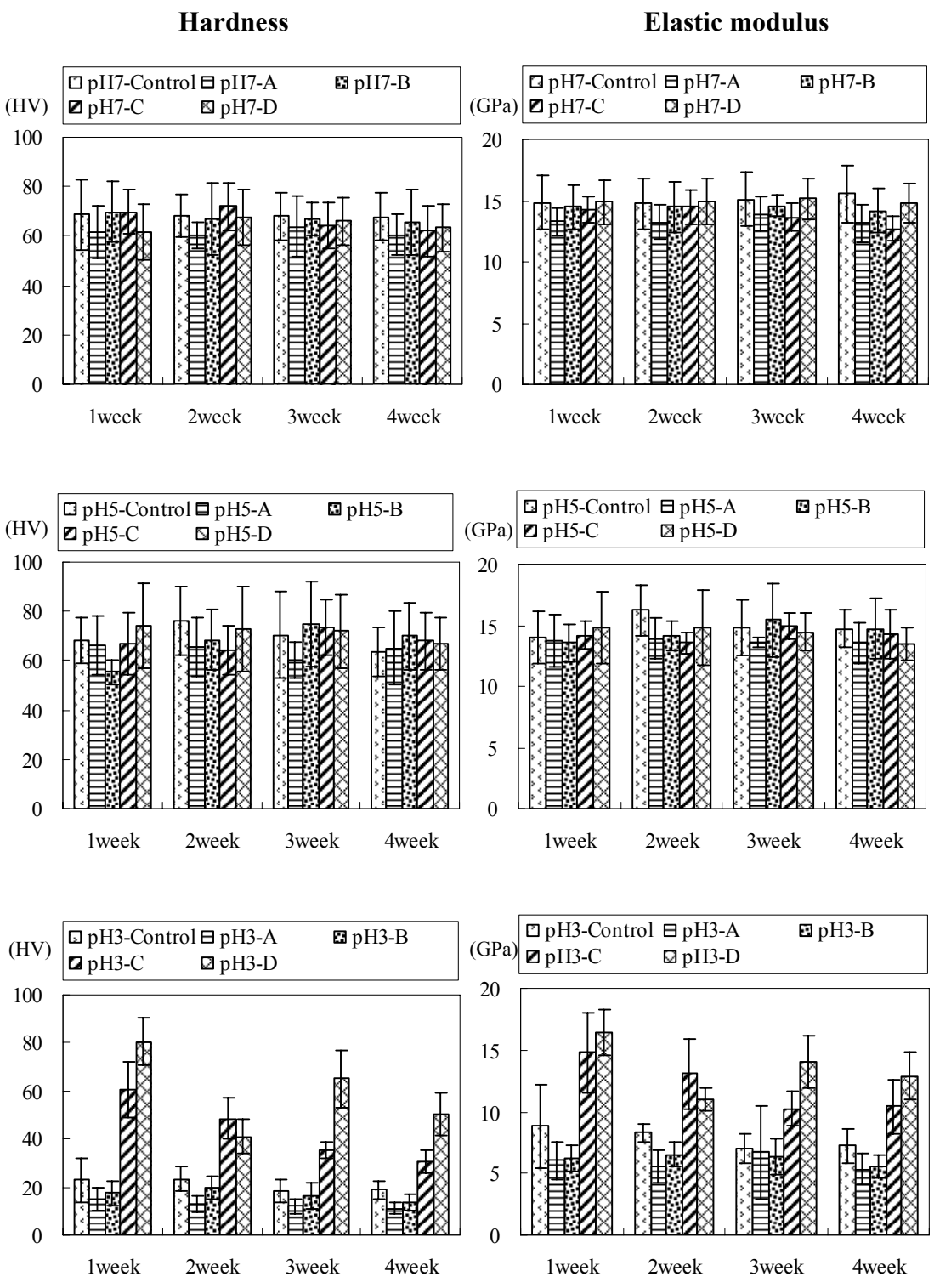

Figure 5-2 Hardness and elastic modulus of KM

*Vertical lines stand for standard deviations.

Table 5-2 Hardness (HV) of FN

		1 week	2 week	3 week	4 week
Group pH7	pH7-Control	111.59 (14.39)	99.78 (9.35)	97.55 (7.48)	98.24 (7.54)
	pH7-A	98.23 (7.29)	88.03 (12.44)	95.84 (16.53)	105.28 (18.94)
	pH7-B	100.08 (21.56)	91.58 (9.14)	93.03 (15.58)	88.06 (9.09)
	pH7-C	86.75 (8.70)	98.72 (13.72)	94.98 (13.11)	89.07 (7.09)
	pH7-D	88.95 (12.25)	95.65 (6.34)	97.31 (23.01)	91.58 (16.92)
	p value	0.022#	0.218*	0.985*	0.093*
Group pH5	pH5-Control	87.56 (16.00)	86.88 (22.83)	90.25 (26.17)	93.42 (21.80)
	pH5-A	93.36 (12.30)	97.64 (9.73)	95.71 (9.75)	93.32 (8.24)
	pH5-B	90.17 (4.79)	87.64 (5.53)	86.94 (16.67)	86.92 (8.26)
	pH5-C	83.56 (11.54)	91.58 (9.67)	95.22 (5.66)	94.40 (9.09)
	pH5-D	91.71 (11.41)	101.48 (20.23)	101.92 (6.97)	95.60 (10.55)
	p value	0.569*	0.152#	0.427#	0.532#
Group pH3	pH3-Control	65.46 (8.10)	52.53 (7.15)	47.15 (4.65)	36.27 (3.63)
	pH3-A	65.24 (11.34)	51.14 (10.05)	38.88 (8.68)	34.54 (7.97)
	pH3-B	91.52 (7.37)	78.76 (10.65)	74.57 (11.10)	69.38 (8.11)
	pH3-C	104.83 (5.79)	96.40 (11.48)	86.97 (12.94)	91.45 (8.68)
	pH3-D	104.56 (15.43)	103.48 (12.48)	114.88 (15.33)	108.22 (17.27)
	p value	0.000*	0.000*	0.000*	0.000#

Standard deviations in parentheses (n=7)

Results of one-way ANOVA* or Nonparametric Test (Kruskal Wallis) #

Table 5-3 Elastic modulus (GPa) of FN

		1 week	2 week	3 week	4 week
Group pH7	pH7-Control	20.13 (1.73)	19.24 (1.51)	19.10 (1.55)	19.32 (1.33)
	pH7-A	19.15 (0.86)	17.24 (1.48)	17.69 (1.71)	19.09 (1.90)
	pH7-B	18.27 (1.79)	17.06 (1.85)	17.53 (2.07)	17.21 (1.35)
	pH7-C	17.04 (1.61)	17.30 (2.10)	16.90 (1.62)	16.94 (1.71)
	pH7-D	17.59 (3.11)	17.64 (2.15)	18.64 (3.34)	18.17 (3.09)
	p value	0.023#	0.192*	0.342*	0.095#
Group pH5	pH5-Control	15.39 (1.52)	15.31 (1.90)	16.01 (3.17)	15.95 (2.29)
	pH5-A	18.89 (2.68)	17.26 (2.10)	18.81 (1.71)	18.76 (1.91)
	pH5-B	17.76 (1.10)	16.78 (1.85)	16.97 (1.93)	16.74 (1.92)
	pH5-C	17.86 (2.52)	18.57 (2.34)	18.23 (1.57)	18.88 (2.02)
	pH5-D	18.67 (3.08)	19.66 (3.19)	20.03 (1.46)	19.07 (2.06)
	p value	0.099#	0.173*	0.131*	0.115*
Group pH3	pH3-Control	12.65 (1.27)	11.85 (1.54)	10.77 (1.04)	10.42 (0.93)
	pH3-A	14.61 (1.97)	12.70 (2.34)	10.81 (1.39)	9.87 (1.78)
	pH3-B	16.36 (1.98)	15.59 (1.91)	15.05 (2.60)	14.67 (2.11)
	pH3-C	19.20 (1.94)	17.18 (2.54)	16.66 (2.67)	16.97 (2.21)
	pH3-D	18.67 (1.67)	19.03 (2.35)	18.64 (2.36)	18.75 (3.11)
	p value	0.000*	0.000*	0.000*	0.000*

Standard deviations in parentheses (n=7)

Results of one-way ANOVA* or Nonparametric Test (Kruskal Wallis) #

Table 5-4 Hardness (HV) of KM

		1 week	2 week	3 week	4 week
Group pH7	pH7-Control	68.62 (14.19)	68.16 (8.58)	68.04 (9.72)	67.83 (9.35)
	pH7-A	61.53 (10.79)	60.15 (5.36)	63.72 (12.39)	60.49 (8.37)
	pH7-B	69.83 (12.54)	66.88 (14.64)	66.99 (6.57)	65.59 (13.40)
	pH7-C	69.71 (8.80)	71.89 (9.31)	64.44 (9.36)	62.14 (10.30)
	pH7-D	61.84 (11.21)	67.68 (11.42)	65.99 (9.65)	63.29 (9.78)
	p value	0.459*	0.335*	0.917*	0.705*
Group pH5	pH5-Control	68.07 (9.39)	76.36 (13.93)	70.33 (17.48)	63.66 (10.09)
	pH5-A	66.09 (11.83)	65.47 (12.11)	60.25 (7.26)	65.09 (14.96)
	pH5-B	55.58 (5.01)	68.53 (12.14)	74.88 (17.34)	69.97 (13.40)
	pH5-C	66.83 (12.58)	64.19 (9.72)	73.45 (11.37)	68.10 (11.66)
	pH5-D	74.03 (17.18)	72.83 (17.05)	71.87 (14.72)	67.03 (10.72)
	p value	0.093*	0.404*	0.344*	0.886*
Group pH3	pH3-Control	22.81 (9.48)	23.46 (4.84)	18.41 (4.97)	18.85 (3.56)
	pH3-A	14.98 (4.86)	13.14 (3.33)	11.97 (2.89)	11.20 (2.64)
	pH3-B	17.46 (4.94)	19.65 (4.89)	16.55 (5.34)	13.52 (3.45)
	pH3-C	60.55 (11.78)	48.56 (8.48)	35.22 (3.50)	30.43 (4.79)
	pH3-D	80.47 (9.90)	40.86 (7.10)	65.02 (12.13)	50.17 (8.88)
	p value	0.000*	0.000*	0.000#	0.000#

Standard deviations in parentheses (n=7)

Results of one-way ANOVA* or Nonparametric Test (Kruskal Wallis) #

Table 5-5 Elastic modulus (GPa) of KM

		1 week	2 week	3 week	4 week
Group pH7	pH7-Control	14.82 (2.20)	14.78 (2.06)	15.09 (2.22)	15.56 (2.33)
	pH7-A	13.28 (1.17)	13.25 (1.37)	13.92 (1.44)	13.16 (1.53)
	pH7-B	14.51 (1.82)	14.50 (2.08)	14.59 (0.82)	14.20 (1.80)
	pH7-C	14.24 (1.05)	14.48 (1.39)	13.65 (1.14)	12.73 (1.01)
	pH7-D	14.88 (1.75)	14.94 (1.85)	15.15 (1.67)	14.77 (1.59)
	p value	0.386*	0.429*	0.351#	0.071*
Group pH5	pH5-Control	13.98 (2.16)	16.22 (2.11)	14.80 (2.27)	14.70 (1.54)
	pH5-A	13.73 (2.14)	13.90 (1.70)	13.57 (0.43)	13.58 (1.65)
	pH5-B	13.54 (1.49)	14.15 (1.18)	15.41 (3.01)	14.71 (2.43)
	pH5-C	14.15 (1.12)	13.57 (0.85)	14.92 (1.07)	14.27 (2.02)
	pH5-D	14.79 (2.92)	14.82 (3.06)	14.46 (1.57)	13.45 (1.33)
	p value	0.818*	0.180#	0.289#	0.568*
Group pH3	pH3-Control	8.86 (3.37)	8.33 (0.73)	6.98 (1.21)	7.26 (1.37)
	pH3-A	6.07 (1.53)	5.58 (1.29)	6.70 (3.78)	5.36 (1.23)
	pH3-B	6.19 (1.06)	6.50 (1.00)	6.33 (1.45)	5.57 (0.90)
	pH3-C	14.77 (3.21)	13.07 (2.89)	10.23 (1.38)	10.41 (2.19)
	pH3-D	16.40 (1.83)	11.01 (0.97)	14.08 (2.13)	12.88 (1.90)
	p value	0.000#	0.000#	0.000*	0.000*

Standard deviations in parentheses (n=7)

Results of one-way ANOVA* or Nonparametric Test (Kruskal Wallis)#

Table 5-6 Statistical comparison of hardness and elastic modulus (after 4 weeks) between storage media

Materials	Variables	Groups	Difference
FN	Hardness (HV)	pH 7	No significant difference*
		pH 5	No significant difference#
		pH 3	pH3-D, pH3-C > pH3-B > pH3-A, pH3-Control#
	Elastic modulus (GPa)	pH 7	No significant difference#
		pH 5	No significant difference*
		pH 3	pH3-D > pH3-B, pH3-Control, pH3-A pH3-C > pH3-Control, pH3-A*
KM	Hardness (HV)	pH 7	No significant difference*
		pH 5	No significant difference*
		pH 3	pH3-D > pH3-C > pH3-Control > pH3-B, pH3-A#
	Elastic modulus (GPa)	pH 7	No significant difference*
		pH 5	No significant difference*
		pH 3	pH3-D, pH3-C > pH3-Control, pH3-B, pH3-A*

Results of one-way ANOVA/Scheff's post-hoc test* and Kruskal-Wallis/Mann-Whitney test#
($p < 0.05$)

> indicates statistically significant difference in hardness/elastic modulus

The representative SEM micrographs are shown in Figure 5-3 to Figure 5-10. Both FN and KM showed similar surface structure in pH 7 and pH 5 storage media regardless of environmental calcium/phosphate levels. The specimen surface was intact and did not show obvious signs of glass particle degradation and matrix dissolution (Figures 5-3, 5-4, 5-7 and 5-8). The irregular cracks shown in these figures seem to be the results of glass-ionomer dehydration due to high vacuum for SEM preparation. A minor number of oval shape voids were also observed which appeared to be air voids formed during material mixing (Fukazawa *et al.*, 1987).

In pH 3 ionic media, a microscopic surface reaction layer was observed for FN and KM (Figure 5-5 and Figure 5-9). Thickness of this layer ranged from 15 to 70 μm and 10 to 75 μm for FN and KM respectively. When phosphate was present in the ionic media (Group pH 3-B, pH 3-C and pH 3-D), the surface reaction layer was thinner than those in phosphate-free storage media (Group pH 3-Control and pH 3-A). At higher magnification (×1000), two types of microstructural features were revealed in this surface reaction layer (Figure 5-6 and Figure 5-10). For Group pH 3-Control and pH 3-A, numerous voids and some protruded glass particles can be seen, which was different from the underlying normal glass-ionomer structure. Most voids were polygonal in shape and appeared to be the remains of lost glass particles. For Group pH 3-B, pH 3-C and pH 3-D, along with the porous structure as mentioned above, densely packed small particles were observed on the superficial surface. The surface reaction layer of these phosphate-containing groups was characteristic of two zones: the outer dense and the inner porous zones. Thickness of the inner porous zone was decreased with an increase in environmental phosphate levels.

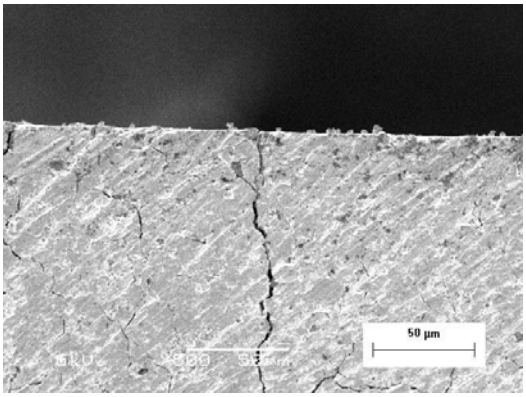

(a) pH 7-Control

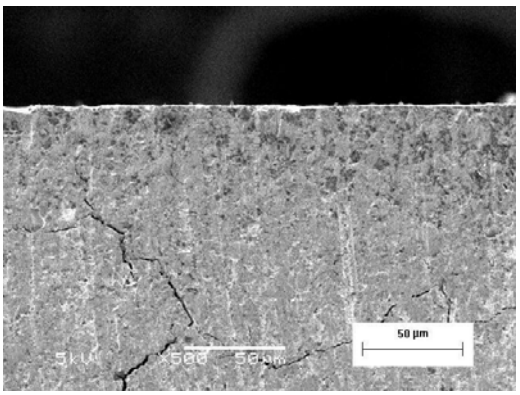

(b) pH 7-A

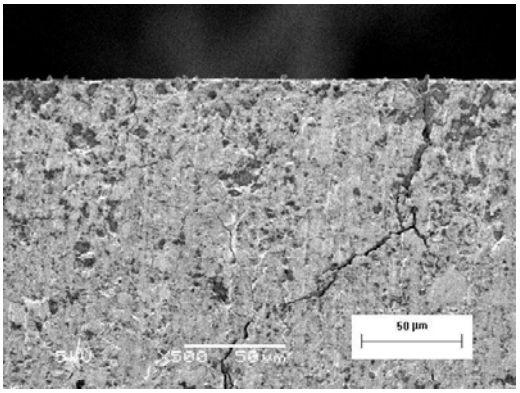

(c) pH 7-B

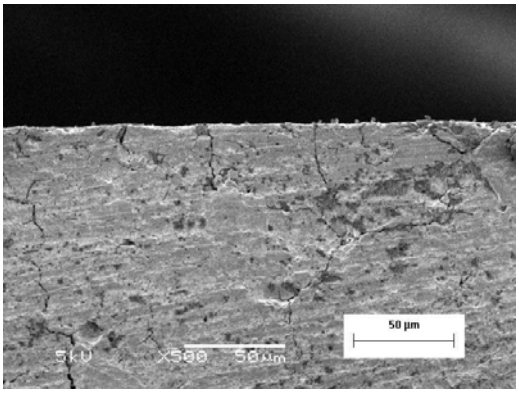

(d) pH 7-C

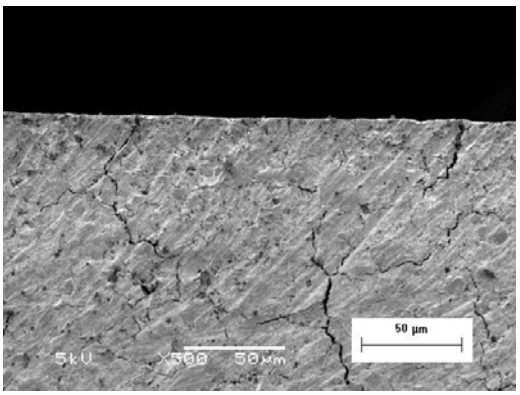

(e) pH 7-D

Figure 5-3 FN after conditioning at pH 7

(a) pH 7-Control, (b) pH 7-A, (c) pH 7-B, (d) pH 7-C, (e) pH 7-D

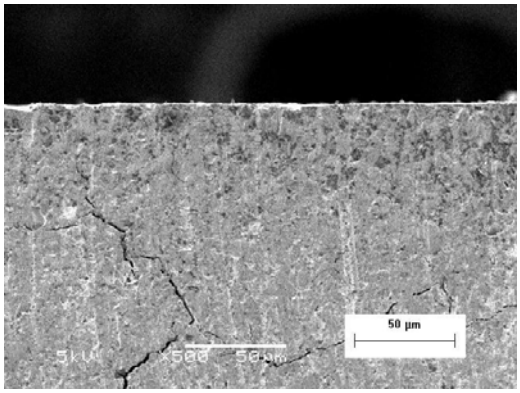

(a) pH 5-Control

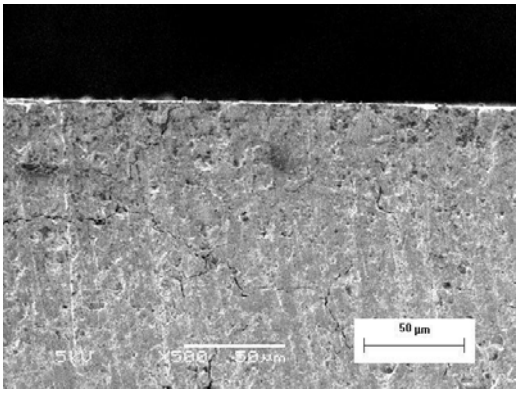

(b) pH 5-A

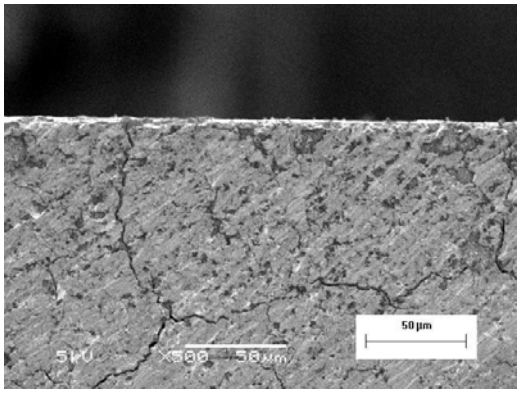

(c) pH 5-B

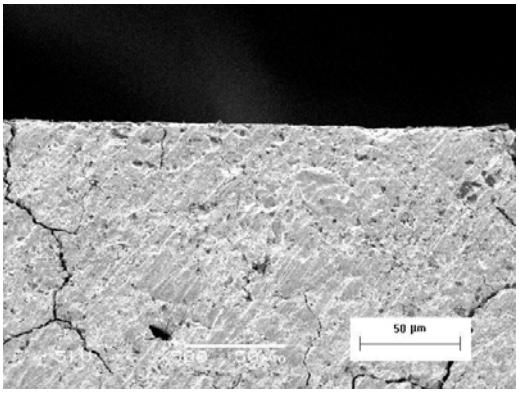

(d) pH 5-C

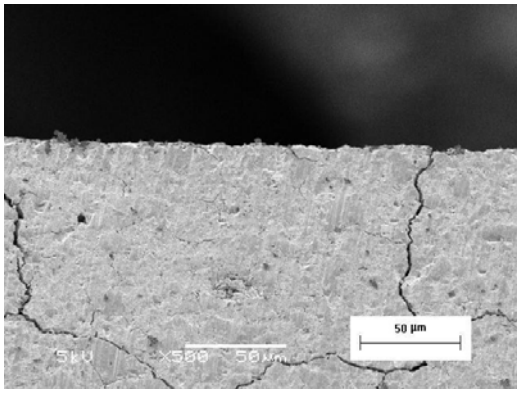

(e) pH 5-D

Figure 5-4 FN after conditioning at pH 5

(a) pH 5-Control, (b) pH 5-A, (c) pH 5-B, (d) pH 5-C, (e) pH 5-D

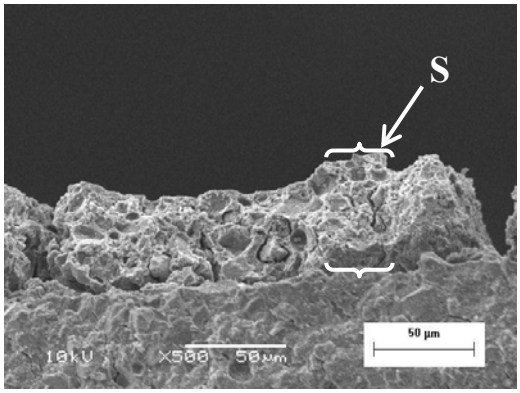

(a) pH 3-Control

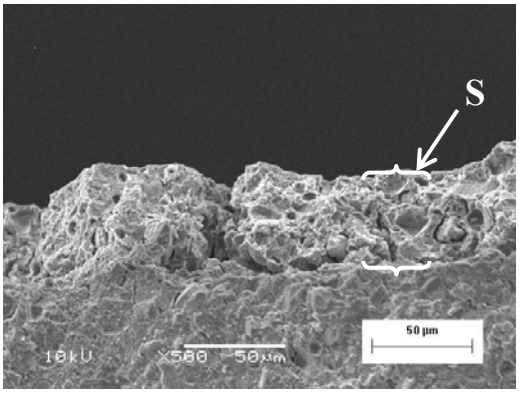

(b) pH 3-A

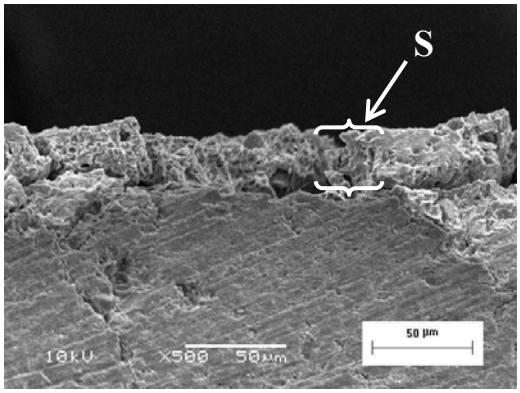

(c) pH 3-B

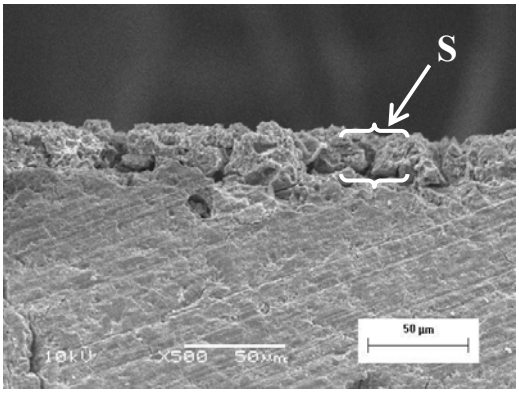

(d) pH 3-C

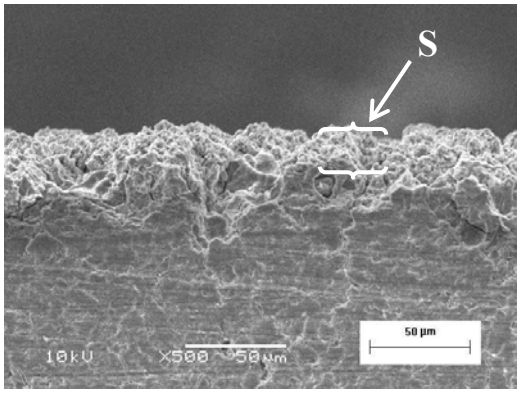

(e) pH 3-D

Figure 5-5 FN after conditioning at pH 3

(a) pH 3-Control, (b) pH 3-A, (c) pH 3-B, (d) pH 3-C, (e) pH 3-D

"S": surface reaction layer

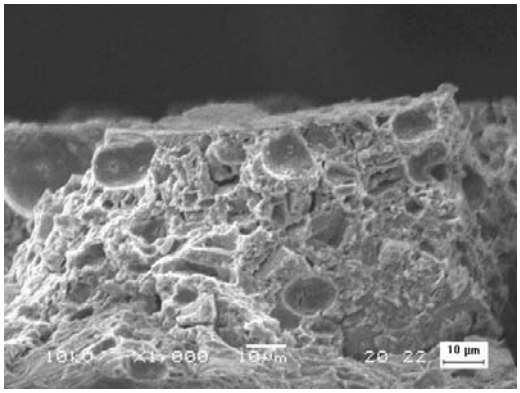

(a) pH 3-Control

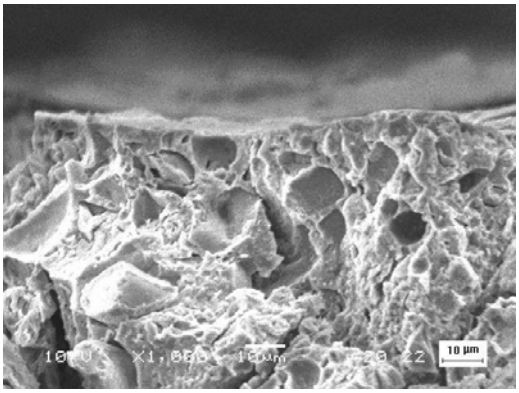

(b) pH 3-A

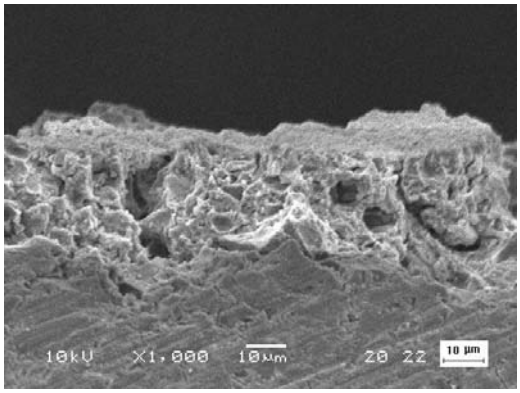

(c) pH 3-B

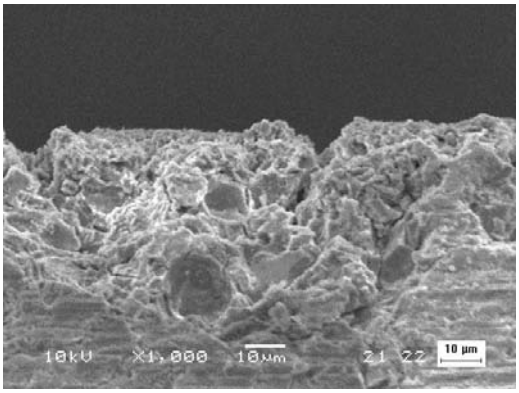

(d) pH 3-C

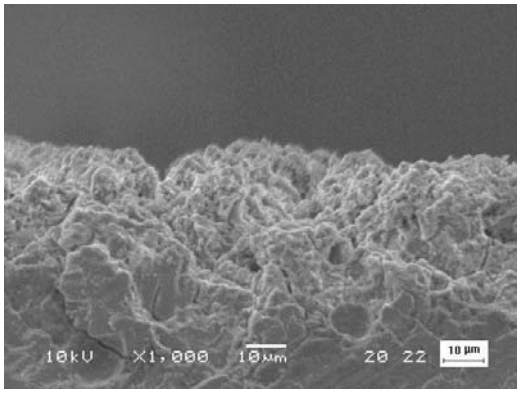

(e) pH 3-D

Figure 5-6 FN after conditioning at pH 3 (Magnification ×1000)

(a) pH 3-Control, and (b) pH 3-A **only show the porous structure;** (c) pH 3-B, (d) pH 3-C, and (e) pH 3-D **show both the outer dense and the inner porous structure**

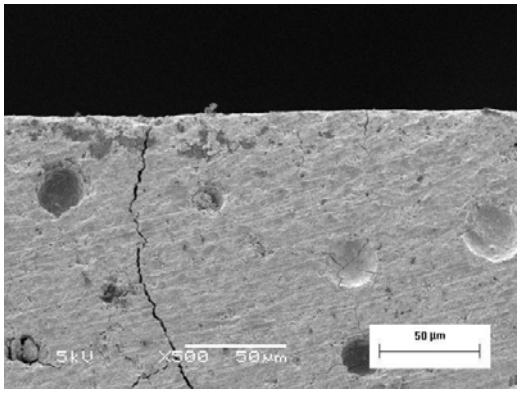

(a) pH 7-Control

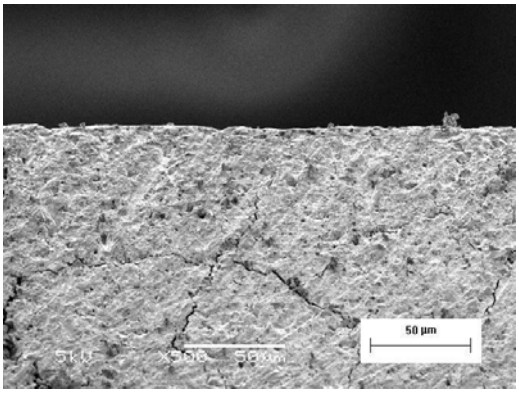

(b) pH 7-A

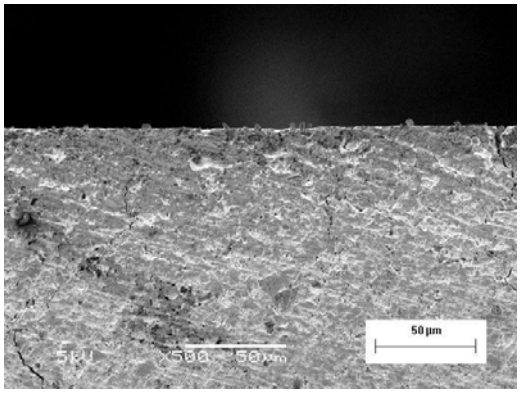

(c) pH 7-B

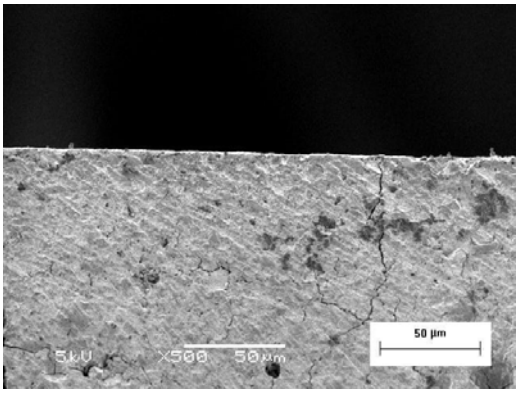

(d) pH 7-C

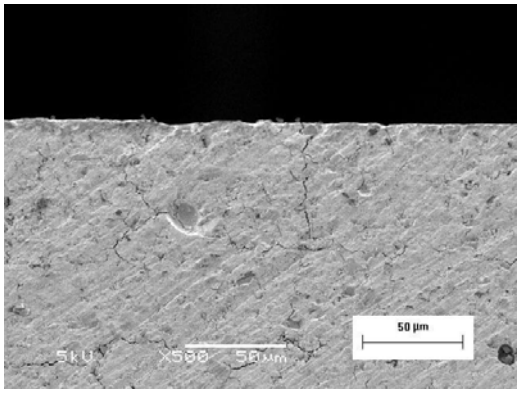

(e) pH 7-D

Figure 5-7 KM after conditioning at pH 7

(a) pH 7-Control, (b) pH 7-A, (c) pH 7-B, (d) pH 7-C, (e) pH 7-D

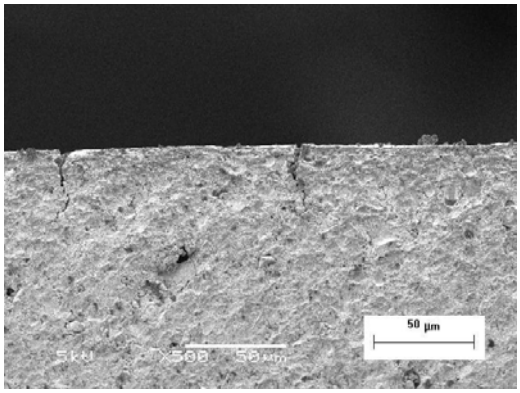

(a) pH 5-Control

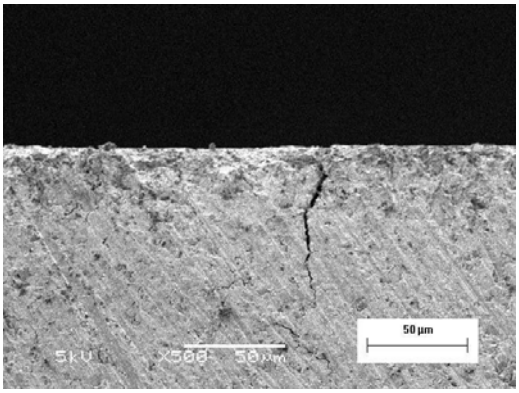

(b) pH 5-A

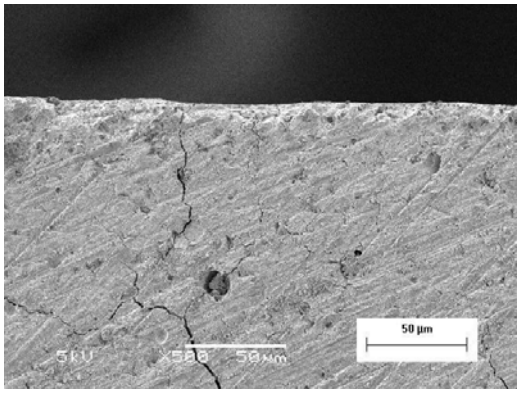

(c) pH 5-B

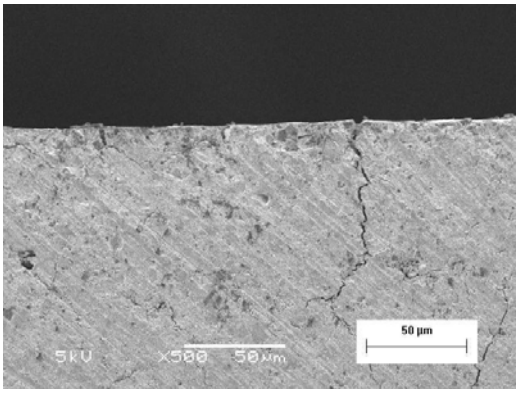

(d) pH 5-C

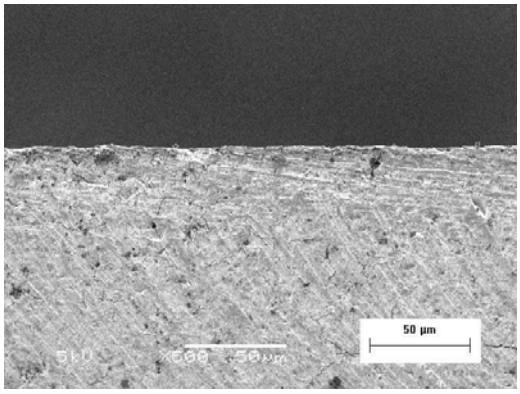

(e) pH 5-D

Figure 5-8 KM after conditioning at pH 5

(a) pH 5-Control, (b) pH 5-A, (c) pH 5-B, (d) pH 5-C, (e) pH 5-D

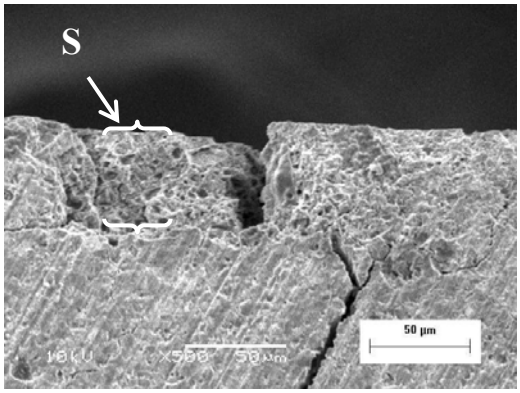

(a) pH 3-Control

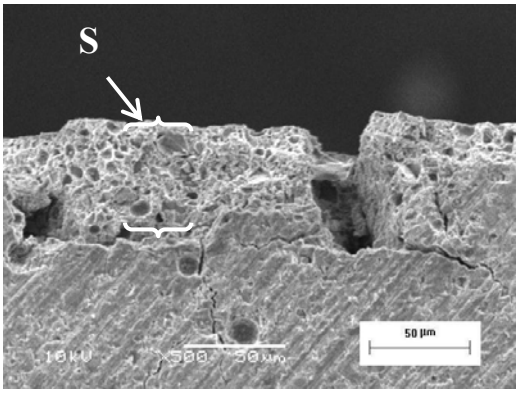

(b) pH 3-A

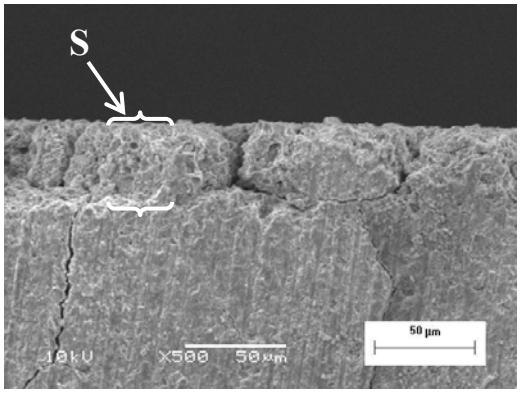

(c) pH 3-B

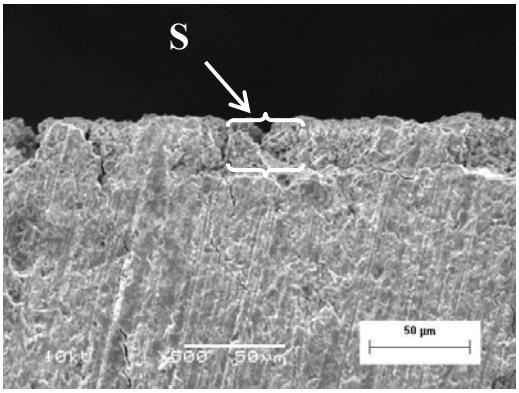

(d) pH 3-C

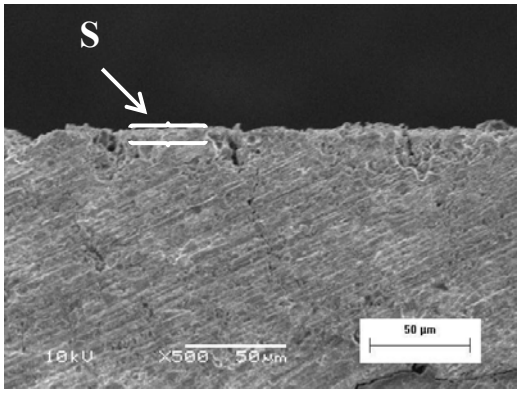

(e) pH 3-D

Figure 5-9 KM after conditioning at pH 3

(a) pH 3-Control, (b) pH 3-A, (c) pH 3-B, (d) pH 3-C, (e) pH3-D

"S": surface reaction layer

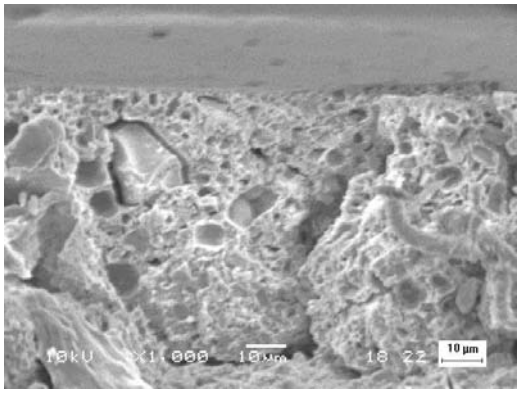

(a) pH 3-Control

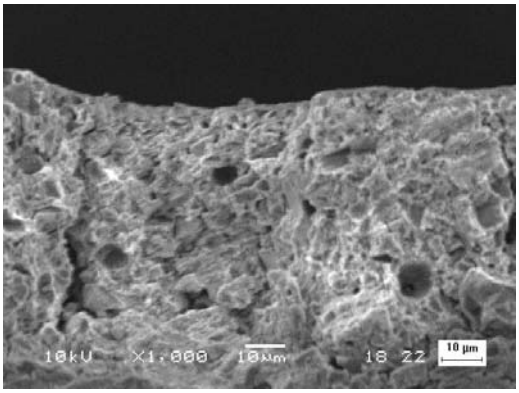

(b) pH 3-A

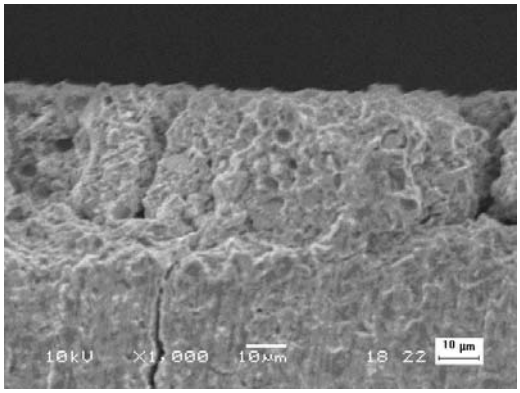

(c) pH 3-B

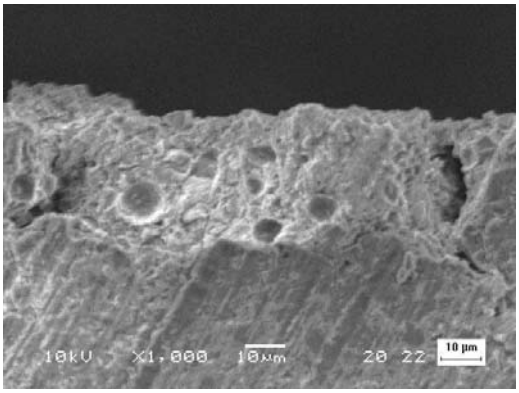

(d) pH 3-C

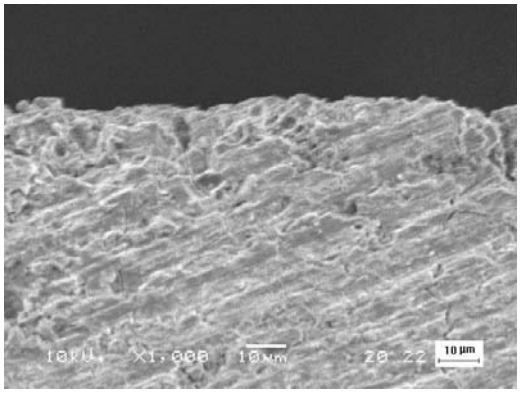

(e) pH 3-D

Figure 5-10 KM after conditioning at pH 3 (Magnification ×1000)

(a) pH 3-Control, and (b) pH 3-A **only show the porous structure;** (c) pH 3-B, (d) pH 3-C, and (e) pH 3-D **show both the outer dense and the inner porous structure**

5.4 Discussion

In this study, the effects of environmental calcium/phosphate and pH on GICs were evaluated with a depth-sensing micro-indentation testing and SEM. The most significant finding was that the effects of environmental calcium/phosphate on the properties of GIC were pH dependent.

In neutral media, FN and KM in the current study exhibited relatively constant hardness and elastic modulus within the four-week observation period. This indicates that the HVGICs gained most of their properties one week after setting. In this study, environmental calcium and phosphate in the range found in saliva did not "positively" influence surface hardness of FN and KM. This was in contrast with a previous study that reported a GIC in natural saliva had higher hardness than in water (Okada *et al.*, 2001). The disparity may be accounted by different glass-ionomer materials and hardness testing methods used. Fuji IX Fast used in this study is fast setting version of Fuji IX observed by Okada *et al.* (2001). The smaller glass particles and higher powder to liquid ratio in Fuji IX Fast (Yap *et al.*, 2003a) may lead to varied reactivity to environmental conditions. With regard to the methods, hardness testing is consistent for homogenous materials regardless of indentation loads applied (Chandler, 1999). However, for inhomogeneous materials, indentation load and resulting indentation depth influence hardness measurements. Using the depth-sensing micro-indentation testing in this study, depth of penetration was 20 ~ 40 μm. This was larger than most glass particles and the readings thus reflect the bulk property of

glass-ionomers. McKenzie *et al.* (2003b) found that the strength of GICs was not improved by exposure to natural saliva. Their results were supported by those of the present study. Cross-sectional view of the specimens with SEM revealed a non-disturbed surface structure, which suggests environmental calcium/phosphate at neutral pH had no significant effect on GICs evaluated in this study.

Previous studies have reported that the solubility of GICs increased with a decrease in environmental pH (Eisenburger *et al.*, 2003). Walls *et al.* (1988) found that GICs had good resistance to erosion at pH 6 or higher but were prone to erosion at pH 4. In this study, both FN and KM tested at pH 5 did not show a significant decrease in surface hardness and elastic modulus. Additionally, variation of environmental calcium/phosphate levels at pH 5 had no significant effects on these GICs. This phenomenon may be due in part to the improved properties of HVGICs. The latter was achieved by removing excess calcium ions from glass particles, decreasing particle size and increasing powder to liquid ratio (Guggenberger *et al.*, 1998). Combined with a relatively intact surface structure observed with SEM, the hardness and elastic modulus results suggest that HVGICs are not apt to degradation at pH 5.

Both FN and KM in this study exhibited diverse mechanical properties at pH 3 depending on environmental phosphate level. The hardness and elastic modulus of both materials were significantly lower in pH 3 than in pH 7 and pH 5 conditions when environmental calcium and phosphate were absent. This was in agreement with

other studies that found GICs degraded in acetic acid of pH 3 (Fukazawa *et al.*, 1990). However, when environmental phosphate was introduced to the acidic conditions of pH 3, both FN and KM showed improved surface hardness and elastic modulus. The varied mechanical properties correlated well with the changes in surface structure. A thinner surface reaction layer led to higher hardness and elastic modulus.

Thickness and structure of the surface reaction layer were also dependent on environmental phosphate level. The inner zone of the surface reaction layer, which presented numerous voids and some protruded glass particles, may be the result of glass particle degradation and matrix dissolution (el Badrawy *et al.*, 1993). When environmental phosphate level was higher, the inner degradation zone was thinner. On the other hand, the outer zone of dense structure was closely related to the presence of environmental phosphate. This suggests that phosphate salts may be the main component in the outer zone. The outer zone may render GICs less soluble in pH 3 conditions and contribute to a thinner inner degradation zone. The existence of the outer zone may be critical for the decrease in thickness of the microscopic surface reaction layer and maintenance of surface mechanical properties.

Although FN and KM have different compositions (one is strontium based while the other is calcium based), they showed the similar trends under pH 3 conditions. Environmental calcium did not positively affect these materials while environmental phosphate improved surface mechanical properties of GICs. The significant effects of environmental phosphate on GICs in pH 3 acidic conditions may be due to the

following mechanism. When H^+ diffuses into GIC and attacks the matrices and glass particles, Al^{3+}, Ca^{2+} or Sr^{2+} cations are released from the matrix backbone and diffuse outwards. Simultaneously, environmental phosphate may form complexes with these intrinsic metal cations. These phosphate salts may retain mechanical properties of GICs as within silicate cements (Kent *et al.*, 1969). The newly formed salts may also prevent further H^+ diffusion by reaction with H^+ in situ, therefore, causing less matrix salt bridge and glass particle decomposition by H^+. Thus, thickness of the inner degradation zone in the surface reaction layer may be decreased by supplementary environmental phosphate.

From the results of this study, the positive effect of environmental phosphate on GICs at low pH (pH 3) should be given more attention. The mechanism of this phenomenon warrants further investigations. From a clinical view point, increasing environmental phosphate may lead to better performance of glass-ionomer restoratives when challenged by acids *in vivo*.

5.5 Conclusions

The effects of environmental calcium/phosphate and pH on surface mechanical properties and structure of HVGICs were evaluated in this study. Both FN and KM showed relatively consistent hardness/elastic modulus and intact surface structure in pH 7 and pH 5 conditions regardless of environmental calcium/phosphate levels. When exposed to pH 3 acidic conditions, hardness and elastic modulus of HVGICs

varied depending on environmental phosphate levels. With increasing phosphate levels, hardness and elastic modulus of these GICs were significantly increased. A surface reaction layer which featured outer dense and inner porous zones was observed. The thickness of these layers differed in accordance with environmental phosphate levels. The results suggest that environmental phosphate may protect GICs from acid degradation through surface modifications of GICs.

Chapter 6

Surface Characterization of GICs Exposed to Acidic Conditions: Effects of Environmental Calcium/Phosphate

6.1 Introduction

In Chapter 5, the interaction of two HVGICs with environmental calcium/phosphate and pH was investigated using a depth-sensing micro-indentation method and SEM approach. Results showed that the interaction was pH and environmental calcium/phosphate dependent. At pH 7 and pH 5, environmental calcium/phosphate had no significant effects on surface hardness and elastic modulus of these HVGICs, while environmental phosphate protected GICs at pH 3.

A reaction layer on the surface of glass-ionomer specimens was observed at pH 3. The thickness of the surface reaction layer was decreased by environmental phosphate. The surface reaction layer had two characteristic zones. The inner zone was porous while the outer zone was dense. The presence of the outer zone was closely related to environmental phosphate.

These results indicate that surface compositions, structures and mechanical properties of GICs may be changed after interaction with environmental phosphate anion in acidic conditions. Surface analytical techniques are thus warranted to analyze the surface reaction layer in depth.

As mentioned in chapter 2.4, a variety of surface analytical methods have been

used to characterize the surface of GICs. These include scanning electron microscopy (SEM), laser scanning confocal microscopy (LSCM), acoustic microscopy, solid state nuclear magnetic resonance spectroscopy (NMR), Raman spectroscopy (RM), Fourier transform infrared spectroscopy (FTIR), secondary ion mass spectrometry (SIMS), X-ray photoelectron spectroscopy (XPS), electron probe microanalysis (EPMA) and energy dispersive X-ray analysis (EDS) *etc.* (el-Badrawy *et al*., 1993; Fano *et al*., 2001; Denisova *et al*., 2004; Watts, 1998; Lloyd *et al*., 1999; Young *et al*., 2000, 2004; Jones *et al*., 2003; Okada *et al*., 2001; Yli-Urpo *et al*., 2005b). As each technique has its strength and weakness, a detailed surface characterization therefore requires the use of more than one technique.

In this study, the mechanical properties, chemical compositions and morphological features of the surface reaction layer were investigated using a nano-indentation testing, FTIR-ATR, EDS, SEM and mechanical profiler respectively. Nano-indentation testing allows for the determination of mechanical properties (hardness and elastic modulus) of nm to μm scale layers by low loading and high spatial resolution. FTIR-ATR and EDS provide organic and inorganic information (chemical bond and element constitution) of the superficial surface of samples. Surface microstructure was observed using SEM and surface roughness was measured using profilometry. The details of these methods have been reviewed earlier in Chapter 2.4.

The present study examined and compared the surface characteristics of GICs

exposed to acidic conditions (pH 3) with varying concentrations of calcium/phosphate. The aim was to characterize the surface reaction layer and explore the possible mechanism of interaction between GICs and environmental calcium/phosphate and pH.

6.2 Materials and methods

6.2.1 Specimen preparation

Fuji IX Fast (FN) and KetacMolar (KM) were activated/mixed according to manufacturers' instructions and injected into customized molds. An acrylic mold with square recesses (3 mm long × 3 mm wide × 2 mm deep) was used for nano-indentation testing while a split Teflon mold (10mm in diameter and 1mm in thickness) was employed for other measurements. The molds were filled with materials, covered with an acetate strip and compressed using finger pressure with a glass slide to extrude excess material. The specimens were randomly divided into 5 groups (n=3), kept in 100% humidity at 37 ºC for 1 hour and stored in acidic conditions for 4 weeks. The pH of the storage media was fixed at 3 and the levels of calcium/phosphate were varied as shown in Table 6-1, which was similar to those in chapter 5. The calcium and phosphate concentration of Group B solution was equal to that of remineralization/demineralization solutions recommended by ten Cate and Duijsters (1982). The total amount of calcium and phosphate of Group A, C and D were all equal to that of Group B. Group A and D only contained calcium or phosphate, while Group C consisted of equal ratio of calcium and phosphate. After conditioning, the specimens were subjected to the following surface analysis.

Table 6-1 Compositions of acidic conditions

	$CaCl_2 \cdot 2H_2O$ (mM)	KH_2PO_4 (mM)	KCl (mM)	Acetic Acid (mM)	pH
Control group	0	0	150	50	3
Group A	2.4	0	150	50	3
Group B	1.5	0.9	150	50	3
Group C	1.2	1.2	150	50	3
Group D	0	2.4	150	50	3

6.2.2 Nano-indentation testing

Hardness and elastic modulus of specimens were determined using a nano-indentation testing (MTS Nano Indenter® XP, USA) (Figure 6-1). The nano-indentation testing employed a CSM technique and was capable of continuously recording load, displacement and stiffness throughout an indentation cycle. Hardness and elastic modulus were reported as a function of indentation penetration depth.

A Berkovich triangular pyramidal indenter with a resonant frequency of 45 Hz (for CSM technique) was used in this study. The indentation procedures were computer-controlled and consisted of four segments: approaching to surface, loading to the maximum depth, holding at the maximum depth and unloading. In the loading segment, a constant strain rate of 0.05 (1/s) was imposed until a penetration depth of 10 μm was reached and the load was defined as the maximum load. This maximum load was held constant for 10 s (holding segment) and subsequently unloaded at the same rate as loading. At the end of the unloading segment, a second hold segment at 10% of the maximum load was used to correct thermal drift (Shen *et al.,* 2003).

Hardness and elastic modulus were determined using the following equations.

$$H = \frac{P_{\max}}{A_{\max}} \tag{6-1}$$

$$E = \frac{\sqrt{\pi}}{2}\frac{1}{\sqrt{A_{\max}}}S\left(1-\nu^2\right) \tag{6-2}$$

where P_{max} is the maximum indentation load, A_{max} is the maximum projected contact area, and S is contact stiffness. ν is Possion's ratio and 0.35 was chosen in this study.

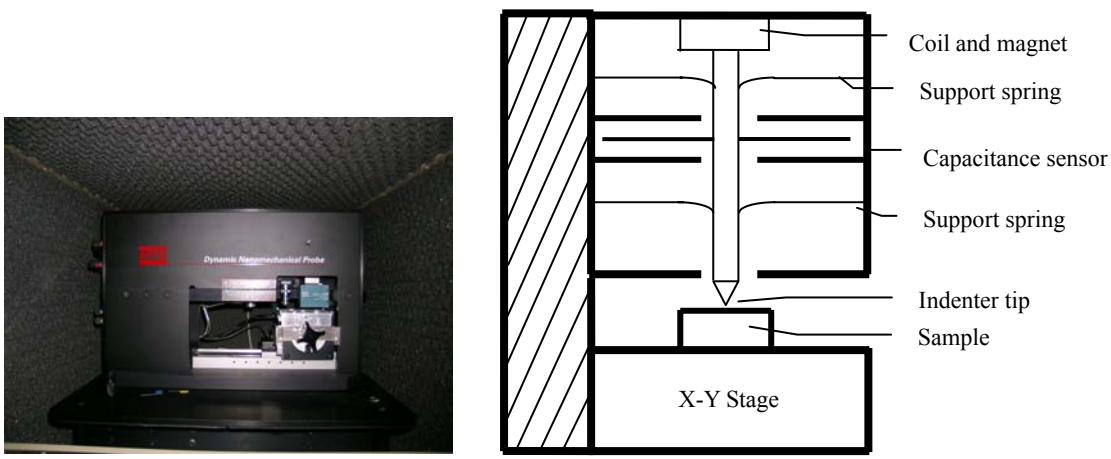

Figure 6-1 Photo and schematic of MTS Nano Indenter® XP

Ten indentations were performed on different locations of each specimen. Therefore, a total of 30 stiffness, hardness and elastic modulus measurements were obtained for each group of testing. Hardness and elastic modulus at maximum displacement (10μm) were compared between acidic conditions using Kruskal-Wallis/Mann-Whitney test ($p<0.05$).

6.2.3 FTIR-ATR

Chemical bond information of the specimens was determined with a Fourier transform infrared (FTIR) spectrometer. An attenuated total reflectance (ATR) accessory was attached and allowed for solid specimen sampling (FTIR Spectrum 2000, PerkinElmer Instruments Inc., USA) (Figure 6-2). The FTIR-ATR system was controlled by commercial software (Spectrum, PerkinElmer Instruments Inc., USA).

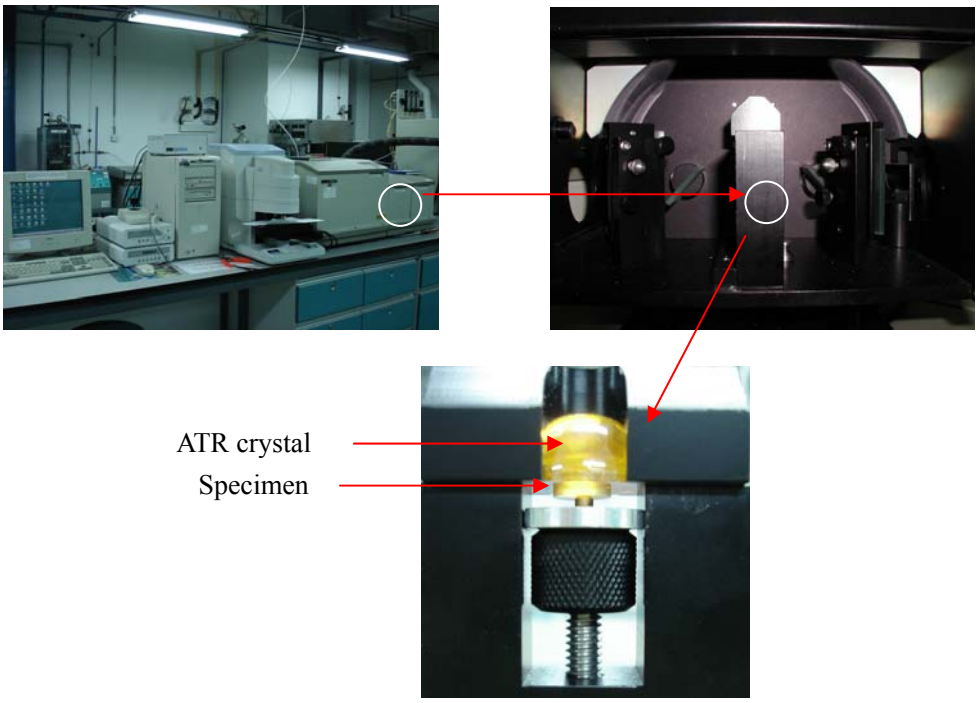

Figure 6-2 FTIR instrumentation and ATR apparatus

After background scanning was executed, the specimen was secured in the ATR apparatus. The number of scans was fixed at 16 for spectrum collection. FTIR spectra were obtained using a mid-infra red source with wavelength range between 400 and 4000 cm^{-1} and resolution of 4 cm^{-1}.

6.2.4 SEM-EDS

Surface structure was observed with a JSM-5600 SEM (JEOL, Japan). Element constitution analysis was carried out using an Oxford ISIS EDS system connected to the JSM-5600 SEM microscope. Specimens were coated with a thin layer of gold and mounted in the vacuum chamber. Secondary electron images and energy dispersive X-ray analysis (EDS) were taken with a standardized method using an accelerating voltage of 15 KV and a working distance of 21 mm. The analysis was done using a spot size of 40 nm and a magnification of ×2000. Element composition was recorded as atomic percentage.

6.2.5 Surface profilometry

Surface roughness was measured and recorded using a stylus profilometer with a probe diameter of 2 μm (Surftest SV-402, Mitutoyo Instruments, Tokyo, Japan). The vertical and horizontal magnifications were set at ×2000 and ×50. One measurement was taken across a length of 0.25 mm × 4. Ten measurements were performed on different locations of each specimen and a total of 30 readings were obtained for each group. The roughness parameter was recorded as average roughness (Ra). Ra was compared between acidic conditions with different calcium/phosphate concentrations using ANOVA/post-hoc Scheffe's test ($p<0.05$).

6.3 Results

6.3.1 Nano-indentation testing

Figure 6-3 and Figure 6-4 show the depth profile of contact stiffness as a function of indentation depth for FN and KM respectively. At the very beginning of indenter

penetration, there was a linear relation between stiffness and indentation depth. With increasing indentation depth, stiffness deviated from the linear trend as seen from the representative curves in Figures 6-3(b), 6-3(c), 6-4(b) and 6-4(c). As mentioned in chapter 2.4.1.2, contact stiffness and penetration depth is not in linear relationship for non-uniform materials. The contact stiffness results suggest that the surface layers of FN and KM in acidic conditions may not be uniform and have different properties from the original material.

The hardness and elastic modulus as a function of indentation depth for FN and KM are shown in Figure 6-5 and Figure 6-6, respectively. For nano-indentation testing, calculation errors are generally present in the first few hundred nm due to the indentation size effect arising from uncertainty of indentation tip area function, surface roughness of the specimens and others (Padama *et al.*, 2003). In this study, hardness and elastic modulus of the first penetration depth of 1 μm were not reported for these reasons. The hardness and elastic modulus value at the maximum depth of 10 μm for both FN and KM are shown in Table 6-2. The statistical comparison between acidic conditions is summarized in Table 6-3.

Similar patterns of hardness and elastic modulus with indentation penetration depth were observed for both FN and KM in the acidic conditions with different calcium/phosphate levels. Hardness and elastic modulus value increased with the increasing indentation penetration depth. The magnitude of increase in hardness and elastic modulus for Group D, C and B was higher than that of Group A and Control group (Figure 6-5 and Figure 6-6). At the maximum penetration depth of 10 μm, the higher phosphate level group (Group D and C) showed significantly greater hardness and elastic modulus than the control group (Table 6-3).

(a)

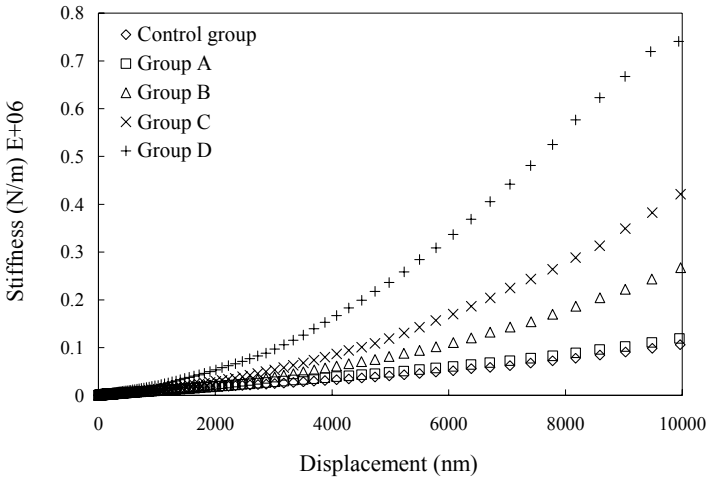

(b)

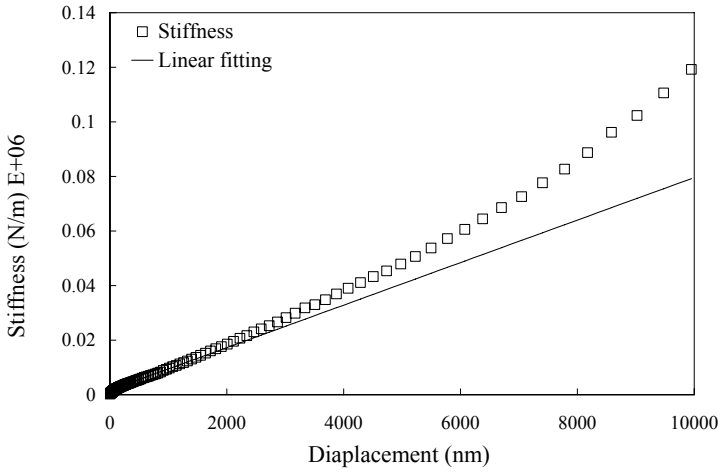

(c)

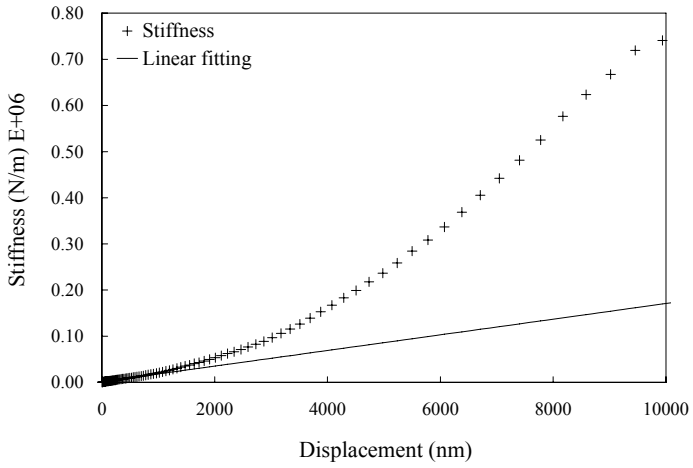

Figure 6-3 Contact stiffness *vs.* displacement curves for FN

(a) Acidic conditions, (b) Group A, (c) Group D

*The solid line represents the linear extrapolation based on the initial linear part of the curve

(a)

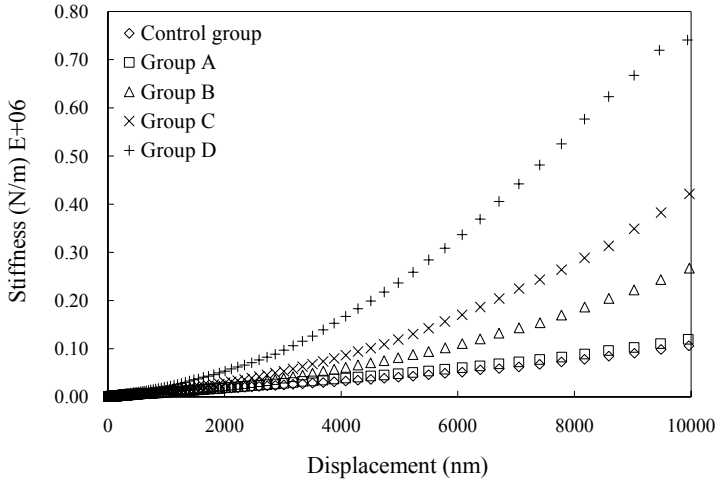

(b)

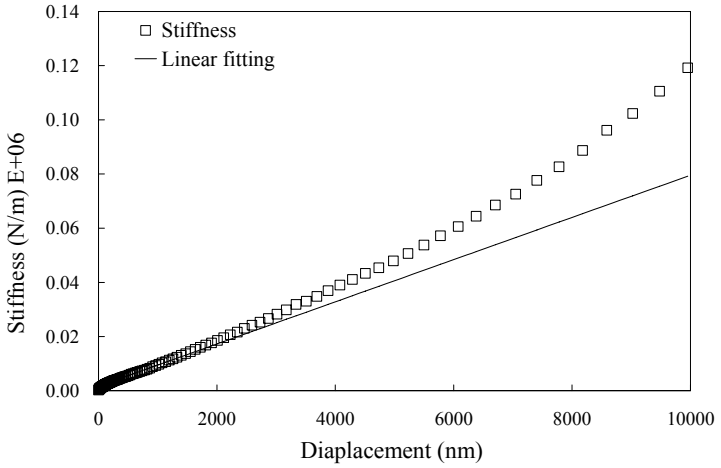

(c)

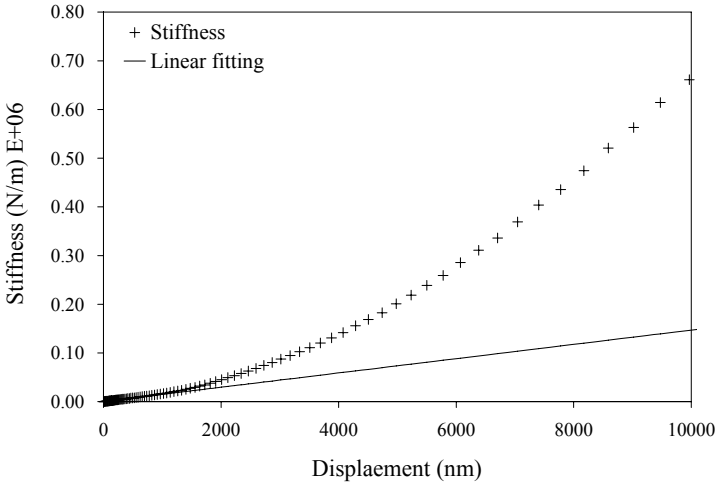

Figure 6-4 Contact stiffness *vs.* displacement curves for KM

(a) Acidic conditions, (b) Group A, (c) Group D

*The solid line represents the linear extrapolation based on the initial linear part of the curve

(a)

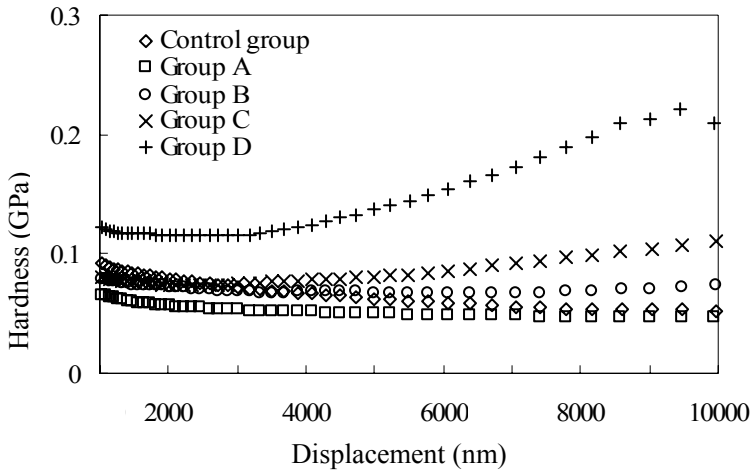

(b)

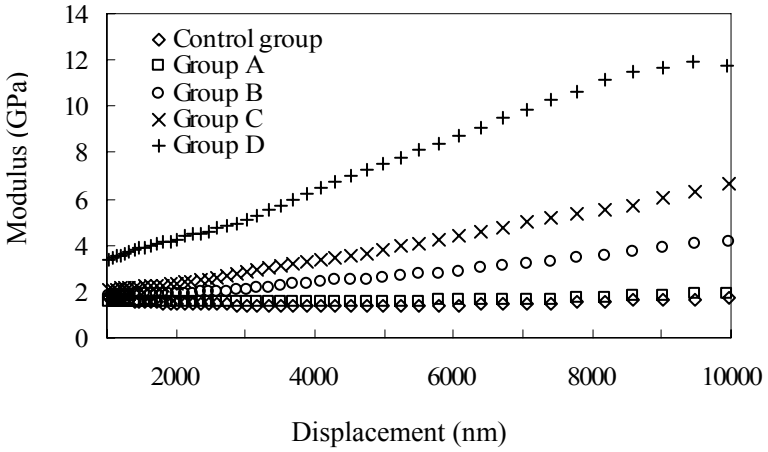

Figure 6-5 Hardness (a) and elastic modulus (b) as a function of displacement for FN

(a)

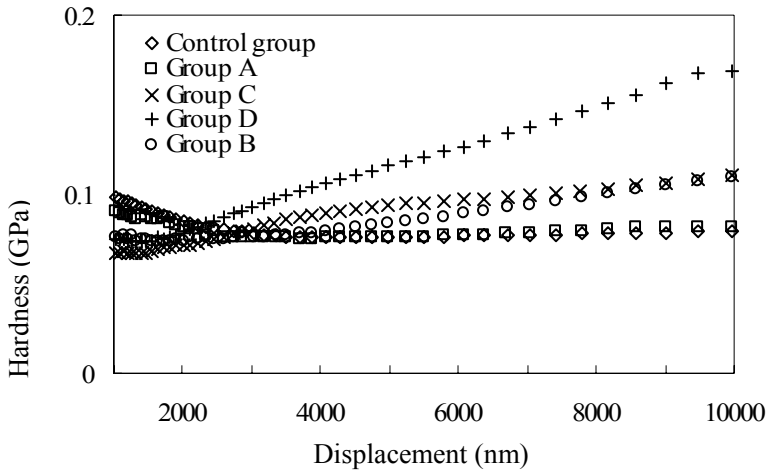

(b)

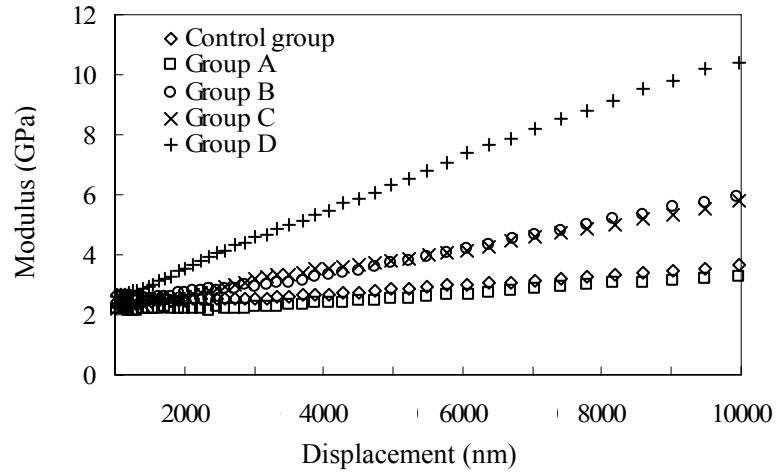

Figure 6-6 Hardness (a) and elastic modulus (b) as a function of displacement for KM

Table 6-2 Hardness and elastic modulus of FN and KM (at displacement of 10 μm)

	FN		KM	
	Hardness (GPa)	**Elastic modulus (GPa)**	**Hardness (GPa)**	**Elastic modulus (GPa)**
Control group	0.053 (0.025)	1.730 (0.755)	0.079 (0.008)	3.591 (0.355)
Group A	0.046 (0.012)	1.911 (0.420)	0.082 (0.018)	3.269 (0.457)
Group B	0.075 (0.015)	4.256 (0.685)	0.110 (0.020)	5.966 (0.841)
Group C	0.112 (0.026)	6.660 (0.997)	0.110 (0.022)	5.834 (0.770)
Group D	0.240 (0.071)	12.747 (2.024)	0.176 (0.047)	10.567 (1.406)

Standard deviations in parentheses

Table 6-3 Statistical comparison of hardness and elastic modulus between acidic conditions (at displacement of 10μm)

Materials	**Variables**	**Difference**
FN	Hardness	Group D > Group C > Group B > Control group, Group A
	Elastic modulus	Group D > Group C > Group B > Control Group, Group A
KM	Hardness	Group D > Group C , Group B > Group A, Control group
	Elastic modulus	Group D > Group C , Group B > Group A, Control group

Results of Kruskal-Wallis/Mann-Whitney test[#] ($p < 0.05$)

> indicates statistically significant difference in hardness and elastic modulus

6.3.2 FTIR-ATR

FTIR spectra of FN and KM between 800 cm^{-1} and 1800 cm^{-1} are shown in Figure 6-7 and Figure 6-8. To clearly show the location of peaks, the Y-axis scale of peak height was slightly varied for different groups.

In the spectra, two groups of peaks (corresponding to polycaboxylates and glass particles) were observed. As reviewed in chapter 2.4.3, the band assigned to symmetric and asymmetric stretch of COO- for metal polycarboxylate and carboxylate salts occur between 1400 cm^{-1} and 1620 cm^{-1}. Si-O-Si asymmetric stretching and Si-O vibration band are within 900 cm^{-1} to 1200 cm^{-1}, which are overlapped by phosphate stretching (Young, 2002; Deb and Nicholson, 1999). In this study, the aluminum polyacrylate (Al-PAA) band detected was at 1625~1630 cm^{-1} and 1460 cm^{-1}. For strontium/calcium polyacrylates (Sr-PAA and Ca-PAA), the band was at 1560 cm^{-1} and 1410 cm^{-1}. The peak centered at 1060 cm^{-1} was assigned to silicate network or phosphate. The strong peak at 1630/1625, 1560 and 1060 cm^{-1} was used to interpret Al-PAA, Sr/Ca-PAA and silicate/phosphate as shown in Figure 6-7 and Figure 6-8.

The variation of the band at 1060 cm^{-1} was significant and correlated well with environmental phosphate level. Compared to the weak band at 1060 cm^{-1} in control group, this peak was relatively higher with increasing environmental phosphate levels. This trend was observed for both FN and KM. The increased 1060 cm^{-1} peak in Group B, C and D may correlate to the increased phosphate level.

The peaks of polyacrylates also varied with environmental phosphate or calcium. When calcium was added (Group A), the peak height ratio of 1560 cm^{-1}:1625 cm^{-1} (Sr/Ca-PAA : Al-PAA) increased in FN and KM. The addition of environmental phosphate (Group D) increased the peak height of Sr-PAA (1560 cm^{-1}) for FN and Al-PAA (1630 cm^{-1}) for KM.

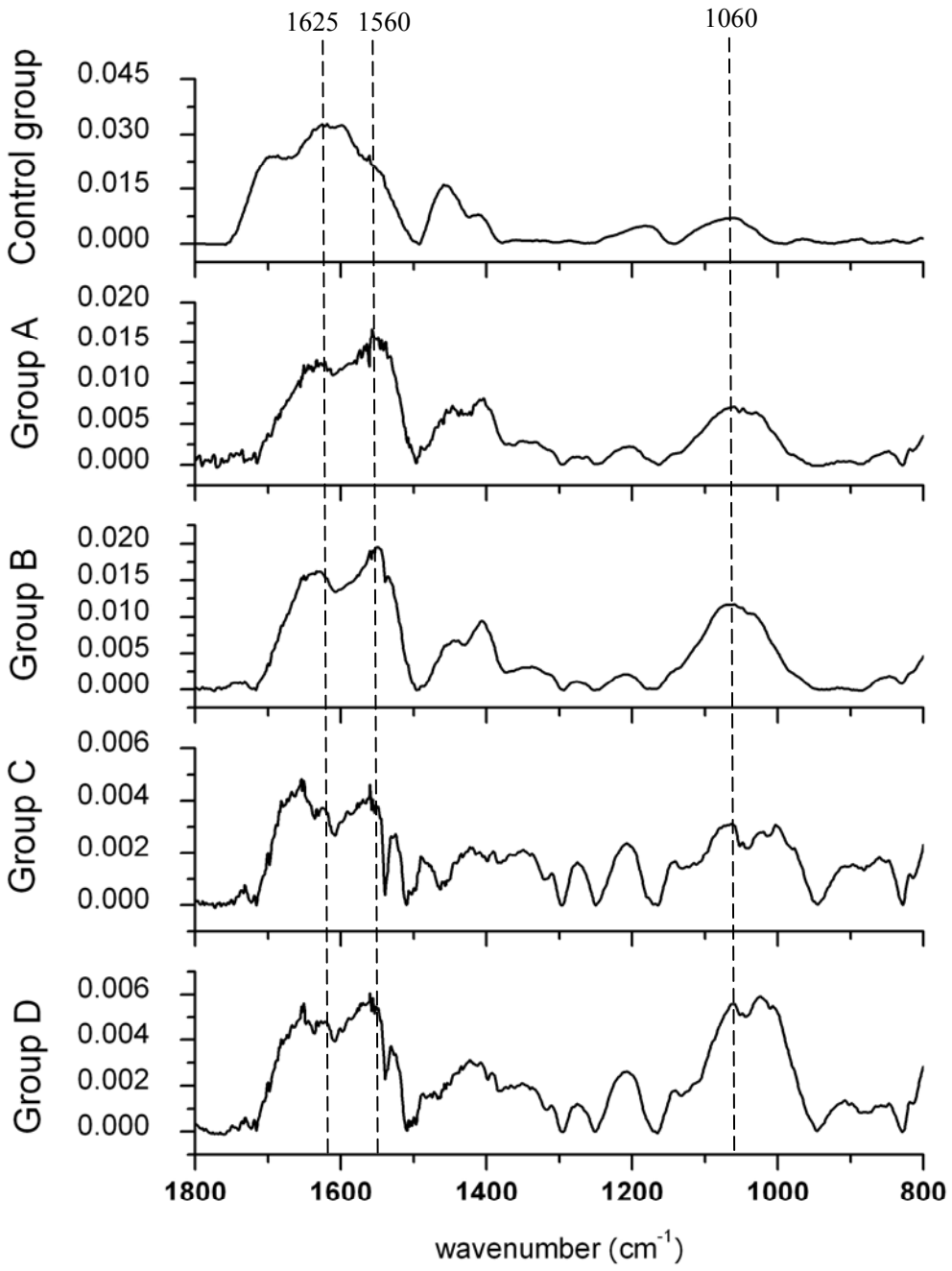

Figure 6-7 FTIR spectra of FN

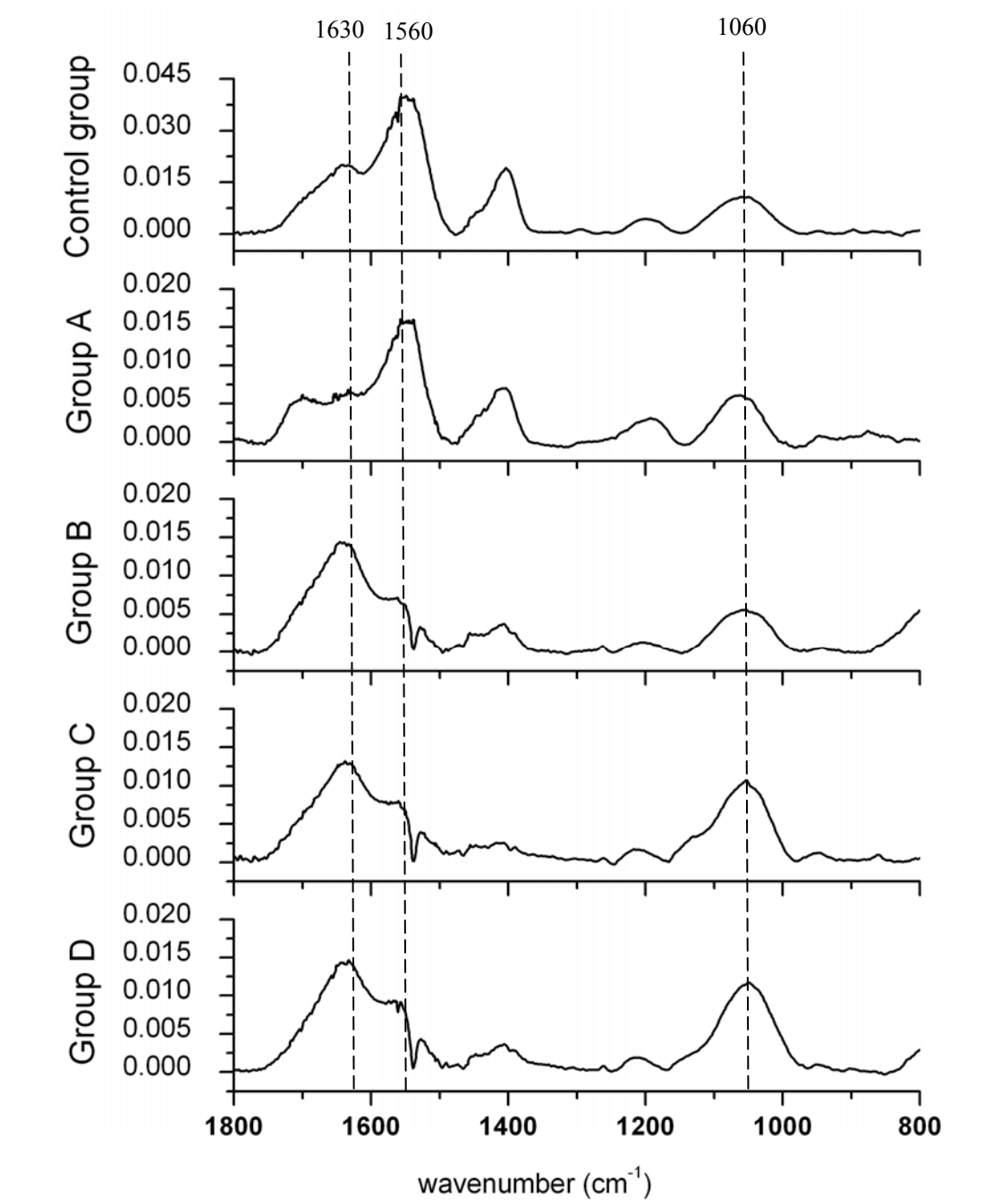

Figure 6-8 FTIR spectra of KM

6.3.3 EDS

Surface element compositions (atomic %) of FN and KM in acidic conditions of varying calcium/phosphate levels are reflected in Table 6-4 and Table 6-5. The main components of FN and KM, i.e. sodium (Na), aluminum (Al), silicon (Si), phosphorus (P), calcium (Ca) and strontium (Sr), were present. FN and KM also contained fluoride which was not measured due to technique limitation.

Exposure to acidic conditions without additional calcium/phosphate (Control group) resulted in a surface with high Si, Al and Sr content for FN, and high Si, Al and Ca content for KM.

When environmental calcium was present (Group A), the Ca content of KM increased significantly while FN only showed a lower increase in Ca content.

When environmental phosphate was present (Group B, C and D), P was detected in both FN and KM. The P content in FN and KM surface increased with increasing environmental phosphate level. Sr content for FN and Ca content for KM were increased accordingly.

Table 6-4 Surface compositions (atomic %) of FN measured with EDS

	Na (%)	Al (%)	Si (%)	P (%)	Ca (%)	Sr (%)
Control group	1.49 (0.20)	30.38 (0.73)	64.53 (1.38)	*	0.81 (0.10)	2.78 (0.50)
Group A	0.78 (0.32)	41.34 (0.41)	54.28 (0.07)	*	1.97 (0.38)	1.64 (0.43)
Group B	1.03 (0.08)	16.04 (0.35)	75.05 (0.39)	4.69 (0.40)	1.10 (0.07)	2.06 (0.31)
Group C	0.66 (0.09)	12.21 (1.38)	77.18 (1.89)	5.77 (0.47)	1.16 (0.23)	3.03 (0.25)
Group D	0.80 (0.12)	15.99 (0.58)	67.79 (1.05)	10.86 (0.82)	0.87 (0.31)	3.70 (0.25)

Standard deviations in parentheses

* stands for element concentration lower than the detection limits

Table 6-5 Surface compositions (atomic %) of KM measured with EDS

	Na (%)	Al (%)	Si (%)	P (%)	Ca (%)	Sr (%)
Control group	7.23 (0.54)	20.09 (0.20)	59.17 (0.47)	*	13.52 (0.28)	*
Group A	4.87 (0.86)	22.60 (0.88)	51.08 (1.15)	*	21.45 (0.54)	*
Group B	4.89 (0.23)	7.00 (0.34)	40.80 (0.50)	4.42 (1.04)	42.89 (0.38)	*
Group C	5.02 (0.61)	11.14 (0.21)	43.15 (0.29)	5.63 (0.48)	35.06 (0.23)	*
Group D	4.27 (0.09)	8.95 (0.32)	37.20 (0.98)	6.48 (0.59)	43.10 (0.73)	*

Standard deviations in parentheses

* stands for element concentration lower than the detection limits

6.3.4 SEM

The topographical changes in FN and KM conditioned in acidic conditions with varying calcium/phosphate levels are shown in Figure 6-9 and Figure 6-10. The occasional cracks observed in photomicrograph are largely the result of dehydration under vacuum.

As can be seen in Figure 6-9 (a) and Figure 6-10 (a), FN and KM exposed to the acidic condition without additional calcium and phosphate (Control group) had relatively smooth surfaces interrupted by intermittent pores.

With an addition of calcium (Group A) as shown in Figure 6-9 (b) and Figure 6-10 (b), both FN and KM exhibited similar surface morphology to the control group.

When phosphate was added (Group D) as shown in Figure 6-9 (e) and Figure 6-10 (e), the surface of both FN and KM was covered by numerous small particles. These particles had irregular shape and varying particle size. The particles were in range of 5 μm for FN and larger for KM. A similar change, but to a lesser extent, was also noted in Group B and C shown in Figures 6-9 (c), (d) and Figures 6-10 (c), (d).

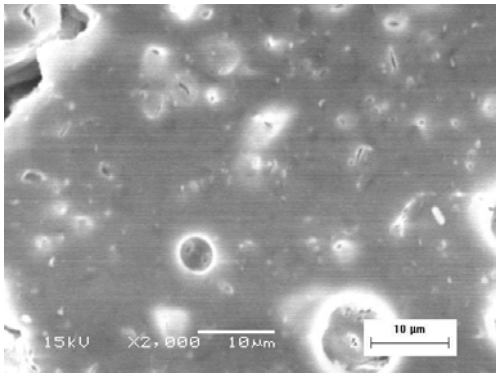

(a) Control group

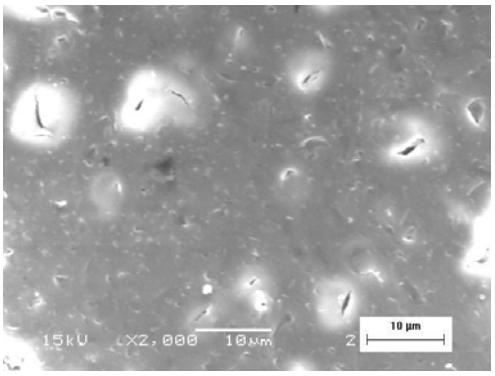

(b) Group A

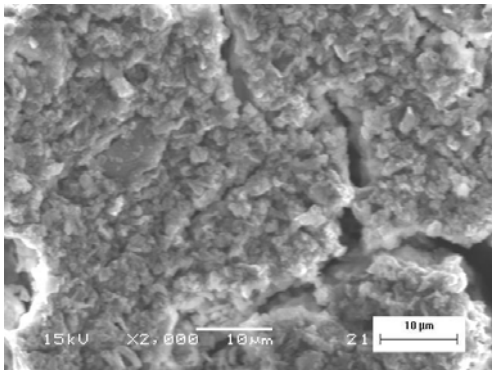

(c) Group B

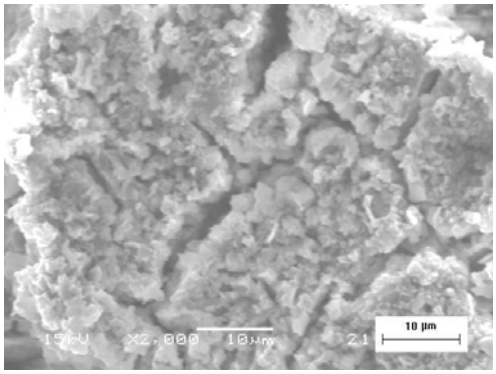

(d) Group C

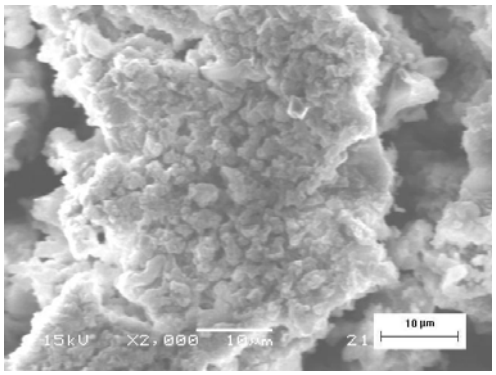

(e) Group D

Figure 6-9 SEM of FN

(a) Control group, (b) Group A, (c) Group B, (d) Group C, (e) Group D

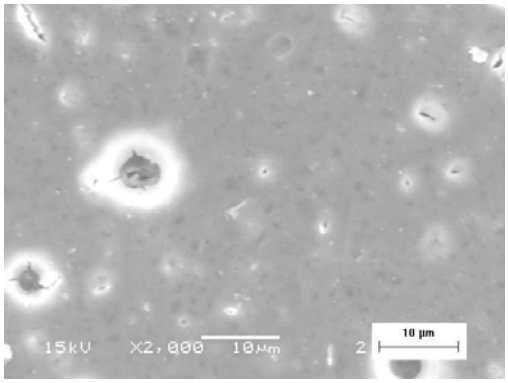

(a) Control group

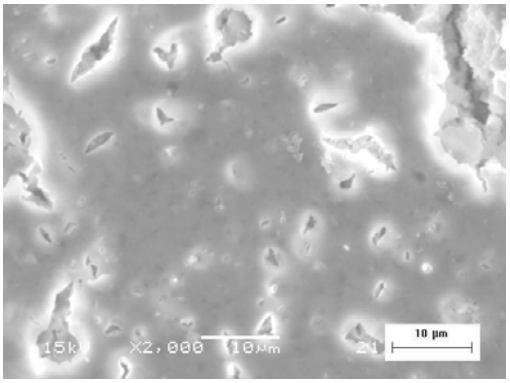

(b) Group A

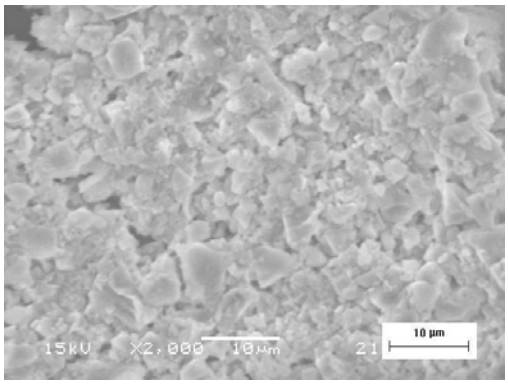

(c) Group B

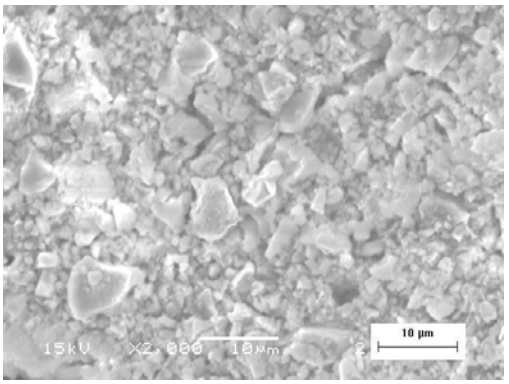

(d) Group C

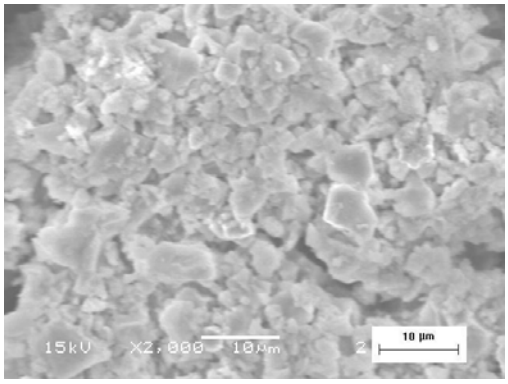

(e) Group D

Figure 6-10 SEM of KM

(a) Control group, (b) Group A, (c) Group B, (d) Group C, (e) Group D

6.3.5 Surface profilometry

The surface roughness (Ra) of both FN and KM as shown in Figure 6-11 and Table 6-6 increased when environmental phosphate was present (Group B, C and D). The increase in Ra for FN and KM was dependent on environmental phosphate level. Higher environmental phosphate level led to higher Ra of FN and KM (Table 6-7). On the other hand, the addition of calcium in acidic conditions (Group A) did not change the surface roughness of both FN and KM.

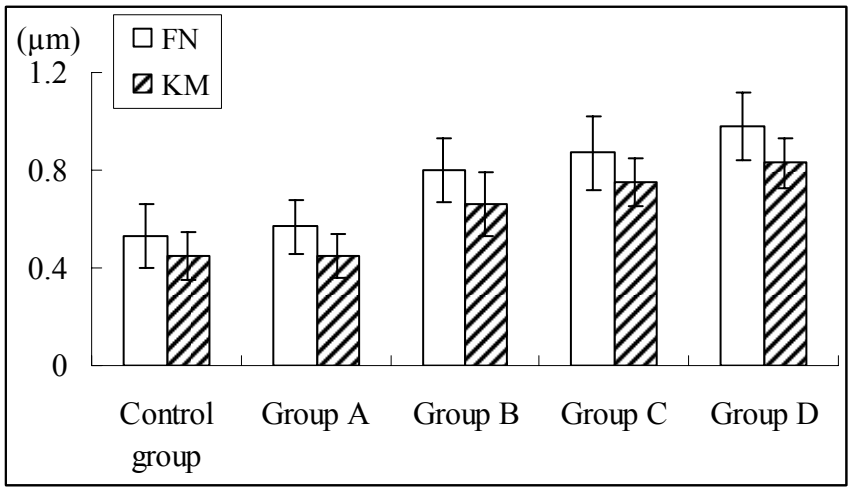

Figure 6-11 Mean surface roughness values (Ra) for FN and KM

*Vertival lines stand for standard deviations

Table 6-6 Mean surface roughness values (Ra) (μm) for FN and KM

	FN	KM
Control group	0.53 (0.13)	0.45 (0.10)
Group A	0.57 (0.11)	0.45 (0.09)
Group B	0.80 (0.13)	0.66 (0.13)
Group C	0.87 (0.15)	0.75 (0.10)
Group D	0.98 (0.14)	0.83 (0.10)

Standard deviations in parentheses

Table 6-7 Statistical comparison of Ra (μm) between acidic conditions

Materials	Difference
FN	Group D > Group C, Group B > Group A, Control group
KM	Group D > Group C > Group B > Group A, Control group

Results of one-way ANOVA/Scheff's post-hoc test ($p<0.05$)

> indicates statistically significant difference in Ra

6.4 Discussion

In Chapter 5, a surface reaction layer was reported under similar conditions. In this study, several surface analytical techniques were used to characterize the surface reaction layer. The depth resolution of FTIR-ATR was around 2~3 μm. SEM/EDS and profilometry provided surface information at submicrometer or micrometer scale. Nano-indentation testing gave mechanical properties of the surface of up to 10 μm. As observed in Chapter 5, the surface layer consisted of two zones with different

structural features. The control group and Group A showed only an inner zone with thickness of more than 10 μm while Group B, C and D showed an outer zone on top of the inner zone in the surface reaction layer (Figure 5-6 and Figure 5-10). Results from the control group and Group A were thus used to interpret the inner zone, while results from Group B, C and D reflected the characteristics of the outer zone.

Based on the microstructure, chemical compositions and mechanical properties, the inner zone of the surface reaction layer may be described as a degradation zone due to acid erosion. As mentioned in Chapter 5, numerous voids corresponding to lost glass particles were observed in the inner zone from a cross-sectional view (Figure 5-6 and Figure 5-10). The topography in this study further substantiated the structural feature of the inner zone (Figure 6-9 and Figure 6-10). FTIR spectra also showed strong polycarboxylates peaks and a weak glass particle band (Figure 6-7 and Figure 6-8). Fukazawa *et al.* (1990) reported similar findings and pointed out that immersion in acids for extended time periods resulted in complete dissolution of glass particles and many pores were left. Element analysis by EDS revealed that the inner zone mainly consisted of Si, Al and Ca/Sr. Sr was absent in KM and Ca was of trace level in FN. This result was in accordance with previous reports on compositions of FN and KM (Smith, 1998). The inner zone was not uniform, according to the results of nano-indentation testing (Figure 6-3 and 6-4). Moreover, the inner zone generally exhibited low hardness and elastic modulus (Figure 6-5 and 6-6). This also supported the point that the inner zone was degraded and thus had inferior mechanical

properties.

The outer zone was different in microstructure from the inner zone. On the cross-sectional view and the surface micrographs, the outer zone was composed of fine particles (Figure 5-6, Figure 5-10, Figure 6-9 and Figure 6-10). The surface roughness also increased (Table 6-6). It can be seen that the particles were irregular in shape and were distributed uniformly on the surface without forming agglomerates. These particles were about 5 μm in size for FN and 10 μm for KM.

Element analysis by EDS showed that the outer zone consisted of P in addition to Si, Al, Sr/Ca. In FTIR spectra, the peaks assigned to phosphate and polycarboxylates were also strong. This suggested that the outer zone consist of both polycarboxylates and phosphate. Due to technique limitations, data on fluoride content in the outer zone was not possible.

The presence of phosphate in the outer zone suggests that the outer zone may possess higher mechanical properties than the inner zone (Driessens, 1995; Morris *et al*., 1997). This was confirmed by hardness and elastic modulus data from nano-indentation testing. Hardness and elastic modulus of the outer zone were significantly higher than that of the inner zone (control group and Group A) during depth profiling.

Additionally, the properties of the outer zone varied according to environmental phosphate level. With an increase in environmental phosphate level, more phosphate was observed in the outer zone (Table 6-4). This was also supported by increased

surface roughness with higher environmental phosphate (Table 6-7). The increased phosphate in the outer zone, thus, resulted in improved hardness and elastic modulus of the outer zone (Figure 6-5 and Figure 6-6).

From this study, it was found that surface layers of different structure, physico-mechanical properties and chemical compositions were formed on GICs depending on environmental phosphate and pH. To further understand the interaction of GICs with environmental calcium/phosphate and pH, studies on the changes in ion concentrations of the surrounding environments are warranted.

6.5 Conclusions

In this study, a series of surface analytical techniques was employed to characterize the surface of HVGICs after interaction with environmental calcium/phosphate and pH. The results of this study showed that the inner zone of the surface reaction layer possessed low mechanical properties which resulted from acid degradation of matrices and glass particles in GICs. An outer zone which exhibited higher mechanical properties than the inner zone was also observed. Along with polycarboxylates, phosphate was involved in the formation of the outer zone.

Chapter 7

Ion Release by GICs Exposed to Acidic Conditions: Effects of Environmental Calcium/Phosphate

7.1 Introduction

GICs are attractive to the dental profession due to their unique cariostatic properties. Compared with other direct filling materials, such as composite resins and amalgam, GICs has been reported to significantly reduce secondary caries in xerostomic patients (McComb *et al.*, 2002; Haveman *et al.*, 2003; Wood, 1993). Their cariostatic properties have been attributed to fluoride release by GICs (Forsten, 1998). Other ions released by GICs, such as calcium or strontium and phosphate, may also assist in the remineralization of decayed tooth (Smales, *et al.*, 2005; Mazzaoui *et al.*, 2003).

Ion release is an intrinsic property of GICs due to their essential compositions and structure (Wilson and McLean, 1988a). According to their sites in GICs, ions can be categorized into cement-forming and non-cement-forming ions. Cement-forming ions include calcium (Ca), strontium (Sr), aluminum (Al) and silicon (Si). Ca, Sr, and Al ions are bound to polycarboxylic acid chains forming hydrophilic matrix. Si ion is involved in the formation of the siliceous gel around glass particles and inorganic network penetrating in polycarboxylate matrices (Wilson, 1996; Wilson and McLean, 1988). Additionally, sodium (Na) and fluorine (F) ions, so-called non-cement-forming

ions, attach to the matrix to balance charges locally and do not contribute to the cement formation. Once GICs have fully set, ion mobility becomes more constricted. In neutral aqueous conditions, the ions released are mainly non-cement-forming ions, notably F and Na ions, and cement-forming ions released are only at trace level. The release of non-cement-forming ions does not cause disintegration of GICs and thus will have no effect on the durability of GICs (Eisenburger *et al.*, 2003; Wilson and Mclean, 1988b).

The level of ions released by GICs is related closely to their ambient acidity. Under low pH conditions, there is a significant increase in fluoride release, which is due to the result of further degradation of glass particles by acids (Gandolfi *et al.*, 2005). This point is supported by a simultaneous increase in the release of matrix-forming ions in acidic conditions (Czarnecka *et al.*, 2002). The level of ions released by GICs is also affected by their surrounding ionic environment. It has been shown that GICs released less fluoride in artificial saliva than in water, regardless of glass-ionomer type (Hayacibara *et al.*, 2004; Levallois *et al.*, 1988).

In Chapter 5, it was observed that environmental phosphate improved hardness and elastic modulus of two HVGICs exposed to acidic conditions. The surface structure and compositions were also altered by environmental phosphate (Chapter 6). In this study, a hypothesis was put forward that environmental phosphate would affect the ion release by GICs in acidic conditions. The aims of this study were twofold: (1) to determine the ion/ligand release by these HVGICs in acidic conditions of varying

environmental calcium and phosphate levels; (2) to evaluate effects of environmental calcium and phosphate on fluoride release profile of these HVGICs in acidic conditions.

7.2 Materials and methods

The same HVGICs (FN and KM) were investigated (Table 4-1). Specimens were prepared with customized Teflon rings (10 mm in diameter and 1 mm in thickness). All specimens were allowed to set in 100% humidity at 37 ºC for 1 hour before being conditioned in different acidic media. The thickness of specimens was measured with an electronic digital caliper (Mitutoyo, Japan) for calculation of surface area.

To determine ions released by GICs, a total 15 specimens for each material were manufactured and randomly divided into five groups (n=3). Each specimen was put into a plastic bottle with 200 ml acidic storage solutions at 37 ºC. The storage solutions were the same to those used in Chapter 6 (Table 6-1). After 4 weeks, the storage solutions were analyzed for Al^{3+}, Si^{4+}, Ca^{2+}, Sr^{2+}, Na^{+} and PO_4^{3+} by inductively coupled plasma optical emission spectrometry (ICP-OES), carboxyl group ($RCOO^{-}$) by UV-Vis spectrometry and F^{-} by ion selective electrode (ISE) potentiometry. The pH value of the storage media were measured with a pH electrode (Orion 91-0, USA).

To obtain fluoride release profile, four storage solutions were selected (Control group, Group A, Group C and Group D). Group A contained only calcium, Group D

contained only phosphate, while Group C contained equal level of calcium and phosphate. Twenty specimens for each material were prepared and randomly divided into four groups (n=5). Each specimen was stored in a plastic bottle of 7 ml solution and transferred into fresh storage solutions every 24 hour for 7 days. The fluoride level of the storage solutions was measured with a fluoride electrode as mentioned below.

The ICP-OES analysis was carried out with Optima 3000 (PerkinElmer, USA), which was controlled by ICP Winlab Software. The wavelength (nm) used was 396 for Al^{3+}, 315 for Ca^{2+}, 460 for Sr^{2+}, 251 for Si^{4+}, 588 for Na^{+} and 213 for PO_4^{3-}. Before measurement, the standard curve for each element was created. The sample solutions were acidified and filtered with 0.2 μm syringe filter. The ion concentration of sample solutions was expressed in unit of ppm.

The carboxyl group was measured by an UV-Vis spectrometer (UVmini-1240, Shimadzu Corp., Japan) using standard one-wavelength quantitative method. The calibration curve was obtained using acidic solutions with known carboxyl group concentration. Each sample solution in the quartz cuvette was measured repeatedly three times and the mean value (mM) was recorded.

Fluoride was determined using fluoride ISE (Accumet fluoride combination electrode, Fisher Scientific, UK) and an ion analyzer (Orion 370 PerpHect meters, Thermo, USA). Before measurement, each sample solution was mixed with the same amount of total ionic strength adjustment buffer (TISAB II) to adjust ionic strength

and pH. TISAB II was prepared based on the formula recommended by US environmental protection agency (Appendix B). The electrode was calibrated using fluoride standard solutions diluted with TISAB II (1:1). The calibration was repeated before measurement of each group of sample solutions. The electrode was immersed into sample solutions and the meter reading (ppm) was recorded after 15 min. Fluoride concentration was calculated and expressed in unit of $\mu g/cm^2$.

The concentration of ion/ligand released from FN and KM was compared between storage conditions using ANOVA/Scheffe's post-hoc test ($p<0.05$).

To evaluate effects of environmental calcium and phosphate on ion/ligand release from GICs, the storage media used in this study were assumed to be unsaturated and no phosphate precipitation occurred. The chemical equilibrium of phosphate in these acidic conditions was calculated using computer software MINEQL+ (Schecher and McAvoy, 1998). The software is a powerful modeling system to calculate chemical equilibrium in aqueous system and is widely used in aquatic chemistry. The parameters of the simulating system were equal to the actual experiment system in this study (37 ºC, 150 mM KCl and 50 mM acetic acids). pH was set as 3.30, which was the pH of the solutions after conditioning GIC samples. The levels of Sr^{2+}/Ca^{2+} and PO_4^{3-} were varied in range of 0~200 mM, which greatly exceeded the real concentration.

7.3 Results

After 4 weeks, the pH values of sample solutions were all changed from 3.00 to 3.25~3.37 (Table 7-1). Group B, C and D showed lower final pH than control group and Group A. When phosphate was added into acidic conditions (Group B, C and D), the pH change was less but independent of the environmental phosphate level.

Table 7-1 pH of storage media after 4 weeks

	FN	KM
Control group	3.36 (0.01)	3.35 (0.01)
Group A	3.37 (0.01)	3.35 (0.00)
Group B	3.28 (0.01)	3.25 (0.01)
Group C	3.28 (0.01)	3.26 (0.00)
Group D	3.27 (0.01)	3.24 (0.01)

Standard deviations in parentheses

* Initial pH of storage media was 3.00

The ion/ligand release by FN and KM are shown in Figure 7-1, Figure 7-2, Table 7-2 and Table 7-4. As FN is strontium based and KM is calcium based, Sr^{2+} release from FN and Ca^{2+} release from KM were reported. In consideration of calcium and phosphate present in the storage solutions before conditioning specimens, calcium and phosphate release were shown with ΔCa^{2+} and ΔPO_4^{3-}, which were derived as follows:

$$\Delta Ca^{2+} = [Ca^{2+}]_f - [Ca^{2+}]_i \text{ and } \Delta PO_4^{3-} = [PO_4^{3-}]_f - [PO_4^{3-}]_i$$

where, $[Ca^{2+}]_f$ and $[PO_4^{3-}]_f$ were the final ion concentration of storage solutions after immersion of GIC specimen; $[Ca^{2+}]_i$ and $[PO_4^{3-}]_i$ were the initial ion concentration of

storage solutions before immersion of GIC specimen.

The substantial ion release from GICs in acidic environments as shown in Figure 7-1, Figure 7-2, Table 7-2 and Table 7-4 supported the results of other studies (Fukazawa *et al.*, 1987; Eisenburger *et al.*, 2003). For both FN and KM, Group A showed similar levels of Al^{3+}, Si^{4+}, Sr^{2+}/Ca^{2+}, F^-, Na^+, $RCOO^-$ and ΔPO_4^{3-} as control group. This suggests that environmental calcium has no significant effects on ion/ligand release by GICs in acidic conditions.

When phosphate was present in acidic conditions (Group B, C and D), the ion/ligand released by FN and KM were slightly different. For FN, the concentration of Al^{3+}, Si^{4+}, Sr^{2+}, F^- and ΔPO_4^{3-} was significantly lower than that of control group (Table 7-3). For KM, the level of Al^{3+}, Si^{4+}, ΔCa^{2+}, F^-, ΔPO_4^{3-} as well as Na^+ was significantly lower than that of control group (Table 7-5). It was clearly shown that the presence of phosphate in acidic conditions retarded these ions release from GICs.

With regard to phosphate release, negative values of ΔPO_4^{3-} were observed for both FN and KM. The negative value means GICs may take up phosphate from the storage media. It was shown that when the environmental phosphate level was high, more environmental phosphate was taken up by GICs.

In terms of $RCOO^-$ release, FN and KM showed the same trend. With increasing environmental phosphate level, $RCOO^-$ level dropped down and then rose up again. Results suggest that environmental phosphate may affect $RCOO^-$ release from GICs through more than one mechanism.

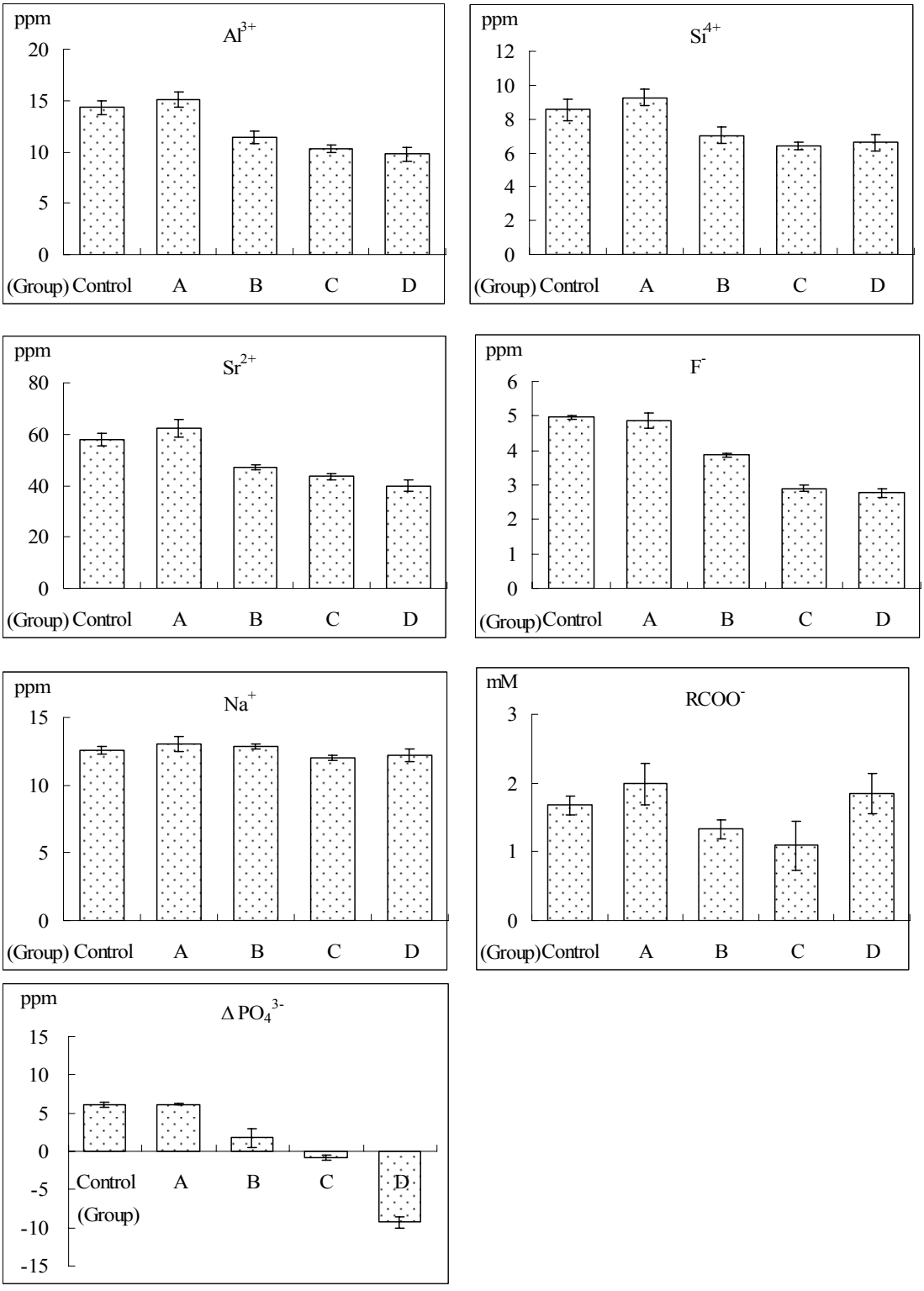

Figure 7-1 Ion/ligand release by FN

* ΔPO_4^{3-} represents phosphate release

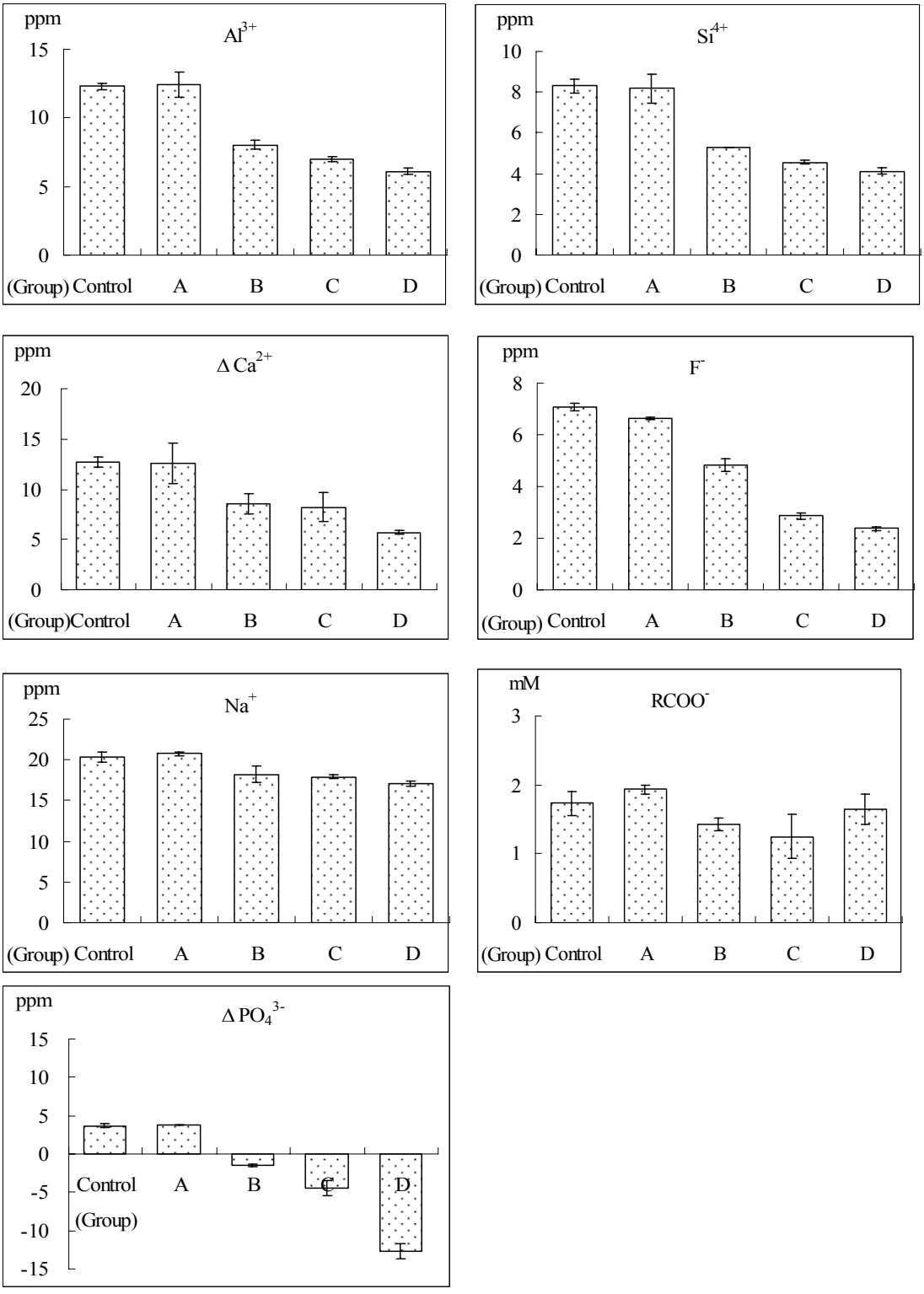

Figure 7-2 Ion/ligand release by KM

* ΔCa^{2+} and ΔPO_4^{2+} represent calcium and phosphate release respectively

Table 7-2 Ion/ligand release by FN

	Control group	Group A	Group B	Group C	Group D
Al^{3+}(ppm)	14.30 (0.70)	15.07 (0.76)	11.40 (0.66)	10.30 (0.35)	9.77 (0.65)
Si^{4+}(ppm)	8.55 (0.63)	9.25 (0.48)	7.03 (0.49)	6.38 (0.23)	6.60 (0.47)
Sr^{2+}(ppm)	57.87 (2.61)	62.17 (3.5)	47.20 (1.05)	43.47 (1.30)	39.93 (2.32)
F^{-}(ppm)	4.97 (0.06)	4.87 (0.21)	3.87 (0.06)	2.90 (0.10)	2.77 (0.12)
Na^{+}(ppm)	12.60 (0.26)	13.03 (0.55)	12.87 (0.21)	12.00 (0.20)	0.47 (12.23)
$RCOO^{-}$(mM)	1.68 (0.14)	1.99 (0.30)	1.33 (0.14)	1.09 (0.36)	1.85 (0.29)
ΔPO_4^{3-}(ppm)	6.10 (0.26)	6.18 (0.08)	1.77 (1.20)	-0.77 (0.35)	-9.30 (0.69)

Standard deviation in parentheses (n=3)

* ΔPO_4^{3-} represents phosphate release

Table 7-3 Statistical comparison of ion/ligand release by FN between acidic storage media

Variables	Difference
Al^{3+}	Group A, Control group > Group B, Group C, Group D*
Si^{4+}	Group A, Control group > Group B, Group D, Group C*
Sr^{2+}	Group A, Control group > Group B, Group C, Group D Group B > Group D*
F^{-}	Group A, Control group > Group B > Group C, Group D*
Na^{+}	No significant difference*
$RCOO^{-}$	Group A > Control Group > Group B, Group C Group D > Group B, Group C#
ΔPO_4^{3-}	Group A, Control group > Group B > Group C > Group D*

Results of one-way ANOVA/Scheff's post-hoc test* and Kruskal-Wallis/Mann-Whitney test#
($p < 0.05$)

> indicates statistically significant difference in concentration of ions/ligands

ΔPO_4^{3-} represents phosphate release

Table 7-4 Ion/ligand release by KM

	Control group	Group A	Group B	Group C	Group D
Al^{3+}(ppm)	12.30 (0.26)	12.40 (0.92)	8.05 (0.33)	6.97 (0.19)	6.09 (0.22)
Si^{4+}(ppm)	8.30 (0.33)	8.18 (0.72)	5.28 (0.02)	4.55 (0.09)	4.11 (0.16)
ΔCa^{2+}(ppm)	12.73 (0.51)	12.53 (2.02)	8.50 (1.00)	8.23 (1.50)	5.72 (0.23)
F^-(ppm)	7.07 (0.15)	6.63 (0.06)	4.83 (0.25)	2.87 (0.12)	2.37 (0.06)
Na^+(ppm)	20.33 (0.67)	20.77 (0.98)	18.20 (0.29)	17.93 (0.29)	17.10 (0.26)
$RCOO^-$(mM)	1.73 (0.18)	1.93 (0.06)	1.42 (0.09)	1.25 (0.32)	1.65 (0.22)
ΔPO_4^{3-}(ppm)	3.68 (0.22)	3.79 (0.07)	-1.43 (0.17)	-4.47 (1.05)	-12.70 (0.92)

Standard deviation in parentheses (n=3)

ΔCa^{2+} and ΔPO_4^{2+} represent calcium and phosphate release respectively

Table 7-5 Statistical comparison of ion/ligand release by KM between acidic storage media

Variables	Difference
Al^{3+}	Group A, Control group > Group B, Group C, Group D Group B > Group D
Si^{4+}	Control group, Group A > Group B, Group C, Group D Group B > Group D
Sr^{2+}	Group A, Control group > Group B, Group C, Group D
F^-	Group A, Control group > Group B > Group C > Group D
Na^+	Group A, Control group > Group B, Group C, Group D
$RCOO^-$	Group A, Control group > Group B, Group C Group D > Group C
ΔPO_4^{3-}	Group A, Control group > Group B > Group C > Group D

Results of one-way ANOVA/Scheff's post-hoc test* and Kruskal-Wallis/Mann-Whitney test# ($p < 0.05$)

> indicates statistically significant difference in concentration of ions/ligands

ΔCa^{2+} and ΔPO_4^{3-} represent calcium and phosphate release respectively

The kinetics of fluoride release are shown in Figure 7-3, Figure 7-4, Table 7-6 amd Table 7-7, while the cumulative fluoride release are in Figure 7-5, Figure 7-6, Table 7-8 and Table 7-9. With regard to fluoride release profile, a slight difference between FN and KM was observed. For FN, fluoride release rate was the highest on the first day, then decreased and followed by a constant level (Figure 7-3). The fluoride release rate of KM was different and fluctuated during the 7-day period (Figure 7-4). When phosphate was present in the acidic solutions (Group C and Group D), both FN and KM released fluoride at a slower rate than those in control group. No significant difference in fluoride release rate was observed between control group and Group A containing only calcium. The adverse effect of environmental phosphate on fluoride release was observed as early as after 1 day immersion for KM and 2 days for FN (Table 7-10). In terms of cumulative fluoride release, the amount of fluoride release during the 7 days was significantly affected by environmental phosphate (Figure 7-5 and Figure 7-6). Both FN and KM released lesser fluoride in acidic conditions containing environmental phosphate when compared to in phosphate free acidic conditions. This is consistent with the 4-week results (Figure 7-1 and Figure 7-2).

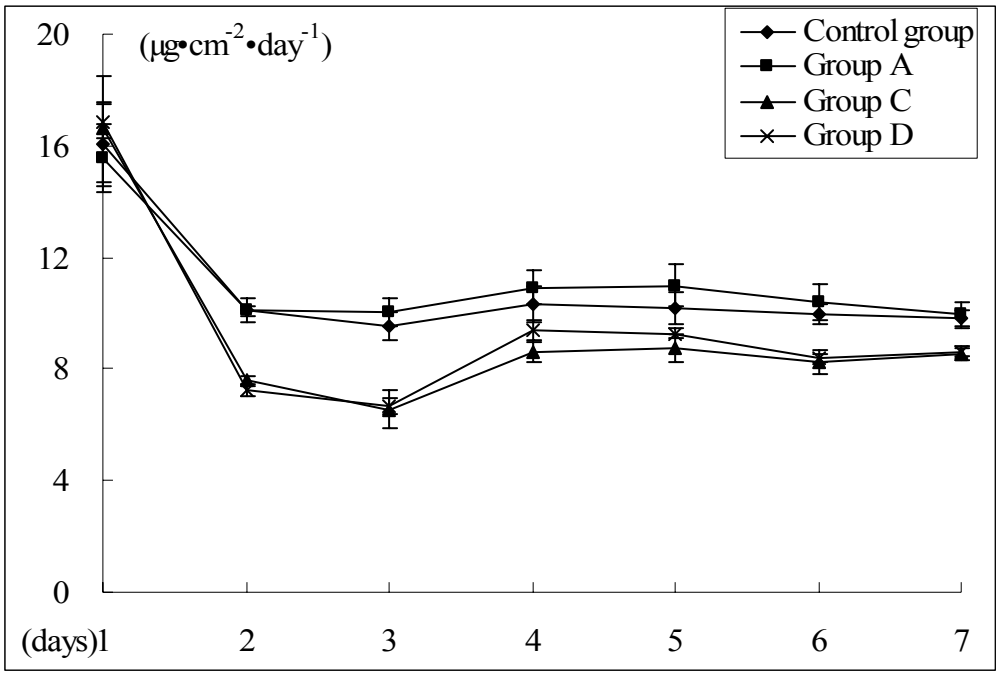

Figure 7-3 Kinetics of fluoride release by FN

*Vertical lines represent standard deviations

Table 7-6 Kinetics of fluoride release (μg•cm^{-1}•day^{-1}) by FN

	Control group	Group A	Group C	Group D
Day 1	16.05 (1.51)	15.55 (1.21)	16.60 (1.90)	16.87 (7.24)
Day 2	10.09 (0.17)	10.13 (0.42)	7.57 (0.17)	7.24 (0.25)
Day 3	9.51 (0.49)	10.05 (0.50)	6.55 (0.68)	6.66 (0.31)
Day 4	10.31 (0.66)	10.92 (0.64)	8.59 (0.34)	9.41 (0.34)
Day 5	10.17 (0.57)	10.99 (0.77)	8.73 (0.51)	9.27 (0.18)
Day 6	9.95 (0.38)	10.41 (0.66)	8.22 (0.43)	8.40 (0.15)
Day 7	9.80 (0.33)	9.98 (0.42)	8.52 (0.21)	8.62 (0.18)

Standard deviation in parentheses (n=5)

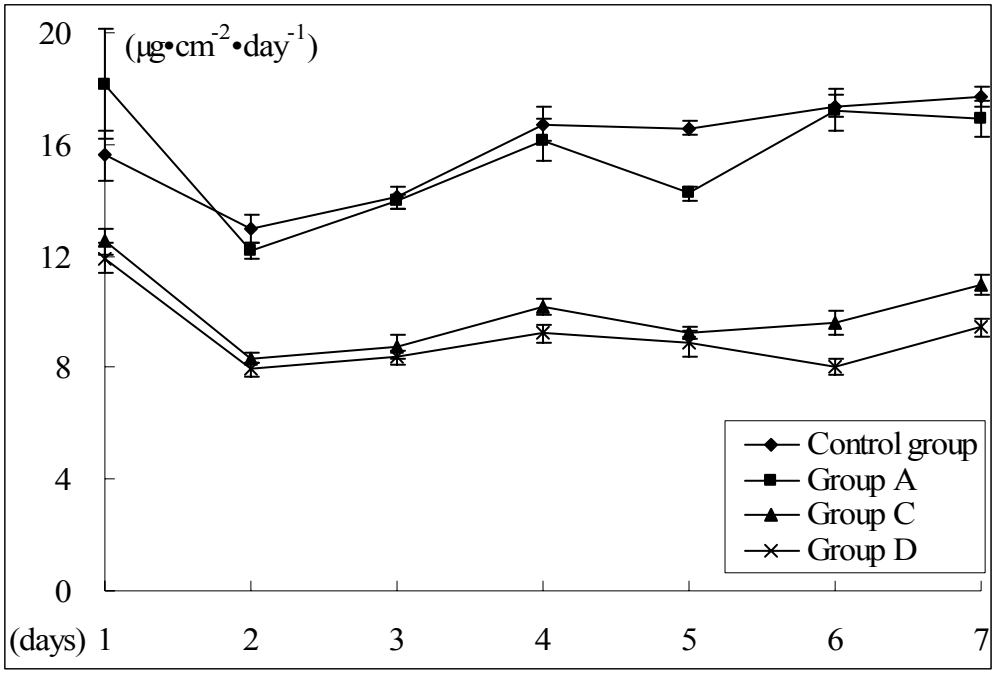

Figure 7-4 Kinetics of fluoride release by KM

*Vertical lines represent standard deviations

Table 7-7 Kinetics of fluoride release (μg•cm^{-1}•day^{-1}) by KM

	Control group	Group A	Group C	Group D
Day 1	15.60 (0.90)	18.15 (1.98)	12.53 (0.48)	11.91 (0.54)
Day 2	12.98 (0.47)	12.17 (0.30)	8.35 (0.17)	7.94 (0.24)
Day 3	14.11 (0.39)	13.95 (0.28)	8.78 (0.43)	8.36 (0.27)
Day 4	16.74 (0.60)	16.15 (0.74)	10.19 (0.31)	9.21 (0.29)
Day 5	16.59 (0.28)	14.23 (0.26)	9.27 (0.21)	8.86 (0.46)
Day 6	17.37 (0.37)	17.22 (0.77)	9.63 (0.43)	8.401 (0.30)
Day 7	17.73 (0.36)	16.94 (0.65)	10.97 (0.36)	9.43 (0.32)

Standard deviation in parentheses (n=5)

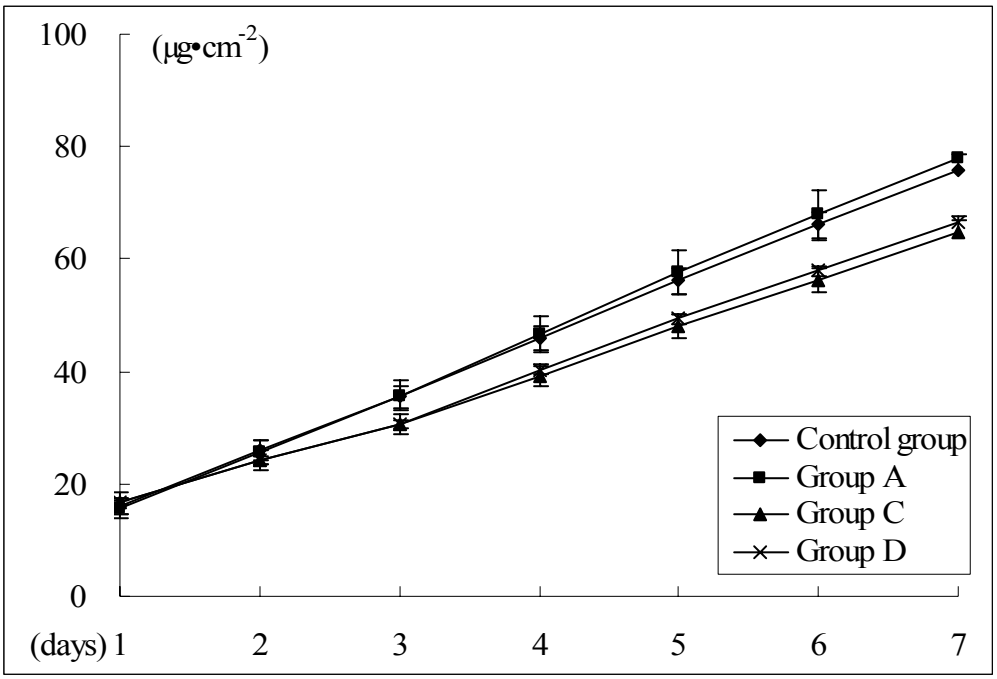

Figure 7-5 Cumulative fluoride release by FN

*Vertical lines represent standard deviations

Table 7-8 Cumulative fluoride release (μg•cm^{-1}) by FN

	Control group	Group A	Group C	Group D
Day 1	16.05 (1.51)	15.55 (1.21)	16.60 (1.90)	16.87 (7.24)
Day 2	26.14 (1.60)	25.68 (1.62)	24.17 (1.99)	24.11 (0.63)
Day 3	35.65 (1.81)	35.73 (2.09)	30.72 (1.59)	30.77 (0.65)
Day 4	45.97 (2.17)	46.65 (2.62)	39.30 (1.82)	40.18 (0.81)
Day 5	56.13 (2.27)	57.65 (3.33)	48.04 (1.97)	49.45 (0.85)
Day 6	66.08 (2.40)	68.06 (3.96)	56.26 (1.98)	57.85 (0.94)
Day 7	75.88 (2.64)	78.04 (4.33)	64.78 (2.03)	66.47 (0.98)

Standard deviation in parentheses (n=5)

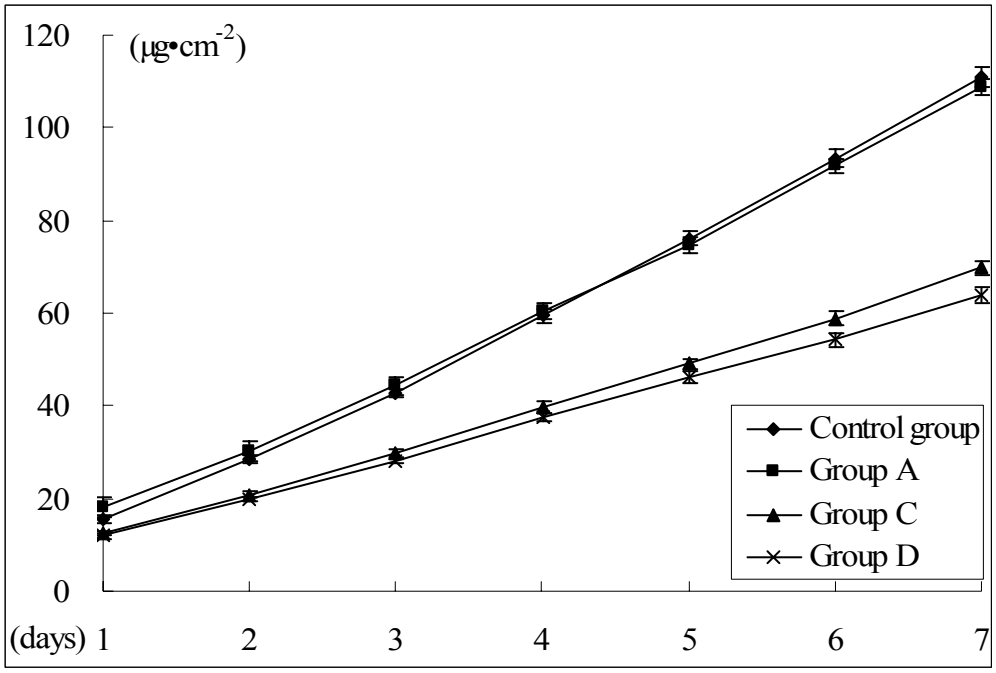

Figure 7-6 Cumulative fluoride release by KM

*Vertical lines represent standard deviations

Table 7-9 Cumulative fluoride release (μg•cm^{-1}) by KM

	Control group	Group A	Group C	Group D
Day 1	15.60 (0.90)	18.15 (1.98)	12.53 (0.48)	11.91 (0.54)
Day 2	28.58 (0.87)	30.32 (2.25)	20.88 (0.57)	19.84 (0.48)
Day 3	42.69 (0.89)	44.26 (2.11)	29.65 (0.98)	28.21 (0.58)
Day 4	59.43 (1.44)	60.41 (1.60)	39.84 (1.22)	37.42 (0.82)
Day 5	76.02 (1.55)	74.64 (1.56)	49.12 (1.11)	46.28 (1.19)
Day 6	93.40 (1.83)	91.87 (1.58)	58.74 (1.52)	54.29 (1.42)
Day 7	111.12 (2.17)	108.80 (1.76)	69.72 (1.56)	63.72 (1.70)

Standard deviation in parentheses (n=5)

Table 7-10 Statistical comparison of fluoride release (daily) between acidic storage media

Materials	Time	Difference
FN	Day 1	No significant difference*
	Day 2	Control group, Group A > Group B, Group D*
	Day 3	Control group, Group A > Group B, Group D*
	Day 4	Control group > Group B Group A > Group B, Group D*
	Day 5	Control group > Group B Group A > Group B, Group D*
	Day 6	Control group, Group A > Group B, Group D*
	Day 7^{-}	Control group, Group A > Group B, Group D*
KM	Day 1	Group A > Control group > Group B, Group D*
	Day 2	Control group >Group A > Group B, Group D*
	Day 3	Control group, Group A > Group B, Group D*
	Day 4	Control group, Group A > Group B > Group $D^{\#}$
	Day 5	Control group > Group A > Group B, Group D*
	Day 6	Control group, Group A > Group B > Group D*
	Day 7^{-}	Control group, Group A > Group B > Group D*

Results of one-way ANOVA/Scheff's post-hoc test* and Kruskal-Wallis/Mann-Whitney test$^{\#}$ ($p < 0.05$)

> indicates statistically significant difference in concentration of fluoride ion

The percentage of phosphate precipitations ($SrHPO_4$ and $CaHPO_4$) as a function of Sr^{2+}/Ca^{2+} and PO_4^{3-} level are reported in Figure 7-7 and Figure 7-8. The arrows indicate the highest PO_4^{3-} level (2.4 mM) in storage media.

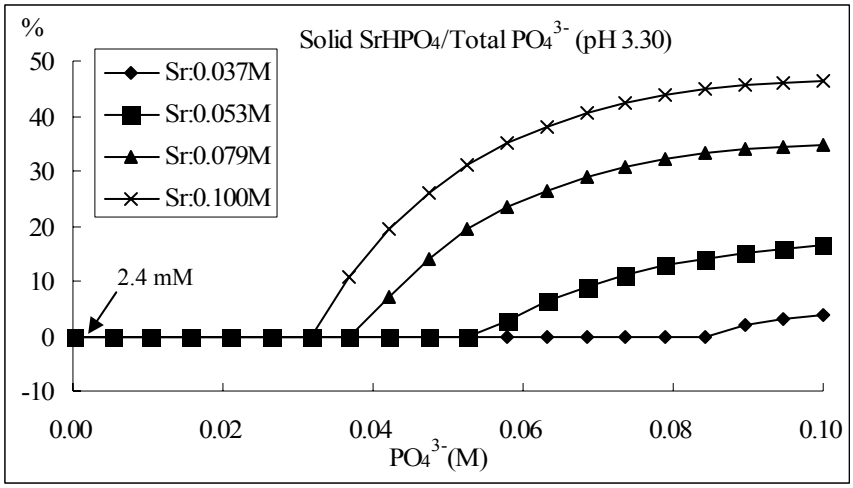

Figure 7-7 Percentage of $SrHPO_4$ precipitations as a function of Sr^{2+} and PO_4^{3-} level

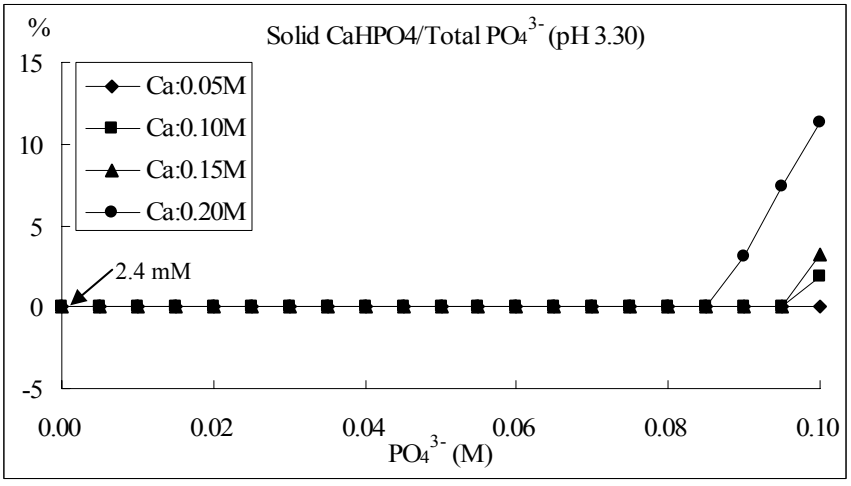

Figure 7-8 Percentage of $CaHPO_4$ precipitations as a function of Ca^{2+} and PO_4^{3-} level

As clearly seen from Figure 7-7 and Figure 7-8, no precipitation is possible when PO_4^{3-} level is 2.4 mM. The storage medium after interaction with GICs was an

unsaturated solution of strontium/calcium phosphate in the current study. The results suggest that there is no phosphate precipitation in storage media before and after conditioning GIC specimens.

7.4 Discussion

ICP-OES has the ability to perform rapid multi-element analysis at trace level. This technique, however, is not available for some elements, such as O, C, H, N, halides and radioactive elements (Brundle *et al.*, 1992). With the exception of F^- and $RCOO^-$, all ions/ligands were examined using ICP-OES in this study. $RCOO^-$ was measured using UV-Vis spectrometry at a wavelength of 205 nm as recommended by the manufacturer. A spectrum scan of storage solutions with a wavelength of 190~250 nm was done to confirm the location of $RCOO^-$ peak. With regards to F^- measurement, plastic containers were used for storage of sample solutions and TISAB II was also added into sample solutions to minimize fluoride measurement errors.

It was found that environmental phosphate reduced the levels of ion/ligands (with the exception of $RCOO^-$) released by GICs in acidic conditions. In general, GICs release more ions in low pH than in neutral situations. The increased ion release is the result of glass particle and matrix degraded by acids (Fukazawa *et al.*, 1987; Smales *et al.*, 2005). The lesser ion/ligands release when phosphate was present in the acidic conditions indicates that environmental phosphate may retard acid degradation of GICs. This was supported by the results from the previous SEM study. When

phosphate was present in storage media, the surface reaction layer was thinner than that in phosphate-free storage solutions (Chapter 5). The relatively smaller change in pH value of the sample solutions consisting of phosphate is consistent with this point. The smaller increase in solution pH suggests that less H^+ hydrolysis of matrices and glass particles occurs in GICs.

With regard to environmental calcium, the results of this study indicated that the addition of calcium to acidic conditions has no significant effects on ion/ligand release by GICs. It further supported the point that environmental calcium was not critical in the interaction between GICs and environmental calcium/phosphate and pH.

Another significant finding of this study was that environmental phosphate level was decreased after interaction with GIC. Generally, the removal of anions and cations from a solution phase is the result of surface adsorption or bulk solution precipitation. The bulk precipitation process is less likely to be responsible for the decreased phosphate level due to the acidity of solutions in this study as shown in Figure 7-7 and Figure 7-8. In the current study, the changes of phosphate anion in storage media were most probably the result of surface adsorption on GICs.

The extent of phosphate uptake by GICs appeared to be dependent on environmental phosphate level. When environmental phosphate concentration was higher, GICs took more phosphate from the surrounding environment. This concurs with our EDS results. A higher environmental phosphate led to higher phosphorus

content in the GIC surface (Chapter 6). The uptake of phosphate by GICs in acidic conditions may be caused by an ion exchange process.

Most metallic ions in GICs, such as Al^{3+}, Ca^{2+} and Sr^{2+}, are complex ions and have a co-ordination number of six. These complex ions are generally covalently bound by carboxyl group, water molecule, fluoride or hydroxyl group (Hosoda, 1993) (Figure 7-9).

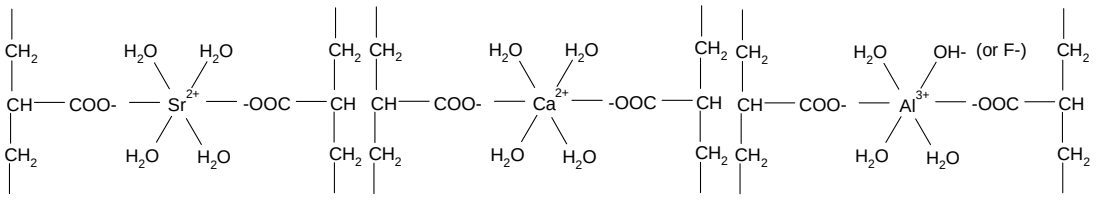

Figure 7-9 The possible molecular structures in set GICs

These ligands can be interchanged with other surrounding ligands. At low pH, H^+ will dissociate the covalent bond between ligands and central metal cations, thus, promoting the ligand exchange. Fluoride anion, hydroxyl and carboxyl groups may interchange with environmental phosphate due to their anionic nature.

If environmental phosphate moved into GICs by ion exchange with OH^-, the uptake of phosphate should be accompanied by a rise in pH value of sample solutions, due to OH^- leaching out of GICs. The pH results, however, showed that sample solutions presenting with phosphate uptake had lower pH value than others. This implies that the exchange between OH^- and PO_4^{3-} had no significant effect on the

phosphate uptake process. In respect to fluoride anion, the fluoride released by GICs did not increase to accompany phosphate uptake. The result indicates that PO_4^{3-}/F^- exchange is also not responsible for phosphate uptake. The carboxyl group showed a dissimilar release profile from other matrix-forming ions, e.g. Al^{3+}, Sr^{2+}, Ca^{2+} and Si^{4+}. With increasing environmental PO_4^{3-} levels, a decrease of Al^{3+}, Sr^{2+}, Ca^{2+} and Si^{4+} release was observed, while $RCOO^-$ release was increased. This suggests that the increased $RCOO^-$ release observed with increasing environmental PO_4^{3-} cannot be attributed to acid degradation of the GIC. The increased $RCOO^-$ was associated with decreased PO_4^{3-} after conditioning GICs, which suggests that an ion exchange has occurred between carboxyl group and PO_4^{3-}, i.e. PO_4^{3-} uptake by GIC happened.

As fluoride release is an important characteristic of GICs, the effect of environmental calcium and phosphate on the fluoride release profile was also examined. Considering the fact that most fluoride is released from GICs in the initial period (Dunne *et al.*, 1996), a short-term fluoride release profile was studied. FN and KM showed substantial amount of fluoride release in all acidic conditions, but the amount and the rate of fluoride release were lowered by phosphate in acidic conditions. The decreased fluoride release was also due to the retardation of acid degradation of GICs by environmental phosphate. The effect of environmental phosphate on fluoride release started as soon as in Day 1 for KM and Day 2 for FN. The reduced fluoride release level may result in extended fluoride releasing characteristic. This may be of clinical relevance as a long and low level fluoride

release is preferred *in vivo* (Forsten, 1998).

7.5 Conclusions

This study investigated the effects of environmental phosphate/calcium on ion/ligand release by GICs in acidic conditions. The fluoride release profile in acidic conditions with varying calcium/phosphate levels was also examined. It was found that in acidic conditions, the ion/ligand release by GICs was substantially increased. With the exception of carboxyl group, matrix-forming ions/ligands released from GICs in acidic conditions were retarded by environmental phosphate. This is consistent with the beneficial effects of environmental phosphate on GICs observed in previous studies. It was additionally found that environmental phosphate was taken up by GICs. The phosphate uptake was environmental phosphate level dependent. This may be due to a ligand exchange between phosphate and carboxyl group. Fluoride release was reduced by environmental phosphate. The retardation effect of environmental phosphate may maintain a long-term and low-level fluoride release, thus, prolonging the cariostatic potential of glass-ionomer restoratives *in vivo*.

Chapter 8

Effects of Environmental Calcium/Phosphate on OCA Wear and Shear Strength of GICs Subject to Acidic Challenge

8.1 Introduction

GICs are cariostatic, biocompatible and can adhere to tooth structure. Glass-ionomer restoratives are commonly used in deciduous teeth as alternatives to dental amalgam. In permanent teeth, they are mainly employed for restoring cervical lesions and with atraumatic restorative (ART), tunnel and sandwich techniques, due to their excellent bonding and moderate mechanical properties. GICs are also recommended for high caries risk patients (e.g. post-radiation therapy, xerostomia etc.), because of their cariostatic potential through fluoride release (Hu *et al.*, 2002; McComb *et al.*, 2002).

The longevity of glass-ionomer restoratives varies widely among different clinical surveys. Reported failure rates range from 0.7% to 60% (Ostlund *et al.*, 1992; Gao *et al.*, 2003; Kilpatrick *et al.*, 1995; Ho *et al.*, 1999). With regards to failure modes of GICs *in vivo*, clinical studies have shown that bulk fracture and loss of anatomy form are the main reasons for failure of glass-ionomer restoratives in general practice (Mjör, 1997; Mandari *et al.*, 2001, Burke *et al.*, 2001). For xerostomic patients, the primary failure modes for GICs are loss of anatomy, marginal deterioration and erosion of material (McComb *et al.*, 2002; Gao *et al.*, 2003; Hu *et*

al., 2002).

The degradation of glass-ionomer restoratives *in vivo* is a chemo-mechanical process. It has been shown that glass-ionomer restoratives suffer more bulk fracture when inserted in large conventional Class I and Class II cavities in stress-bearing areas (Smales *et al.*, 1990; Qvist *et al.*, 1997). In addition, it was found that glass-ionomer restoratives in contact free areas (CFA) were as worn as those in occlusal contact areas (OCA) (McKinney *et al.*, 1987). These results suggest that both chemical and mechanical environments play an important role in degradation of glass-ionomer restoratives (Mair *et al.*, 1996; Maeda *et al.*, 1999). To improve clinical performance, GICs must have greater resistance to the chemo-mechanical degradation *in vivo*.

More recently, McKenzie *et al.*, (2003a, 2004) found that GICs conditioned in Coca-Cola had higher hardness and strength than those in other acidic drinks and were comparable to those in neutral media. They postulated that the phosphoric acid in Coca-Cola may contribute to this phenomenon. In our earlier studies, we found that GICs showed higher surface hardness and elastic modulus in acidic conditions when environmental phosphate level was high (Chapter 5).

The purpose of this study was to determine the effects of environmental phosphate on clinically related mechanical properties of GICs, when exposed to acidic conditions. Due to the fact that loss of anatomy and fracture are the main causes for GIC restoration failure, this study investigated OCA wear resistance and shear

strength of two HVGICs. In this study, a simple reciprocating compression-sliding system was used. The wear process was simplified to two body wear without considerations of the exogenous third body. Despite these limitations, the derived results provide insight into the effects of environmental phosphate on GICs when challenged by acids.

8.2 Materials and methods

Capsulated Fuji IX Fast and KetacMolar were activated and mixed according to manufacturers' instructions (Table 4-1). Shear strength specimens were made using stainless steel washers (12.0 mm in outer diameter, 5.0 mm in inner diameter and 1.0 mm in thickness) and wear specimens were prepared using customized acrylic moulds with rectangular recess (8.0 mm long × 4.0 mm wide × 2.0 mm deep). The molds filled with the mixed materials and covered with acetate strips and glass slides. Pressure was applied gently to remove excess material. The specimens were allowed to set, kept in 100% humidity at 37 ºC for 1 hour, randomly divided into five groups and conditioned in acidic storage media (pH 3). The detail of storage media is listed in Table 6-1. After 4 weeks, the specimens were subjected to shear punch testing (n=8) or OCA wear testing (n=6) for shear strength and wear depth.

Shear punch testing was conducted using a custom designed micro-punch apparatus mounted on an Instron Micro-tester (Model 5848, Instron Corp, Massachusetts, USA) (Figure 8-1). Each specimen was measured with a digital vernier caliper (Mitutoyo, Tokyo, Japan) for thickness and then positioned in the apparatus with the holding washer. The specimen was restrained by tightening a screw clamp. To minimize frictional force, the entire experimental set-up was calibrated to ensure the punch and the punch hole in specimen jig were aligned. The testing was controlled by a computerized program (Merlin, Instron Corp.). A steel punch with a flat end of 2 mm diameter was used to create shear force and the testing was done at a crosshead speed of 1.5 mm/min. The maximum load was recorded and shear strength was subsequently computed using the following formula:

$$\text{Shear strength } (MPa) = \frac{W}{\pi DT}$$

where W is the load to fracture (N); D is the diameter of the punch (mm); T is the thickness of the specimen (mm).

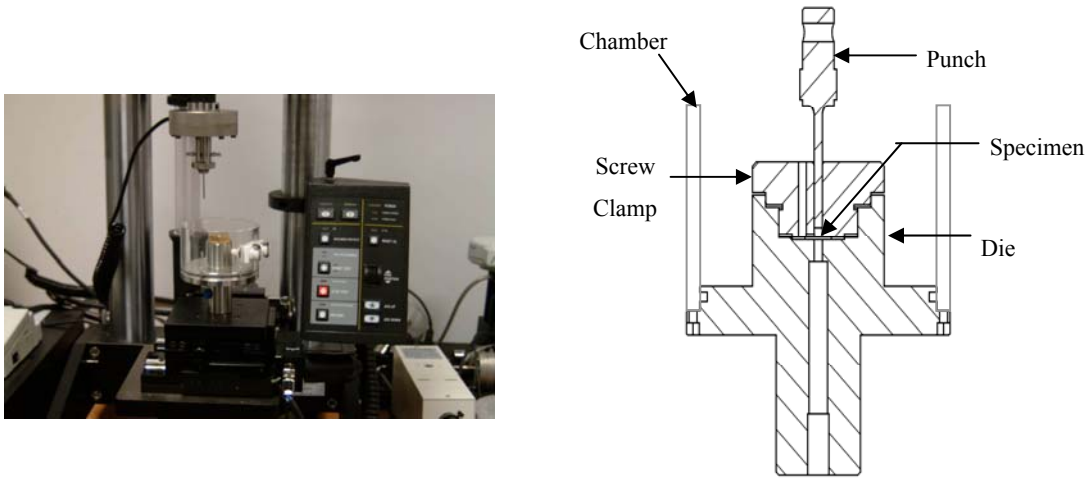

Figure 8-1 Photograph and schematic presentation of the micro-punch apparatus

The OCA wear testing was achieved with a reciprocating compression-sliding wear instrument, which allowed specimens to move back and forth against counter wear body. This testing has been described in detail by Yap *et al.* (2001b) (Figure 8-2). The specimens were fixed on the sliding platform in holders with storage solutions as lubricating media. Flat-ended SS304 stainless steel of 1mm diameter polished to 1200 grit with a series of sandpapers were used as abrading counter bodies. A constant stress of 20 MPa was applied and specimens were tested at a speed of 100 cycles/minute. Wear depths (μm) were measured and recorded with a profilometer (Surftest SV-402, Japan) after 500, 1000, 2000 and 3000 wear cycles. Five measurements were performed at the center of each specimen and total 30 readings were obtained for each group.

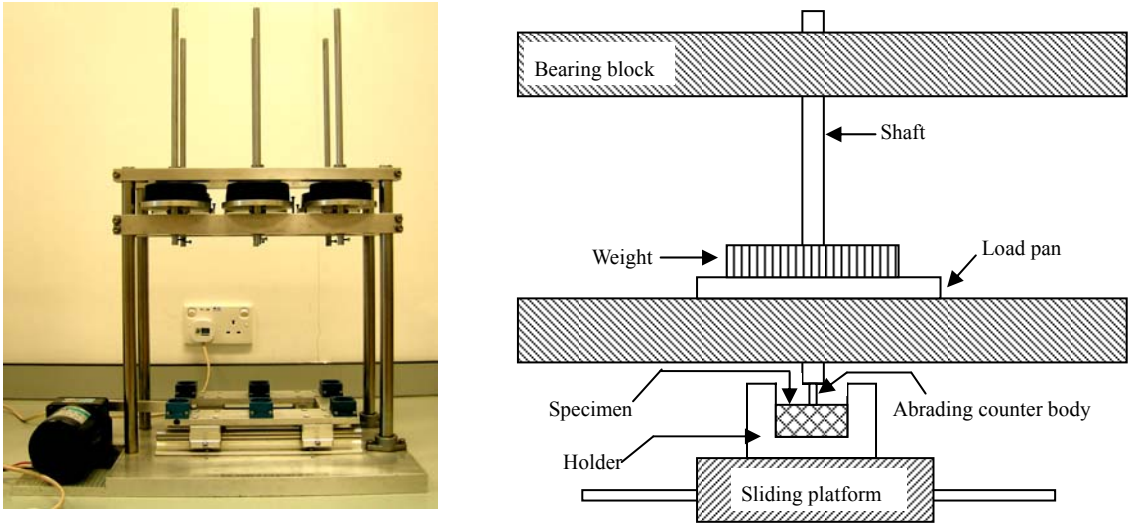

Figure 8-2 Photograph and schematic presentation of the wear instrumentation

All statistical analysis was carried out at significance level 0.05. One-way ANOVA and Scheffe's post-hoc tests were used to determine storage medium differences in shear strength and wear depth.

8.3 Results

8.3.1 Wear depth

The cumulative wear depth of FN and KM are shown in Figure 8-3, Figure 8-4 and Table 8-1. As can be seen, the cumulative wear depth of FN and KM in all acidic conditions increased as a function of wear cycles. For both FN and KM, the increase in wear depth within the first 500 wear cycles was much higher than after 500 wear cycles. It can also be seen that the wear depth of FN and KM in acidic conditions was dependent on environmental phosphate levels. FN and KM both experienced the highest wear depth in the control group and Group A, where environmental phosphate was absent. With the addition of phosphate in acidic conditions (Group B, C and D), wear depth of FN and KM significantly decreased. With increasing environmental phosphate levels, the wear depth of FN and KM decreased. Exposure to the highest phosphate level (Group D) resulted in the lowest wear depth of FN and KM (Table 8-2).

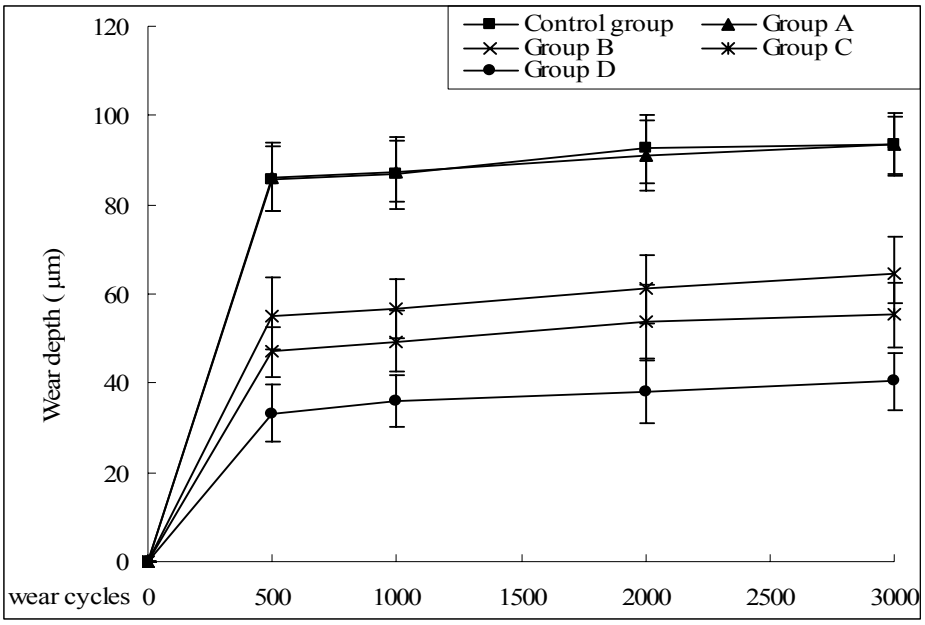

Figure 8-3 Mean cumulative wear of FN in different acidic conditions

*Vertical lines represent standard deviations

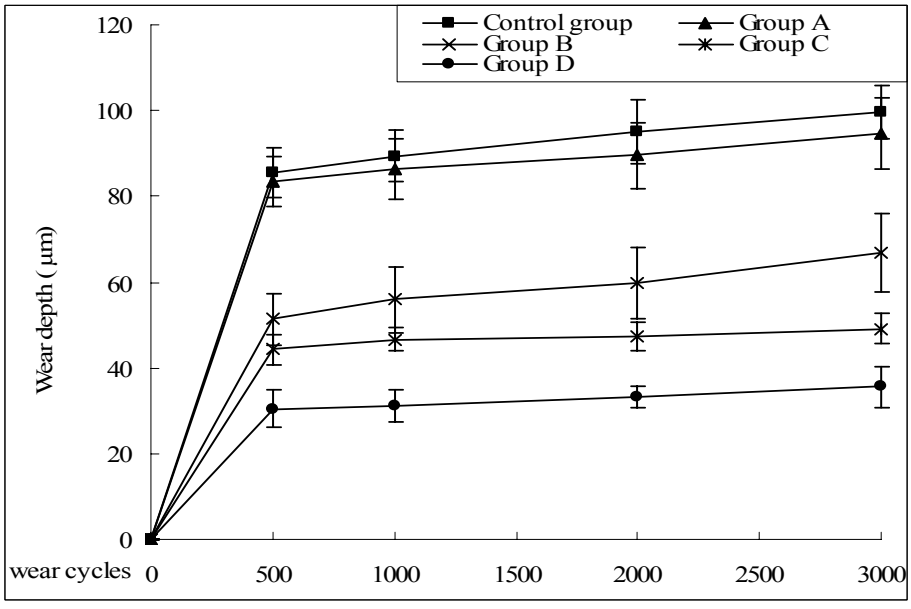

Figure 8-4 Mean cumulative wear of KM in different acidic conditions

*Vertical lines represent standard deviations

Table 8-1 Cumulative wear depth (μm) of FN and KM in different acidic conditions

Materials	Wear cycles	Control group	Group A	Group B	Group C	Group D
FN	500	85.8 (7.3)	86.1 (7.7)	55.2 (8.5)	47.0 (5.6)	33.3 (6.5)
	1000	87.0 (8.1)	87.4 (6.8)	56.9 (6.4)	49.4 (6.7)	35.9 (5.8)
	2000	92.6 (7.6)	91.2 (7.8)	61.4 (7.4)	53.6 (8.3)	38.2 (7.2)
	3000	93.5 (7.2)	93.3 (6.4)	64.4 (8.5)	55.3 (7.3)	40.4 (6.5)
KM	500	85.3 (5.8)	83.4 (5.8)	51.4 (6.0)	44.3 (3.4)	30.5 (4.2)
	1000	89.3 (6.1)	86.3 (6.9)	55.9 (7.5)	46.6 (2.7)	31.0 (3.8)
	2000	95,2 (7.4)	89.5 (7.7)	59.9 (8.3)	47.4 (3.3)	33.1 (2.5)
	3000	99.5 (6.3)	94.9 (8.3)	66.8 (9.2)	49.2 (3.6)	35.6 (4.7)

Standard deviation in parentheses (n=6)

Table 8-2 Statistical comparison of wear depth between acidic conditions

Materials	Wear cycles	Difference
FN	500	Control group, Group A > Group B > Group C > Group D*
	1000	Control group, Group A > Group B > Group C > Group D*
	2000	Control group, Group A > Group B > Group C > Group D*
	3000	Control group, Group A > Group B > Group C > Group D*
KM	500	Control group, Group A > Group B > Group C > Group D$^{\#}$
	1000	Control group, Group A > Group B > Group C > Group D$^{\#}$
	2000	Control group > Group A > Group B > Group C > Group D$^{\#}$
	3000	Control group > Group A > Group B > Group C > Group D$^{\#}$

Results of one-way ANOVA/Scheff's post-hoc test* and Kruskal-Wallis/Mann-Whitney test$^{\#}$ ($p < 0.05$)

> indicates statistically significant difference in wear depth

8.3.2 Shear strength

The shear strength of FN and KM in the various acidic conditions are listed in Figure 8-5 and Table 8-3. Group D and Group C showed significantly higher shear strength than control group, while Group B did not. When only calcium was present in acidic conditions (Group A), a similar shear strength to control group was observed (Table 8-4).

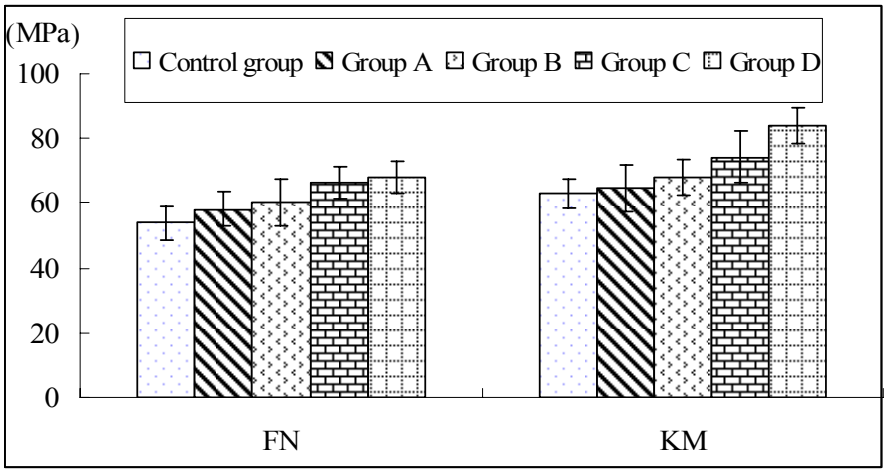

Figure 8-5 Shear strength of FN and KM

*vertical lines represent standard deviations

Table 8-3 Shear strength (MPa) of FN and KM

	FN	KM
Control group	53.87 (5.21)	63.09 (4.53)
Group A	58.11 (5.31)	64.67 (7.28)
Group B	60.15 (7.15)	67.87 (5.53)
Group C	66.37 (4.85)	74.20 (7.87)
Group D	68.01 (5.16)	84.00 (5.45)

Standard deviations in parentheses

Table 8-4 Statistical comparison of shear strength between acidic conditions

Materials	Difference
FN	Group D > Group A, Control group Group C > Control group
KM	Group D > Group B, Group A, Control group Group C > Control group

Results of one-way ANOVA/Scheff's post-hoc test ($p<0.05$)
> indicates statistically significant difference in shear strength

These results suggest that environmental phosphate improves the wear resistance and shear strength of GICs in acidic conditions. The beneficial effects of environmental phosphate were dependent on the phosphate level, that is, the higher environmental phosphate level led to the greater wear resistance and shear strength of GICs when exposed to acids.

8.4 Discussion

Traditionally, conventional GICs are contraindicated in stress bearing occlusal restorations as they suffer bulk fracture and wear due to their insufficient strengths, poor wear resistance and sensitivity to acids. With improvements in the formulation, HVGICs present with increased strength and resistance to wear (Ellakuria *et al.*, 2003; de Gee, 1999). HVGICs were designed as alternatives to amalgam and have been employed in occlusal areas with the ART technique as well as temporary filling and

deciduous tooth restorations.

The wear of glass-ionomer restoratives *in vivo* is highly complex. Numerous *in vitro* wear testing have been carried out to predict the wear rate of materials under simulated intra-oral conditions. However, a total simulation of clinical behavior is impossible *in vitro* and no wear test has achieved this thus far (Turssi *et al.*, 2002). In this study, a simple reciprocating compression-sliding system, which simulates occlusal contact area (OCA) wear *in vivo*, was used to evaluate wear property of HVGICs (Yap *et al.*, 2001b). A controlled contact stress of 20 MPa was employed based on reported contact stress during mastication (Anderson, 1956). A stainless steel counter-body was used to produce a "plucking" wear, which has been observed in clinically worn composites (Abell *et al.*, 1983). In the wear testing, acidic storage media were placed in specimen holder and acted as a lubricant. The degraded surface was removed during wear testing and the fresh surface was again exposed to the acidic environment.

ISO recommends a compression strength testing for chemical-cured and a flexural strength testing for light-cured GIC materials (ISO 9917). The quality of the surface and edges of specimens are most critical to the strengths of the materials during the compression and flexural testing. Shear punch testing is an appropriate method to evaluate all dental materials, especially GICs (Nomoto *et al.*, 2001). *In vivo*, restorations are placed in shear during the masticatory cycle. Moreover, shear strength obtained from shear punch testing correlates with strength from tensile testing. Shear

strength can be used to estimate tensile property, which is also frequently present during mastication (Guduru *et al.*, 2005). The strength order of dental materials by shear strength testing is consistent with their clinical performance (Nomoto *et al.*, 2001). With regard to sample preparation for shear punch testing, the only requirement is that the two faces are flat and parallel, which is easily achieved. The quality of the specimen edges around the circumstance has no direct influence on the testing outcomes. The shear punch testing also has the advantage of saving material due to use of smaller specimens (Yap *et al.*, 2003b). As suggested by Nomoto *et al.* (2001), the specimens were restrained tightly during the shear punch testing. The recess in the apparatus provides a snug-fit with the specimens and minimizes the bending of specimens. Thus the reliability and reproducibility of the shear punch testing is assured (Yap *et al.*, 2003b).

It has been reported that GICs had inferior wear resistance and strength when exposed to acids (de Gee, 1999; McKenzie *et al.*, 2003a). Acids decompose the matrices and glass particles in GICs leading to degradation of the material (Fukazawa *et al.*, 1987, 1990). Compared with the results of FN in neutral conditions using the same wear testing (Yap *et al.*, 2003a), the results of this study (Control group) confirmed the negative effects of acids on GICs. It is noteworthy that, in this study, environmental calcium had no positive effects on the wear resistance and shear strength of GICs in acidic conditions. The results further supported the finding that environmental calcium had no significant effects on GICs in acidic conditions as

mentioned in previous studies (Chapter 5, 6 and 7).

In the present study, it was found that the wear resistance and shear strength of FN and KM in acidic conditions were improved by environmental phosphate. The positive effects of environmental phosphate are consistent with our previous studies for other properties of GICs.

In general, wear resistance of materials is directly determined by their surface energy, surface morphology and surface composition (Chattopadhyay, 2001). In our previous studies, we found that environmental phosphate altered the surface properties (hardness and elastic modulus, structure and compositions) of GICs when subjected to acidic conditions. The different wear results between acidic conditions with varying phosphate levels were therefore not surprising. Wear depth at different test intervals were in the following order: Control group and Group A > Group B > Group C > Group D. This is in accordance with the order of surface reaction layer thickness (Chapter 5). Findings suggest that the thickness of the surface reaction layer may be critical to the wear resistance of GICs in acid conditions.

The decreased wear resistance with an increase in surface reaction layer thickness also implies that the surface reaction layer is more susceptible to OCA wear than the unaffected normal GICs. Wear depth of the first 500 wear cycles in this study was generally beyond the thickness of the surface reaction layer (Figure 5-5 and Figure 5-9). Thus, differences in the wear rate between 500 cycles and 2000~3000 cycles can be used to predict the wear resistance of the surface reaction layer. It can be clearly

seen that the wear rate of the first 500 cycles was much higher than that for 2000~3000 cycles (Figure 8-3 and Figure 8-4). This suggests further that the surface reaction layer had lower wear resistance than the unaffected normal structure. The inferior wear resistance of the surface reaction layer may arise from the increased porosity or small particles and decreased hardness due to acid degradation (Chapter 6).

Our previous studies showed that the structure, compositions and physico-mechanical properties of the surface reaction layer were different when environmental phosphate level was varied. Higher environmental phosphate level led to a thinner and harder surface reaction layer (Chapter 6). In general, for the same material, higher hardness is related to higher wear resistance (Chattopadhyay, 2001). Along with the varied thickness, the altered properties (microstructure, roughness, hardness and elastic modulus) of the surface reaction layer may also contribute to the differences in wear resistance of GICs. However, the wear results from this study were insufficient to provide direct evidence for this assumption, due to the dominant role of surface reaction layer thickness in the wear process.

With regards to bulk mechanical property, shear strength of GICs in acidic conditions was also increased by environmental phosphate. The beneficial effects of environmental phosphate may be also due to the surface reaction layer as mentioned above. In the shear punching process, the sample is “punched out” by a shear linkage of microvoids in materials. Before the final catastrophic failure, the sample

experiences a combination of shear, bending and tension deformation (Lucas, 1983). Due to the sensitivity to microcrack like defects, strength is generally affected by material structure, surface treatment, testing methods and testing environment, *etc* (Kelly, 1995). It has been shown that chemical degradation will promote microcrack initiation in polymers, thus, accelerate the ultimate failure of materials under an applied load (Choi *et al.*, 2005). In this study, the surface reaction layer arising from the combined effects of environmental pH and phosphate is characterized with increased porosity or small particles. It is therefore anticipated that a thicker surface reaction layer may lead to a decreased strength. The latter was supported by the shear strength results.

Intra-oral pH is often decreased by intrinsic and extrinsic acids, such as gastric and dietary acids, and pH 3 is clinically realistic. It should be noted that the consumption of potentially erosive foodstuffs and beverages has increased nowadays, and this correlates closely to the prevalence of dental erosion (Lussi *et al.*, 2004). Although clinical surveys have shown that a long duration of exposure to low intra-oral pH has the potential to promote degradation of glass-ionomer restoratives *in vivo*, it must be highlighted that the detrimental effects of acids resulting from a four week conditioning period *in vitro* may take months or years to occur *in vivo*. In addition, the *in vitro* accelerated wear testing and shear punch testing are unable to completely simulate the “clinical” conditions for GIC restorations. The results of this laboratory study, however, provide important information regarding the performance

of GIC restoratives when exposed to acidic and stress-bearing conditions *in vivo*. To minimize acid degradation of GICs and increase their longevity *in vivo*, the following are suggested: (1) reduce acid exposure; and (2) modify the local environment by introducing beneficial agents. It was found in this study that environmental phosphate can positively affect wear process and strength of GICs. Hence, we suggest that the creation of a local high phosphate environment of GICs may improve the clinical performance of GICs, especially when challenged by acids. This could be achieved by coating GICs with high phosphate containing varnishes or resins or espousing GIC restorations to high phosphate foams or gel using a tray.

8.5 Conclusions

In the current study, the effects of environmental phosphate on OCA wear and shear strength of GICs subject to acidic conditions were investigated. Within the limitations of this study, the wear and shear strength of HVGICs in acidic conditions varied significantly with environmental phosphate level. It was found that adding phosphate to acidic conditions improved wear resistance and shear strength for both FN and KM. This phenomenon was attributed to the surface reaction layer of GICs, which was dependent on phosphate level in acidic conditions. The results suggest that environmental phosphate may improve clinical performance of glass-ionomer restorations when challenged by acids.

Chapter 9

General Conclusions, Proposed Mechanism and Future Perspectives

This study investigated the interaction of glass-ionomer restoratives with environmental calcium/phosphate and pH. The effects of environmental calcium/phosphate and pH on surface properties and other clinically related properties were examined. Based on analysis of surface changes of GICs and ion release/uptake from GICs, possible underlying mechanism was explored and proposed.

9.1 Results and general conclusions

In the preliminary study (Chapter 4), the suitability of a depth-sensing micro-indentation testing for GICs was investigated and the results showed that this technique was efficient and effective for characterizing mechanical properties of GICs. In the preliminary study, the effects of environmental conditions (100% humidity, water, ionic media with pH 7, 5 and 3) on GICs were also investigated using the depth-sensing micro-indentation testing. It was found that hardness and elastic modulus of the tested GICs were dependent on those storage conditions.

With regards to the influence of environmental calcium/phosphate and pH on the strontium based Fuji IX Fast and calcium based KetacMolar (Chapter 5), it was found that the effects of environmental calcium/phosphate on these two GICs were pH

dependent. The hardness, elastic modulus and surface structure did not change when pH were at 7 and 5, regardless of concentration of calcium and phosphate. However, at pH 3, hardness and elastic modulus of these GICs were influenced by the environmental phosphate level. An increased level of environmental phosphate led to higher hardness and elastic modulus. In general, a microscopic surface reaction layer was observed in specimens conditioned at pH 3 and it was thinner when the environmental phosphate level was higher.

In Chapter 6, a series of surface analytical techniques were employed to characterize the surface reaction layer. It was found that this layer was composed of two distinct zones. The inner zone was porous and had low hardness and elastic modulus. It was suggested that this zone was the result of acid degradation of the matrix and glass phases in GICs. The outer zone contained small particles and showed higher hardness and elastic modulus than the inner zone. It was also found that storage in a solution with high concentration of phosphate led to an outer zone with greater mechanical properties and a thinner inner degradation zone.

The ion/ligand release from GICs was investigated in Chapter 7. It was found that levels of cement-forming ions released from the tested GICs, e.g. Al^{3+}, Ca^{2+}, Sr^{2+}, and Si^{4+}, were decreased with the presence of phosphate in acidic conditions. The results confirmed the inhibition effect of environmental phosphate on acid degradation of GICs, as shown in Chapter 6. It was also found that environmental phosphate was taken up by GICs. The phosphate uptake was increased with increasing environmental phosphate

levels. Phosphate uptake may be the result of ligand exchange between environmental phosphate and intrinsic carboxyl group.

With regard to clinically related properties (Chapter 8), wear resistance and shear strength of the tested GICs were improved when environmental phosphate was present in the pH 3 solutions. On the other hand, fluoride released from GICs under acidic conditions was slightly reduced by environmental phosphate. The improved clinically related properties suggest that the introduction of local phosphate to GICs may result in better clinical performance. This should be included in future investigations.

9.2 Proposed mechanism of interaction between GICs and environmental calcium/phosphate and pH

Based on the results and conclusions mentioned above, a schematic representation of the proposed mechanism is shown in Figure 9-1. The mechanism of interaction of GIC with environmental calcium/phosphate and pH may be described using the following model.

--- Hydrogen ions (H^+) diffuse into GIC due to concentration gradient. The diffusion process is controlled by the GIC matrix and concentration of H^+ at GIC surface (Fukazawa *et al.*, 1990) (Figure 9-1a).

--- As illustrated below, the hydrogen ions (H^+) dissociate the cross-linking of polycarboxylate chains by exchanging with matrix-forming cations (Fukazawa *et al.*, 1990):

$(RCOO^-)_2M^{2+} + 2H^+ \Leftrightarrow 2RCOO^-H^+ + M^{2+}$

(M= metal cations, such as Ca^{2+}, Sr^{2+} and Al^{3+}; $RCOO^-$ = polycarboxylate anion)

--- The metal cations (Ca^{2+}/Sr^{2+} and Al^{3+}) diffuse outwards due to the existing concentration gradients (Figure 9-1a).

--- With the removal of cross-linking and metal cations, the GIC matrix is degraded and

glass particles are lost (Fano *et al.*, 2001; Roulet, 1984; Fukazawa *et al.*, 1987). Microstructure of severely degraded GIC is shown in Figure 9-1c.

--- Meanwhile, phosphate anions (PO_4^{3-}) are adsorbed on GIC surface *via* ligand exchange with carboxyl groups (Chapter 7: discussion).

--- The phosphate anions (PO_4^{3-}) adsorbed on the surface of GIC forms phosphate complexation with intrinsic metal cations (Figure 9-1b,d).

--- The complexation of phosphate on the surface of GIC hinders the penetration of further H^+, and also inhibits matrix-forming ion (Ca^{2+}, Sr^{2+} and Al^{3+}) from moving outwards (Figure 9-1b), thus, retards further dissolution of GIC and leads to a thinner inner zone of degraded GIC (Figure 9-1d).

The results of this study suggest that an increase in the concentration of phosphate in its immediate surrounding would provide some protection to GIC, especially when the environment is acidic. An in depth understanding of the involved mechanisms is required before the clinical implications can be fully appreciated.

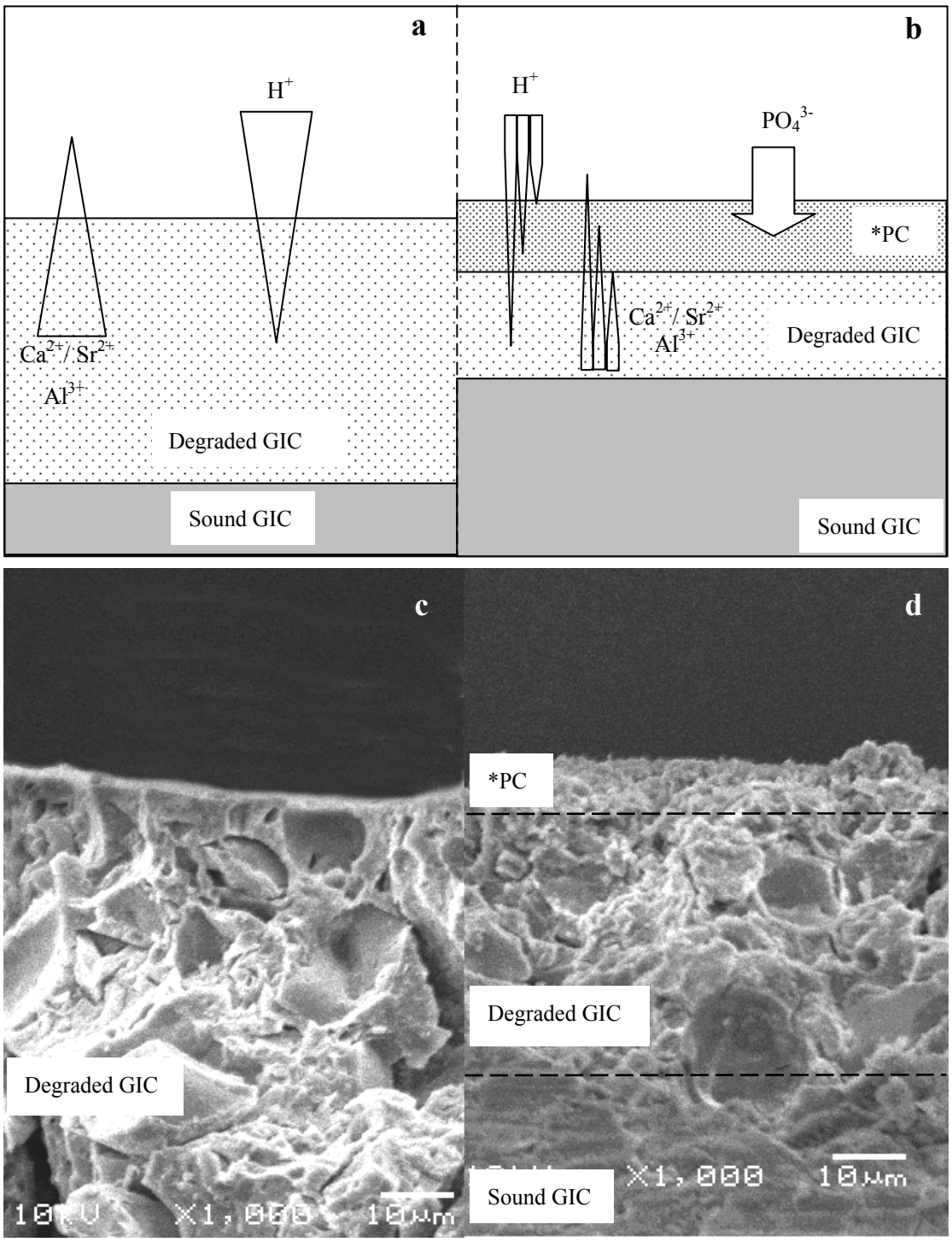

*PC: phosphate complexation

Figure 9-1 Illustration of interaction of GIC with environmental phosphate and pH

a. Diagram showing degradation of GIC

b. Diagram showing the effect of environmental phosphate on degradation of GIC

c. SEM photograph of degraded GIC

d. SEM photograph of GIC exposed to acidic conditions with phosphate

9.3 Future perspectives

Within the limitations of this study, it was found that environmental phosphate improved hardness, elastic modulus, wear resistance and shear strength of GICs under acidic conditions through surface modifications of GICs. Results of the current research suggest that the introduction of phosphate to glass-ionomer restoratives may improve their clinical performance, especially when challenged by acids. Further studies are warranted to clarify and confirm the findings of the present study.

In the current study, the accelerated *in vitro* experiments were carried out to investigate the interaction of GICs with environmental calcium/phosphate and pH. The GIC specimens were continuously exposed to environmental phosphate under neutral or acidic conditions for a prolonged period of time. The intra-oral pH as reviewed in Chapter 2 may drop during or after intake foods and acidic beverage. The dropped intra-oral pH then rises due to the effect of saliva clearance. In future work, a pH cycle program can be employed to simulate the pH variation in oral environment. Comparisons between the effects of phosphate-containing and phosphate-free pH cycling on glass-ionomers could more precisely predict the environmental phosphate effect on GICs *in vivo*.

In this study, the environmental phosphate levels (0 ~ 2.4 mM) employed were in the ranges found in saliva and most drinks. It was noted that increasing environmental phosphate level improved mechanical properties of GICs when challenged by acids. A wider range of phosphate levels should be investigated in future studies.

The two HVGICs tested in this study were either strontium or calcium based. These GICs were in capsule form, prepared according to manufacturers' instructions and set by traditional acid-base reaction. To verify that the findings of this study are universal across all GICs, more types of GICs of different powder to liquid ratios and mixing requirements should be investigated in future.

In this study, potassium orthophosphates $(PO_4)^{3-}$ were used as environmental phosphate source. It was found that the adsorption and complexation of phosphate on GIC surface inhibited further degradation of GICs, thus, improving their mechanical properties. However, this adsorption/complexation process of environmental phosphate under current experimental conditions was controlled by environmental pH. In future works, the introduction of environmental phosphate to GICs independent of environmental pH should be investigated. The phosphate may be grafted to new molecules which have more affinity to GICs, such as 3,4-dihydroxyphenylalanine (DOPA)-containing polypeptide, casein phosphopeptides (CPP), polymerizable phosphates, *etc*., which have shown effective binding to hydroxyapatite and biofilm (Tay and Pashley, 2002; Rose, 2000).

The adsorption/complexation process of environmental phosphate may also be enhanced through other approaches, such as varying the metal counterion. It was reported that fluoride uptake by GICs was significantly affected by the counterion type (Hadley *et al.*, 2001). The knowledge of counterion effect on phosphate uptake by GICs, however, is limited and should be investigated further.

Although HVGICs have significantly superior properties than their earlier counterparts, in this study they still degrade when they were exposed to a low pH environment. Improvements in GIC compositions are still warranted to increase their acid resistance. Various types of phosphates have been incorporated into GICs. It was shown that GICs with low phosphate concentration in the glass component have extended setting / working time and slightly increased compressive strength of GICs (Griffin and Hill, 2000). In addition, incorporation of casein phosphopeptide – amorphous calcium phosphate (CPP-ACP) nanocomplexes into glass particles increased bond and compressive strength of GICs (Mazzaoui *et al.,* 2003). However, the acid resistance of these experimental GICs is not known. The incorporation of phosphate into glass-ionomer components could potentially to improve GIC properties.

According to results of this study, environmental phosphate improved acid resistance of GICs. Future studies could also focus on how to effectively introduce environmental phosphate to GIC restoratives. Introduction of phosphate in the forms of topical agents has the most potential and is feasible in the clinic. Investigations on the effects of different phosphate-containing topical agents, such as surface coating, varnish, foam, gel, and oral rinse, on GICs are also warranted.

References

Abdalla AI, Alhadainy HA, Garcia-Godoy F. Clinical evaluation of glass ionomers and compomers in Class V carious lesions. Am J Dent 1997;10:18-20.

Abell AK, Leinfelder KF, Turner DT. Microscopic observations of the wear of a tooth restorative composite in vivo. J Biomed Mater Res 1983;17:501-507.

Anderson DJ. Measurement of stress in mastication. J Dent Res 1956;35:664-671.

Arita K, Lucas ME, Nishino M. The effect of adding hydroxyapatite on the flexural strength of glass ionomer cement. Dent Mater J 2003;22:126-136.

Attin T, Hannig C, Wiegand A, Attin R. Effect of bleaching on restorative materials and restorations--a systematic review. Dent Mater 2004;20:852-861.

Barkmeier WW, Jabro MH, Latta MA. Scanning electronic microscopic analysis of the local effects of a periodontal scaling gel on selected surfaces. J Clin Dent 1992;3:39-42.

Bibby BG, Mundorff SA, Zero DT, Almekinder KJ. Oral food clearance and the pH of plaque and saliva. J Am Dent Assoc 1986;112:333-337.

Billington RW, Hadley PC, Towler MR, Pearson GJ, Williams JA. Effects of adding sodium and fluoride ions to glass ionomer on its interactions with sodium fluoride solution. Biomaterials 2000;21:377-383.

Billington RW, Williams JA, Pearson GJ. Variation in powder/liquid ratio of a restorative glass-ionomer cement used in dental practice. Br Dent J 1990;169:164-167.

Billington RW, Williams JA, Strang R. Effects of 'neutral' sodium fluoride on glass-ionomers in vitro. J Dent Res 1987;66:844 (Abs no.88).

Bourke AM, Walls AW, McCabe JF. Light-activated glass polyalkenoate (ionomer) cements: the setting reaction. J Dent 1992;20:115-120.

Brackett WW, Dib A, Brackett MG, Reyes AA, Estrada BE. Two-year clinical performance of Class V resin-modified glass-lonomer and resin composite restorations. Oper Dent 2003;28:477-481.

Brackett WW, Gilpatrick RO, Browning WD, Gregory PN. Two-year clinical performance of a resin-modified glass-ionomer restorative material. Oper Dent 1999;24:9-13.

Braybrook JH, Nicholson JW. Incorporation of crosslinking agents into poly(vinyl phosphonic acid) as a route to glass–polyalkenoate cements of improved compressive strength. J. Mater. Chem 1993;3,361-365.

Brundle CR, Evans CA, Wilson JS. Appendixes: Techniques summaries. In: Brundle CR, Evans CA, Wilson JS, editors. Encyclopedia of materials characterization. Greenwich, USA: Manning Publications Co., 1992. p. Appendixes 269-288.

Brunelle JA, Carlos JP. Recent trends in dental caries in US children and the effect of water fluoridation. J Dent Res 1990;69:723-727.

Burke FJ, Wilson NH, Cheung SW, Mjor IA. Influence of patient factors on age of restorations at failure and reasons for their placement and replacement. J Dent 2001;29:317-324.

Causton BE. The physico-mechanical consequences of exposing glass ionomer cements to water during setting. Biomaterials 1981;2:112-115.

Chandler H. Introduction to hardness testing. In: Chandler H, editors. Hardness testing. USA: ASM International, 1999. p. 1-13.

Chattopadhyay R. Surface characterization. In: Chattopadhyay R, editors. Surface wear: analysis, treatment and prevention. USA: ASM International, 2001. p. 1-54.

Choi BH, Zhou Z, Chudnovsky A, Stivala SS, Sehanobish K, Bosnyak CP. Fracture initiation associated with chemical degradation: observation and modeling. International Journal of Solids and Structures 2005;42:681-695.

Chung SM, Yap UJ, Tsai KT and Yap FL. Elastic modulus of resin-based dental restorative materials: a micro-indentation approach. J Biomed Mater Res Part B: Applied Biomaterials 2005;72B:246-253.

Culbertson BM. Glass-ionomer dental restoratives. Prog Polym Sci 2001;26:577-604.

Culbertson BM, Xie D, and Thakur A. New matrix resins for glass polyalkenates or glass-ionomers with pendant amino acid residues. J Macromol Sci, Pure Appl Chem 1999;A36(5-6):681-696.

Czarnecka B, Limanowska-Shaw H, Nicholson JW. Buffering and ion-release by a glass-ionomer cement under near-neutral and acidic conditions. Biomaterials 2002;23:2783-2788.

Darling M, Hill R. Novel polyalkenoate (glass-ionomer) dental cements based on zinc silicate glasses. Biomaterials 1994;15:299-306.

de Gee AJ. Physical properties of glass-ionomer cements: setting shrinkage and wear. In: Davidson CL, Mjör IA, editors. Advances in glass-ionomer cements. Berlin: Quintessence, 1999. P. 51-66.

De Maeyer EA, Verbeeck RM, Vercruysse CW. Infrared spectrometric study of acid-degradable glasses. J Dent Res 2002;81:552-555.

De Maeyer EA, Verbeeck RM, Vercruysse CW. Reactivity of fluoride-containing calcium aluminosilicate glasses used in dental glass-ionomer cements. J Dent Res 1998;77:2005-2011.

Deb S, Nicholson JW. The effect of strontium oxide in glass-ionomer cements. J Mater Sci Mater Med 1999;10:471-474.

Denisova LA, Maev RG, Poyurovskaya IY, Grineva TV, Denisov AF, Maeva EY, Bakulin EY. The use of acoustic microscopy to study the mechanical properties of glass-ionomer cement. Dent Mater 2004;20:358-363.

Dodds MW, Johnson DA, Yeh CK. Health benefits of saliva: a review. J Dent 2005;33:223-233.

Driessens FCM. Chemistry of calcium phosphate cements. Euroceramics 1995;4:877-883.

Dunne SM, Goolnik JS, Millar BJ, Seddon RP. Caries inhibition by a resin-modified and a conventional glass ionomer cement, in vitro. J Dent 1996;24:91-94.

Edgar WM. Saliva: its secretion, composition and functions. Br Dent J 1992;172:305-312.

Eisenburger M, Addy M, Rossbach A. Acidic solubility of luting cements. J Dent 2003;31:137-142.

el-Badrawy WA, McComb D. Effect of home-use fluoride gels on resin-modified glass-ionomer cements. Oper Dent 1998;23:2-9.

el-Badrawy WA, McComb D, Wood RE. Effect of home-use fluoride gels on glass ionomer and composite restorations. Dent Mater 1993;9:63-67.

el Mallakh BF, Sarkar NK. Fluoride release from glass-ionomer cements in de-ionized water and artificial saliva. Dent Mater 1990;6:118-122.

Ellakuria J, Triana R, Minguez N, Soler I, Ibaseta G, Maza J, Garcia-Godoy F. Effect of one-year water storage on the surface microhardness of resin-modified versus conventional glass-ionomer cements. Dent Mater 2003;19:286-290.

Ermis RB. Two-year clinical evaluation of four polyacid-modified resin composites and a resin-modified glass-ionomer cement in Class V lesions. Quintessence Int 2002;33:542-548.

Espelid I, Tveit AB, Tornes KH, Alvheim H. Clinical behaviour of glass ionomer restorations in primary teeth. J Dent 1999;27:437-442.

Fano L, Fano V, Ma WY, Yang GW, Zhu F. Structure of dental glass-ionomer cements by confocal fluorescence microscopy and stereomicroscopy. Biomaterials 2001;22:2353-2358.

Ferguson DB, Botchway CA. A comparison of circadian variation in the flow rate and composition of stimulated human parotid, submandibular and whole salivas from the same individuals. Arch Oral Biol 1980;25:559-568.

Folwaczny M, Loher C, Mehl A, Kunzelmann KH, Hickel R. Class V lesions restored with four different tooth-colored materials--3-year results. Clin Oral Investig 2001;5:31-39.

Forsten L. Fluoride release and uptake by glass-ionomers and related materials and its clinical effect. Biomaterials 1998;19:503-508.

Forsten L. Fluoride release of glass ionomers. J Esthet Dent 1994;6:216-222.

Forsten L. Fluoride release and uptake by glass-ionomers. Scand J Dent Res 1991;99:241-245.

Franco EB, Benetti AR, Ishikiriama SK, Santiago SL, Lauris JR, Jorge MF, Navarro MF. 5-year clinical performance of resin composite versus resin modified glass ionomer restorative system in non-carious cervical lesions. Oper Dent 2006;31:403-408.

Frencken JE, Pilot T, Songpaisan Y, Phantumvanit P. Atraumatic restorative treatment (ART): rationale, technique, and development. J Public Health Dent 1996;56:135-140.

Fukazawa M, Matsuya S, Yamane M. The mechanism for erosion of glass-ionomer cements in organic-acid buffer solutions. J Dent Res 1990;69:1175-1179.

Fukazawa M, Matsuya S, Yamane M. Mechanism for erosion of glass-ionomer cements in an acidic buffer solution. J Dent Res 1987;66:1770-1774.

Gandolfi MG, Chersoni S, Acquaviva GL, Piana G, Prati C, Mongiorgi R. Fluoride release and absorption at different pH from glass-ionomer cements. Dent Mater. 2005; in print.

Ganss C, Klimek J, Giese K. Dental erosion in children and adolescents--a cross-sectional and longitudinal investigation using study models. Community Dent Oral Epidemiol 2001;29:264-271.

Gao W, Peng D, Smales RJ, Yip KH. Comparison of atraumatic restorative treatment and conventional restorative procedures in a hospital clinic: evaluation after 30 months. Quintessence Int 2003;34:31-37.

Griffin SG, Hill RG. Influence of glass composition on the properties of glass polyalkenoate cements Part II: influence of phosphate content. Biomaterials 2000;21:399-403.

Gu YW, Yap AU, Cheang P, Khor KA. Effects of incorporation of HA/ZrO_2 into glass ionomer cement (GIC). Biomaterials 2005;26:713-720.

Gu YW, Yap AU, Cheang P, Kumar R. Spheroidization of glass powders for glass ionomer cements. Biomaterials 2004;25:4029-4035.

Guduru RK, Darling KA, Kishore R, Scattergood RO, Koch CC and Murty KL. Evaluation of mechanical properties using shear–punch testing. Materials Science and Engineering A 2005;395:307-314.

Guggenberger R, May R, Stefan KP. New trends in glass-ionomer chemistry. Biomaterials 1998;19:479-483.

Hadley PC, Billington RW, Williams JA, Pearson GJ. Interactions between glass ionomer cement and alkali metal fluoride solutions: the effect of different cations.

Biomaterials 2001;22:3133-3138.

Hadley PC, Billington RW, Pearson GJ, Williams JA. Effect of monovalent ions in glass ionomer cements on their interaction with sodium fluoride solution. Biomaterials 2000;21:97-102.

Hammesfahr PD. Development in resionomer system. In: Hunt P, editor. Glass ionomers: the next generation. Philadelphia, 1994;47-55.

Hattab FN, Amin WM. Fluoride release from glass ionomer restorative materials and the effects of surface coating. Biomaterials 2001;22:1449-1458.

Haveman CW, Summitt JB, Burgess JO, Carlson K. Three restorative materials and topical fluoride gel used in xerostomic patients: a clinical comparison. J Am Dent Assoc 2003;134:177-184.

Hayacibara MF, Ambrozano GM, Cury JA. Simultaneous release of fluoride and aluminum from dental materials in various immersion media. Oper Dent 2004;29:16-22.

Ho TF, Smales RJ, Fang DT. A 2-year clinical study of two glass ionomer cements used in the atraumatic restorative treatment (ART) technique. Community Dent Oral Epidemiol 1999;27:195-201.

Hosoda H. The composition and setting reaction of glass ionomer cement. In: Katsuyama S, Ishikawa T, Fujii B, editors. Glass ionomer dental cement. Ishiyaku EuroAmerican, Inc. 1993. p.16-24.

Hu JY, Li YQ, Smales RJ, Yip KH. Restoration of teeth with more-viscous glass ionomer cements following radiation-induced caries. Int Dent J 2002;52:445-448.

Hubel S, Mejare I. Conventional versus resin-modified glass-ionomer cement for Class II restorations in primary molars. A 3-year clinical study. Int J Paediatr Dent 2003;13:2-8.

Humphrey SP, Williamson RT. A review of saliva: normal composition, flow, and function. J Prosthet Dent 2001;85:162-169.

International Organization for Standardization. Dentistry – Water-based cements – Part 1: Powder / liquid acid-base cements. 2003: ISO 9917-1.

International Organization for Standardization. Dental water-based cements – Part 2:

Light-activated cements. 1998: ISO 9917-2.

International Organization for Standardization. Dentistry – Polymer-based filling, restorative and luting materials. 2000: ISO 4049.

Jefferson KL, Zena RB, Giammara B. Effects of carbamide peroxide on dental luting agents. J Endod 1992;18:128-132.

Johansson AK, Johansson A, Birkhed D, Omar R, Baghdadi S, Carlsson GE. Dental erosion, soft-drink intake, and oral health in young Saudi men, and the development of a system for assessing erosive anterior tooth wear. Acta Odontol Scand 1996;54:369-378.

Jones FH, Hutton BM, Hadley PC, Eccles AJ, Steele TA, Billington RW, Pearson GJ. Fluoride uptake by glass ionomer cements: a surface analysis approach. Biomaterials 2003;24:107-119.

Kanchanavasita W, Anstice HM, Pearson GJ. Long-term flexural strengths of resin-modified glass-ionomer cements. Biomaterials 1998a;19:1703-1713.

Kanchanavasita W, Anstice HM, Pearson GJ. Long-term surface micro-hardness of resin-modified glass ionomers. J Dent 1998b,26:707-712.

Karantakis P, Helvatjoglou-Antoniades M, Theodoridou-Pahini S, Papadogiannis Y. Fluoride release from three glass ionomers, a compomer, and a composite resin in water, artificial saliva, and lactic acid. Oper Dent 2000;25:20-25.

Karlsbeek H, Verrips GHW. Dental caries prevalence and the use of fluorides in different European countries. J Dent Res 1990;69:728-732.

Kelly JR. Perspectives on strength. Dent Mater 1995;11:103-110.

Kent BE, Wilson AD. Dental silicate cements. 8. Acid-base aspect. J Dent Res 1969;48:412-418.

Kilpatrick NM, Murray JJ, McCabe JF. The use of a reinforced glass-ionomer cermet for the restoration of primary molars: a clinical trial. Br Dent J 1995;179:175-179.

Lacatusu S, Francu L, Francu D. Clinical and therapeutical aspects of rampant caries in cervico-facial irradiated patients. Rev Med Chir Soc Med Nat Iasi 1996;100:198-202.

Larsen MJ, Nyvad B. Enamel erosion by some soft drinks and orange juices relative to their pH, buffering effect and contents of calcium phosphate. Caries Res 1999;33:81-87.

Leirskar J, Nordbo H, Mount GJ, Ngo H. The influence of resin coating on the shear punch strength of a high strength auto-cure glass ionomer. Dent Mater 2003; 19: 87-91.

Leung VW, Darvell BW. Artificial salivas for in vitro studies of dental materials. J Dent 1997;25:475-484.

Levallois B, Fovet Y, Lapeyre L, Gal JY. In vitro fluoride release from restorative materials in water versus artificial saliva medium (SAGF). Dent Mater 1998;14:441-447.

Li X, Bhushan B. A review of nanoindentation continuous stiffness measurement technique and its applications. Materials characterization 2002;48:11-36.

Lloyd CH, Scrimgeour SN, Hunter G, Chudek JA, Lane DM, Mcdonald PJ. Solid state spatially resolved ^{1}H and ^{19}F nuclear magnetic resonance spextroscopy of dental materials by stray-field imaging. J Mater Sci: materials in medicine 1999;10: 369-373.

Loguercio AD, Reis A, Barbosa AN, Roulet JF. Five-year double-blind randomized clinical evaluation of a resin-modified glass ionomer and a polyacid-modified resin in noncarious cervical lesions. J Adhes Dent 2003;5:323-332.

Lucas, GE. The development of small specimen mechanical test techniques. J of nuclear materials 1983;117:327-339.

Lussi A, Jaeggi T, Zero D. The role of diet in the aetiology of dental erosion. Caries Res 2004;38:34-44.

Lussi A, Schaffner M. Progression of and risk factors for dental erosion and wedge-shaped defects over a 6-year period. Caries Res 2000;34:182-187.

Lussi A, Portmann P, Burhop B. Erosion on abraded dental hard tissues by acid lozenges: an in situ study. Clin Oral Investig 1997;1:191-194.

Lussi A, Jaeggi T, Jaeggi-Scharer S. Prediction of the erosive potential of some beverages. Caries Res 1995;29:349-354.

Maeda T, Mukaeda K, Shimohira T, Katsuyama S. Ion distribution in matrix parts of glass-polyalkenoate cement by SIMS. J Dent Res 1999;78:86-90.

Mair L, Joiner A. The measurement of degradation and wear of three glass ionomers following peroxide bleaching. J Dent 2004;32:41-45.

Mair LH, Stolarski TA, Vowles RW, Lloyd CH. Wear: mechanisms, manifestations and measurement. J Dent 1996;24:141-148.

Mallow PK, Durward CS, Klaipo M. Restoration of permanent teeth in young rural children in Cambodia using the atraumatic restorative treatment (ART) technique and Fuji II glass ionomer cement. Int J Paediatr Dent 1998;8:35-40.

Mandari GJ, Frencken JE, van't Hof MA. Six-year success rates of occlusal amalgam and glass-ionomer restorations placed using three minimal intervention approaches. Caries Res 2003;37:246-253.

Mandari GJ, Truin GJ, van't Hof MA, Frencken JE. Effectiveness of three minimal intervention approaches for managing dental caries: survival of restorations after 2 years. Caries Res 2001;35:90-94.

Manhart J, Chen H, Hamm G, Hickel R. Review of the clinical survival of direct and indirect restorations in posterior teeth of the permanent dentition. Oper Dent 2004;29:481-508.

Margolis HC, Moreno EC. Composition and cariogenic potential of dental plaque fluid. Crit Rev Oral Biol Med 1994;5:1-25.

Maryniuk GA, Kaplan SH. Longevity of restorations: survey results of dentists' estimates and attitudes. J Am Dent Assoc 1986;112:39-45.

Matsuya S, Maeda T, Ohta M. IR and NMR analyses of hardening and maturation of glass-ionomer cement. J Dent Res 1996;75:1920-1927.

Mazzaoui SA, Burrow MF, Tyas MJ, Dashper SG, Eakins D, Reynolds EC. Incorporation of casein phosphopeptide-amorphous calcium phosphate into a glass-ionomer cement. J Dent Res 2003;82:914-918.

McCabe JF. Resin-modified glass-ionomers. Biomaterials 1998;19:521-527.

McComb D, Erickson RL, Maxymiw WG, Wood RE. A clinical comparison of glass ionomer, resin-modified glass ionomer and resin composite restorations in the

treatment of cervical caries in xerostomic head and neck radiation patients. Oper Dent 2002;27:430-437.

McKenzie MA, Linden RWA, Nicholson, JW. The effect of Coca-Cola and fruit juices on the surface hardness of glass-ionomers and 'compomers'. J Oral Rehabil 2004;31:1046-1052.

McKenzie MA, Linden RWA, Nicholson, JW. The physical properties of conventional and resin-modified galss-ionomer dental cements stored in saliva, proprietary acidic beverages, saline and water. Biomaterials 2003a;24:4063-4069.

McKenzie MA, Linden RWA, Nicholson, JW. The effect of saliva on surface hardness and water sorption of glass-ionomers and “compomers”. J Mater Sci Mater med 2003b;14:869-873.

McKinney JE, Antonucci JM, Rupp NW. Wear and microhardness of glass ionomer cements. J Dent Res 1987;66:1134-1139.

McLean JW. Dentinal bonding agents versus glass-ionomer cements. Quintessence Int 1996;27:659-667.

McLean JW, Wilson AD, Prosser HJ. Development and use of water-hardening glass-ionomer luting cements. J Prosthet Dent 1984;52:175-181.

Mesu FP, Reedijk T. Degradation of luting cements measured in vitro and in vivo. J Dent Res 1983;62:1236-1240.

Mitra SB, Kedrowski BL. Long-term mechanical properties of glass ionomers. Dent Mater 1994;10:78-82.

Mitsuhashi A, Hanaoka K, Teranaka T. Fracture toughness of resin-modified glass ionomer restorative materials: effect of powder/liquid ratio and powder particle size reduction on fracture toughness. Dent Mater 2003;19:747-757.

Mjör IA. The reasons for replacement and the age of failed restorations in general dental practice. Acta Odontol Scand 1997;55:58-63.

Mjör IA. Glass-ionomer restorations and secondary caries: A preliminary report. Quintessence Int 1996;27:171-174.

Mjör IA, Jokstad A. Five-year study of Class II restorations in permanent teeth using amalgam, glass polyalkenoate (ionomer) cerment and resin-based composite

materials. J Dent 1993;21:338-343.

Mohamed-Tahir MA, Yap AU. Effects of pH on the surface texture of glass ionomer based/containing restorative materials. Oper Dent 2004;29:586-591.

Mojon P, Kaltio R, Feduik D, Hawbolt EB, MacEntee MI. Short-term contamination of luting cements by water and saliva. Dent Mater 1996;12:83-87.

Momoi Y, Hirosaki K, Kohno A, McCabe JF. In vitro toothbrush-dentifrice abrasion of resin-modified glass ionomers. Dent Mater 1997;13:82-88.

Morris JH, Perkins PG, Rose AEA, Smith WE. The chemistry and binding properties of aluminum phosphates. Chem Sov Rev 1977;6:173-194.

Mount GJ. Description of glass-ionomers. In: Mount GJ, editors. An atlas of glass-ionomer cements.UK: Martin Dunitz, 2002. P. 1-42.

Mount GJ. Glass ionomers: a review of their current status. Oper Dent 1999;24:115-124.

Muhlemann HR, Schmid R, Noguchi T, Imfeld T, Hirsch RS. Some dental effects of xylitol under laboratory and in vivo conditions. Caries Res 1977;11:263-276.

Muraguchi K, Suzuki S, Minami H, Tanaka T. In vitro evaluation of bond strength and surface roughness of a resin-paint material. Dent Mater J 2004;23:406-411.

Musanje L, Shu M, Darvell BW. Water sorption and mechanical behavior of cosmetic direct restorative materials in artificial saliva. Dent Mater 2001;17:394-401.

Neo J, Chew CL. Direct tooth-colored materials for noncarious lesions: a 3-year clinical report. Quintessence Int 1996;27:183-188.

Ngo H. Biological potential of glass-ionomers. In: Mount GJ, editors. An atlas of glass-ionomer cements. UK: Martin Dunitz, 2002. p. 43-56.

Nicholson JW, McKenzie MA, Goodridge R, Wilson AD. Variations in the compressive strength of dental cements stored in ionic or acidic solutions. J Mater Sci Mater Med 2001;12:647-652.

Nicholson JW, Czarnecka B, Limanowska-Shaw H. A preliminary study of the effect of glass-ionomer and related dental cements on the pH of lactic acid storage solutions. Biomaterials 1999;20:155-158.

Nomoto R, Komoriyama M, McCabe JF, Hirano S. Effect of mixing method on the porosity of encapsulated glass ionomer cement. Dent Mater 2004;20:972-978.

Nomoto R, Uchida K, Momoi Y, McCabe JF. Erosion of water-based cements evaluated by volumetric and gravimetric methods. Dent Mater 2003;19:240-244.

Nomoto R, McCabe JF. A simple acid erosion test for dental water-based cements. Dental Mater 2001;17:53-59.

Nomoto R, Carrick TE, McCabe JF. Suitability of a shear punch test for dental restorative materials. Dent Mater 2001;17:415-421.

Okada K, Tosaki S, Hirota K, Hume WR. Surface hardness change of restorative filling materials stored in saliva. Dent Mater 2001;17:34-39.

Oliver WC, Pharr GM. An improved technique for determining hardness and elastic modulus using load and displacement sensing indentation experiments. J Mater Res 1992;7:1564-1568.

Onal B, Pamir T. The two-year clinical performance of esthetic restorative materials in noncarious cervical lesions. J Am Dent Assoc 2005;136:1547-1555.

Ostlund J, Moller K, Koch G. Amalgam, composite resin and glass ionomer cement in Class II restorations in primary molars--a three year clinical evaluation. Swed Dent J 1992;16:81-86.

Padma P, Reza AM, Seifollah N, Kun L. Effects of thickness and indenter geometry in nanoindentation of nickel thin films. Thin film – stress and mechanical properties X; material research society symposium – proceedings 2003;795:355-360.

Patel M, Tawfik H, Myint Y, Brocklehurst D, Nicholson JW. Factors affecting the ability of dental cements to alter the pH of lactic acid solutions. J Oral Rehabil 2000;27:1030-1033.

Pearson GJ, Atkinson AB. Long-term flexural strength of glass ionomer cements. Biomaterials 1991;12:658-660.

Pedersen AML, Bardow A, Nauntofte B. Salivary changes and dental caries as potential oral markers of autoimmune salivary gland dysfunction in primary Sjogren's syndrome. BMC Clin Pathol 2005;5:4.

Pluim LJ, Arends J. The relation between salivary properties and in vivo solubility of dental cements. Dent Mater 1987;3:13-18.

Powell LV, Johnson GH, Gordon GE. Factors associated with clinical success of cervical abrasion/erosion restorations. Oper Dent 1995;20:7-13.

Prentice LH, Tyas MJ, Burrow MF. The effect of particle size distribution on an experimental glass-ionomer cement. Dent Mater 2005;21:505-510.

Pyk N, Mejare I. Tunnel restorations in general practice. Influence of some clinical variables on the success rate. Acta Odontol Scand 1999;57:195-200.

Qvist V, Laurberg L, Poulsen A, Teglers PT. Eight-year study on conventional glass ionomer and amalgam restorations in primary teeth. Acta Odontol Scand 2004;62:37-45.

Qvist V, Laurberg L, Poulsen A, Teglers PT. Longevity and cariostatic effects of everyday conventional glass-ionomer and amalgam restorations in primary teeth: three-year results. J Dent Res 1997;76:1387-1396.

Randall RC and Wilson NHF. Glass-ionomer restoratives: A systematic review of a secondary caries treatment effect. J Dent Res 1999;78:628-637.

Rose RK. Binding characteristics of Streptococcus mutans for calcium and casein phosphopeptide. Caries Res 2000;34:427-431.

Roulet JF, Walti C. Influence of oral fluid on composite resin and glass-ionomer cement. J Prosthet Dent 1984;52:182-189.

Ryge G, Jendresen MD, Glantz PO, Mjor I. Standardization of clinical investigators for studies of restorative materials. Swed Dent J 1981;5:235-239.

Sabbagh J, Vreven J, Leloup G. Dynamic and static moduli of elasticity of resin-based materials. Dent Mater 2002;18:64-71.

Saito S, Tosaki S, Hirota K. Characteristics of glass-ionomer cements. In: Davidson CL, Mjör IA, editors. Advances in glass-ionomer cements. Berlin: Quintessence, 1999. P. 15-50.

Sarkar NK. Metal-matrix interface in reinforced glass ionomers. Dent Mater 1999;15:421-425.

Schwarz E, Chiu GK, Leung WK. Oral health status of southern Chinese following head and neck irradiation therapy for nasopharyngeal carcinoma. J Dent 1999;27:21-28.

Schmitt W, Purrmann R, Jochum P, Gasser O. Calcium depleted aluminium fluorosilicate glass powder for use in dental or bone cements. US Patent No. 4376835, 1983.

Setchell DJ, Teo CK, Khun AT. The relative solubilities of four modern glass-ionomer cements. Br Dent J 1985;158:220-222.

Shen L, Zeng K, Wang Y, Narayanan B, Kumar R. Determination of the hardness and elastic modulus of low K thin film and their barrier layer for microelectronic applications. Microelectronic Engineering 2003;70:115-124.

Sherrington I, Smith EH. Modern measurement techniques in surface metrology. Wear 1988;125:271-288.

Smales RJ, Ngo HC, Yip KH, Yu C. Clinical effects of glass ionomer restorations on residual carious dentin in primary molars. Am J Dent 2005;18:188-193.

Smales RJ, Gerke DC, White IL. Clinical evaluation of occlusal glass ionomer, resin, and amalgam restorations. J Dent 1990;18:243-249.

Smith DC. Development of glass-ionomer cement systems. Biomaterials 1998;19:467-478.

Smith GE. Surface deterioration of glass-ionomer cement during acid etching: an SEM evaluation. Oper Dent;1988:13:3-7.

Stephen KW. Fluoride toothpastes, rinses, and tablets. Adv Dent Res 1994,8:185-189.

Strand GV, Nordbo H, Tveit AB, Espelid I, Wikstrand K, Eide GE. A 3-year clinical study of tunnel restorations. Eur J Oral Sci 1996;104:384-389.

Suddick RP, Hyde HJ, Feller RP. Salivary water and electrolytes and oral health. In: Menaker L. editor. The biological basis of dental caries. New York: Harper and Rowe Publishers, 1980. p. 132-147.

Swift EJ Jr, Dogan AU. Analysis of glass ionomer cement with use of scanning electron microscopy. J Prosthet Dent 1990;64:167-174.

Taifour D, Frencken JE, Beiruti N, van 't Hof MA, Truin GJ. Effectiveness of glass-ionomer (ART) and amalgam restorations in the deciduous dentition: results after 3 years. Caries Res 2002;36:437-444.

Tanumiharja M, Burrow MF, Cimmino A, Tyas MJ. The evaluation of four conditioners for glass ionomer cements using field-emission scanning electron microscopy. J Dent 2001;29:131-138.

Tay FR, Pashley DH. Dental adhesives of the future. J Adhes Dent 2002;4(2):91-103.

ten Cate JM, Duijsters PP. Alternating demineralization and remineralization of artificial enamel lesions. Caries Res 1982;16:201-210.

Towler MR, Bushby AJ, Billington RW, Hill RG. A preliminary comparison of the mechanical properties of chemically cured and ultrasonically cured glass ionomer cements, using nano-indentation techniques. Biomaterials 2001;22:1401-1406.

Triana RT, Millan CP, Barrio JG, Garcia-Godoy F. Effect of APF gel on light-cured glass ionomer cements: an SEM study. J Clin Pediatr Dent 1994;18:109-113.

Turker SB, Biskin T. Effect of three bleaching agents on the surface properties of three different esthetic restorative materials. J Prosthet Dent 2003;89:466-473.

Turssi CP, Hara AT, de Magalhaes CS, Serra MC, Rodrigues AL Jr. Influence of storage regime prior to abrasion on surface topography of restorative materials. J Biomed Mater Res B Appl Biomater 2003;65:227-232.

Turssi CP, Hara AT, Serra MC, Rodrigues AL Jr. Effect of storage media upon the surface micromorphology of resin-based restorative materials. J Oral Rehabil 2002;29:864-871.

van Dijken JW, Kieri C, Carlen M. Longevity of extensive class II open-sandwich restorations with a resin-modified glass-ionomer cement. J Dent Res 1999;78:1319-1325.

van Dijken JW. A 6-year evaluation of a direct composite resin inlay/onlay system and glass ionomer cement-composite resin sandwich restorations. Acta Odontol Scand 1994;52:368-376.

van Duinen RN, Kleverlaan CJ, de Gee AJ, Werner A, Feilzer AJ. Early and long-term wear of 'fast-set' conventional glass-ionomer cements. Dent Mater 2005;21:716-720.

Walls AW, McCabe JF, Murray JJ. The effect of the variation in pH of the eroding solution upon the erosion resistance of glass polyalkenoate (ionomer) cements. Br Dent J 1988;164:141-144.

Wasson EA, Nicholson JW. New aspects of the setting of glass-ionomer cements. J Dent Res 1993;72:481-483.

Wasson EA, Nicholson JW. Studies on the setting chemistry of glass-ionomer cements. Clin Mater 1991;7:289-293.

Watson TF. Application of confocol scanning optical microscopy to dentistry. Br Dent J 1991;171:287-291.

Wattanapayungkul P, Yap AU, Chooi KW, Lee MF, Selamat RS, Zhou RD. The effect of home bleaching agents on the surface roughness of tooth-colored restoratives with time. Oper Dent 2004;29:398-403.

Welbury RR, Walls AW, Murray JJ, McCabe JF. The 5-year results of a clinical trial comparing a glass polyalkenoate (ionomer) cement restoration with an amalgam restoration. Br Dent J 1991;170:177-181.

Wilder AD Jr, Swift EJ Jr, May KN Jr, Thompson JY, McDougal RA. Effect of finishing technique on the microleakage and surface texture of resin-modified glass ionomer restorative materials. J Dent 2000;28:367-373.

Williams JA, Billington RW, Pearson G. Silver and fluoride ion release from metal-reinforced glass-ionomer filling materials. J Oral Rehabil 1997;24:369-375.

Wilson AD. Secondary reactions in glass-ionomer cements. J Mater Sci Lett 1996;15:275-276.

Wilson AD, Hill RG, Warrens CP, Lewis BG. The influence of polyacid molecular weight on some properties of glass-ionomer cements. J Dent Res 1989;68:89-94.

Wilson AD, Mclean JW. Setting reaction and its clinical consequences. In: Wilson AD, Mclean JW, editors. Glass-ionomer cement. Chicago: Quint; 1988a. P. 43-55.

Wilson AD, Mclean JW. Erosion and longevity. In: Wilson AD, Mclean JW, editors. Glass-ionomer cement. Chicago: Quint; 1988b. p. 107-123.

Wilson AD, Groffman DM, Powis DR, Scott RP. An evaluation of the significance of the impinging jet method for measuring the acid erosion of dental cements.

Biomaterials 1986;7:55-60.

Wilson AD, Paddon JM, Crisp S. The hydration of dental cements. J Dent Res 1979;58:1065-1071.

Wilson AD, Kent BE. A new translucent cement for dentistry. The glass ionomer cement. Br Dent J 1972;132:133-135.

Wood RE, Maxymiw WG, McComb D. A clinical comparison of glass ionomer (polyalkenoate) and silver amalgam restorations in the treatment of Class 5 caries in xerostomic head and neck cancer patients. Oper Dent 1993;18:94-102.

Xie D, Brantley WA, Culbertson BM, Wang G. Mechanical properties and microstructures of glass-ionomer cements. Dent Mater 2000;16:129-138.

Xie, D, Culbertson BM, Johnston WM. Formulations of light-curable glass-ionomer cements containing N-vinylpyrrolidone. J Macromol Sci, Pure Appl. Chem 1998a;35A:1631-1650.

Xie, D, Culbertson BM, Johnston WM. Improved flexural strength of N-vinylpyrrolidone modified acrylic acid copolymers for glass-ionomers. J Macromol Sci, Pure Appl. Chem 1998b;35A: 1615-1629.

Xie, D, Culbertson BM, Wang G.. Microhardness of N-vinylpyrrolidone modified glass-ionomers cements. J Macromol Sci, Pure Appl. Chem 1998c;35A: 547-561.

Xu HH. Long-term water-aging of whisker-reinforced polymer-matrix composites. J Dent Res 2003;82:48-52.

Yap AU, Wang XY, Wu XW, Chung SM. Comparative hardness and modulus of tooth-colored restoratives: A depth-sensing microindentation study. Biomaterials 2004;25:2179-2185.

Yap AU, Pek YS, Cheang P. Physico-mechanical properties of a fast-set highly viscous GIC restorative. J Oral Rehabil 2003a;30:1-8.

Yap AU, Lee MK, Chung SM, Tsai KT, Lim CT. Effect of food-simulating liquids on the shear punch strength of composite and polyacid-modified composite restoratives. Oper Dent 2003b;28:529-534.

Yap AU, Wattanapayungkul P. Effects of in-office tooth whiteners on hardness of tooth-colored restoratives. Oper Dent 2002;27:137-141.

Yap AU, Tan WS, Yeo JC, Yap WY, Ong SB. Surface texture of resin-modified glass ionomer cements: effects of finishing/polishing systems. Oper Dent 2002;27:381-386.

Yap AU, Mudanbi S, Chew CL, Neo JCL. Mechanical properties of an improved visible light-cured resin-modified glass ionomer cement Oper Dent 2001a;26:295-301.

Yap AUJ, Chew CL, Teoh SH, Ong LFKL. Influence of contact stress on OCA wear of composite restoratives. Oper Dent 2001b;26:134-144.

Yap AU, Sim CP, Loganathan V. Polymerization color changes of esthetic restoratives. Oper Dent 1999;24:306-311.

Yap AU. Post-irradiation hardness of resin-modified glass ionomer cements and a polyacid-modified composite resin. J Mater Sci: Mater Med 1997;8:413-416.

Yli-Urpo H, Vallittu PK, Narhi TO, Forsback AP, Vakiparta M. Compound changes and tooth mineralization effects of glass ionomer cements containing bioactive glass (S53P4), an in vivo study. Biomaterials 2005a;26:5934-5941.

Yli-Urpo H, Lassila LV, Narhi T, Vallittu PK. Compressive strength and surface characterization of glass ionomer cements modified by particles of bioactive glass. Dent Mater 2005b;21:201-209.

Yip HK, To WM. An FTIR study of the effects of artificial saliva on the physical characteristics of the glass ionomer cements used for art. Dent Mater 2005;21:695-703.

Yip HK, To WM, Smales RJ. Effects of artificial saliva and APF gel on the surface roughness of newer glass ionomer cements. Oper Dent 2004;29:661-668.

Yoshida Y, Van Meerbeek B, Nakayama Y, Snauwaert J, Hellemans L, Lambrechts P, Vanherle G, Wakasa K. Evidence of chemical bonding at biomaterial-hard tissue interfaces. J Dent Res 2000;79:709-714.

Young AM, Rafeeka SA, Howlett JA. FTIR investigation of monomer polymerisation and polyacid neutralisation kinetics and mechanisms in various aesthetic dental restorative materials. Biomaterials 2004;25:823-833.

Young AM. FTIR investigation of polymerisation and polyacid neutralisation kinetics in resin-modified glass-ionomer dental cements. Biomaterials 2002;23:3289-3295.

Young AM, Sherpa A, Pearson G, Schottlander B, Waters DN. Use of Raman spectroscopy in the characterisation of the acid-base reaction in glass-ionomer cements. Biomaterials 2000;21:1971-1979.

Yu C, Gao XJ, Deng DM, Yip HK, Smales RJ. Survival of glass ionomer restorations placed in primary molars using atraumatic restorative treatment (ART) and conventional cavity preparations: 2-year results. Int Dent J 2004;54:42-46.

Appendix A: Preparation of storage media of varying calcium/phosphate and pH

Molecular mass and density:

Calcium chloride dehydrate ($CaCl_2$•$2H_2O$)	147.02 g/mol
Potassium dihydro-orthophosphate (KH_2PO_4)	136.09 g/mol
Potassium chloride (KCl)	74.55 g/mol
N-2-hydroxyethylpiperazine-N'-2-ethanesulfonic acid (HEPES, $C_8H_{18}O_4N_2S$)	238.30 g/mol
Acetic acid CH_2COOH	60.05 g/mol
Density of acetic acid	1.053 g/ml

Make stock solution:

1. Make 30 mM $CaCl_2$•$2H_2O$ stock solution:

   Weigh 4.4106 g $CaCl_2$•$2H_2O$, dissolve in 1 L deionized water and store in a labeled bottle.

2. Make 30 mM KH_2PO_4 stock solution:

   Weigh 4.0827 g KH2PO4, dissolve in 1 L deionized water and store in a labeled bottle.

3. Make 40 mM HEPES stock solution:

   Weigh 9.523 g HEPES, dissolve in 1 L deionized water and store in a labeled bottle.

Preparation of storage media (in 1 L volumetric flask):

1. Add 30 mM $CaCl_2$•$2H_2O$ and 30 mM KH_2PO_4 stock solution as follows to achieve desired concentrations.

Storage Media		**Add stock solution**	
$CaCl_2$•$2H_2O$ (mM)	KH_2PO_4 (mM)	30 mM $CaCl_2$•$2H_2O$ (ml)	30 mM KH_2PO_4 (ml)
0	0	0	0
2.4	0	80	0
1.5	0.9	50	30
1.2	1.2	40	40
0	2.4	0	80

2. Weight 11.1825 g KCl and add to flask.
3. Add 500 ml of 40 mM HEPES stock solution for pH 7 storage media **OR** add 2.851 ml of concentrated glacial acetic acid for pH 5 and 3 storage media.
4. Fill flask with deionized water to 1 L and mix.
5. Check pH of solution and add 1 M KOH in a drop-wise manner until the desired pH of 7.0, 5.0 or 3.0 is obtained.

Appendix B: Preparation of TISAB II

(Refer to method 9214, US environmental protection agency, 1996)

Reagents:

1. Sodium hydroxide solution (5 M NaOH): Dissolve 200 g of NaOH in sufficient reagent water to make 1 L of solution. Store in a tightly sealed polyethylene bottle.
2. Glacial acetic acid (CH_3CO_2)
3. Sodium chloride (NaCl)
4. 1,2-cyclohexanediaminetetraacetic acid (CDTA)
5. Deionized water

Preparation of TISAB:

To approximately 500 ml of deionized water add 57.0 ml of glacial acetic acid, 58.0 g of sodium chloride, and 4.00 g of CDTA. Stir to dissolve and cool to room temperature. Adjust the solution pH to between 5.0 and 5.5 with 5 M NaOH (about 150 ml will be required). Transfer the solution to a 1000 ml volumetric flask and dilute to the mark with deionized water. Transfer the solution to a clean polyethylene bottle stored at 4 ^{o}C.